RESEARCH

Mia-Lisa Schmiedt

The CLN5 disease
– protein maturation,
trafficking and pathology

Mia-Lisa Schmiedt

The CLN5 disease – protein maturation, trafficking and pathology

Academic Dissertation

To be presented with the permission of the Medical Faculty of the University

of Helsinki, for public examination in lecture hall 2 at Biomedicum 1,

on 06th of July 2012, at 12 noon

Medical Genetics, Haartman Institute, Faculty of Medicine,
University of Helsinki, Finland
National Institute for Health and Welfare, Public Health Genomics Unit
Institute for Molecular Medicine, Finland (FiMM)
Helsinki Biomedical Graduate School, University of Helsinki, Finland

NATIONAL INSTITUTE
FOR HEALTH AND WELFARE

FiMM
Institute for Molecular Medicine Finland
Nordic EMBL Partnership for Molecular Medicine

UNIVERSITY OF HELSINKI

Cover picture: Ulla Sinikka Schmiedt, title: Für Mia, 2012

YMPÄRISTÖMERKKI
MILJÖMÄRKT
441 729
Painotuote

Supervisors	**Adjunct professor Anu Jalanko**
	National Institute for Health and Welfare
	Public Health Genomics
	Helsinki, Finland
and	
	Adjunct professor Aija Kyttälä
	National Institute for Health and Welfare
	Public Health Genomics
	Helsinki, Finland

Reviewers	**Adjunct professor Mikko Hiltunen**
	Institute of Clinical Medicine / Neurology
	University of Eastern Finland
	Kuopio, Finland
and	
	Adjunct professor Eija Jokitalo
	Institute of Biotechnology
	Electron Microscopy Unit
	University of Helsinki
	Helsinki, Finland

Opponent	**Professor Anu Wartiovaara**
	Research Program for Molecular Neurology
	University of Helsinki
	Helsinki, Finland

Members of the thesis committee

Professor Elina Ikonen
Institute of Biomedicine, Anatomy
University of Helsinki
Helsinki, Finland

and

Adjunct professor Outi Kopra
Folkhälsan Institute of Genetics, Department of Medical Genetics and Research Program's Unit, Molecular Medicine, and Neuroscience Centre
University of Helsinki
Helsinki, Finland

Aerodynamically, the bumble bee shouldn't be able to fly, but the bumble bee doesn't know it, so it goes on flying anyway.

Mary Kay Ash

Dedicated to my family

Abstract

Neurodegenerative disorders are caused by defects in the central nervous system leading to neuronal destruction and devastating conditions. They are often incurable and result in premature death. Neuronal ceroid lipofuscinoses (NCLs) comprise a group of rare, hereditary neurodegenerative disorders. They belong to the family of lysosomal storage disorders primarily affecting children. Patients share common features like accumulation of autofluorescent storage material, neuronal degeneration, and suffer from motor disturbances, progressive loss of vision and premature death. To date, nine genes have been detected to cause NCLs, but the mechanisms and functions of the proteins encoded by these genes are still largely unknown.

One type of NCLs is the CLN5 disease, a late infantile variant phenotype form. This severe neurodegenerative disease of childhood is caused by mutations in the *CLN5* gene, which encodes a highly glycosylated lysosomal protein of unidentified function. The early years of the patients are in most cases normal. First clinical signs usually start between 4-7 years of age with psychomotor disturbances and visual impairment. The disease often progresses rapidly between the ages 9-11 years and from the age of 12 years patients require help with all activities. Patients die young mostly between 12 to 23 years of age.

The aim of this thesis project was to contribute to the understanding of the molecular and cell biological mechanisms underlying CLN5 disease. Thereby, the focus of the first part of the thesis was on the basic characterisation of the maturation and trafficking of the CLN5 protein by *in vitro* studies. Thorough analyses presented proteolytical cleavage of a predicted CLN5 signal peptide in the ER, subsequent maturation/trimming of the proform followed by trafficking to the lysosomes. First evidence indicated that CLN5 might also use mannose-6-phosphate receptor independent trafficking routes to the lysosomes.

Overexpression studies of CLN5 constructs carrying different disease causing mutations revealed that trafficking was disturbed with varying severity depending on the particular mutation. Moreover, the trafficking to lysosomes could be rescued by co-expression of another NCL protein CLN1/PPT1, a suggested interaction partner of CLN5.

Real-time PCR revealed that *Cln5* gene expression rises gradually in the mouse brain with age and its expression is highest in microglia, the so called macrophages

of the brain which are important for the immune system of the central nervous system (CNS). Further, mice lacking the *Cln5* gene (*Cln5* ko) were utilised to study the pathology in more detail. Early microglial activation in *Cln5* ko mice was documented by immunohistochemical staining and thresholding image analysis. Early defective myelination was also observed *in vitro* and *in vivo*, prominently in the superficial laminae of the cortex but not in white matter structures. Additionally, disturbances in the systemic lipid metabolism and lipid transport were detected, pinpointing to a possible role of Cln5 in lipid homeostasis/transport.

Another goal of this thesis project was to investigate possible *in vivo* links between Cln5 and its suggested interaction partner palmitoyl protein thioesterase (Cln1/Ppt1), also a member of NCL proteins. Mutations in the *CLN1* gene are known to cause an infantile form of NCL. *Cln1*- and *Cln5*-deficient mice were crossed, thereby generating *Cln1/Cln5*-double-knockout (*Cln1/5* dko) mice, which were then characterised with the ultimate goal to provide novel insights into NCLs in general. The pathology of *Cln1/5* dko mice was more severe than in the single knockout animals, with widespread accumulation of autofluorescent storage material in the brain, intense astrocytosis and microglial activation especially in the thalamus and cortical regions, defective myelination in the cortex and disturbed lipid metabolism. Gene expression profiling of the cortex of *Cln1/5* dko mice underlined these findings pointing at defects in myelination and immune response pathways.

In conclusion, this thesis work elucidates the controversially discussed maturation and localisation of the CLN5 protein. It provides novel aspects about the early events in the pathogenesis of CLN5 disease, late infantile variant, links Cln5 to lipid metabolism and strengthens the recently reported connection to Cln1/Ppt1. Together, the findings of this thesis work contribute to the basic knowledge of molecular mechanisms underlying these devastating diseases.

Contents

The CLN5 disease - protein
maturation, trafficking and pathology

11

List of original publications

I.   **Mia-Lisa Schmiedt***, Carlos Bessa*, Claudia Heine, Maria Gil Ribeiro, Anu Jalanko, Aija Kyttälä. The neuronal ceroid lipofuscinosis protein CLN5: new insights into cellular maturation, transport, and consequences of mutations. *Human Mutation* 2010 Mar; 31(3):356-65

II. **Mia-Lisa Schmiedt**, Tea S. Blom, Tomas Blom, Outi Kopra, Carina von Schantz-Fant, Mervi Kuronen, Elina Ikonen, Matti Jauhiainen, Jonathan D. Cooper, Anu Jalanko. *Cln5*-deficiency in mice leads to microglial activation, defective myelination and changes in lipid metabolism. *Neurobiology of Disease* 2012 Apr; 46(1):19-29

III. Tea S. Blom, **Mia-Lisa Schmiedt,** Andrew M. Wong, Aija Kyttälä, Jarkko Soronen, Matti Jauhiainen, Jaana Tyynelä, Jonathan D. Cooper, Anu Jalanko. Exacerbated neuronal ceroid lipofuscinosis phenotype in *Cln1/5* double knock-out mice. S*ubmitted*

*These authors contributed equally to this work.

Publication I has appeared previously in the doctoral thesis of Carlos Bessa in Portugal (2009).

These articles are reproduced with the kind permission of their copyright holders.

Abbreviations

Only abbreviations that appear more than once and in more than one chapter are displayed.

aa	amino acid(s)
ab	antibody
ABCA/G	ATP-binding cassette transporter family A/G
ATP	adenosine triphosphate
BBB	blood brain barrier
BFA	brefeldin A
BODIPY-LacCer	boron dipyrromethene-lactoceramide
BSA	bovine serum albumin
Cc	corpus callosum
CD68	cluster of differentiation 68
cDNA	complementary DNA
Chx	cycloheximide
Chol	cholesterol
CL	curvilinear profile
CLN1-10, *CLN1-10*	ceroid lipofuscinosis, neuronal 1-10, human protein, *DNA/RNA*
Cln1-10, *Cln1-10*	ceroid lipofuscinosis, neuronal 1-10, murine protein, *DNA/RNA*
Cln1 ko, *Cln5* ko	*Cln1*-deficient knockout mice, *Cln5*-deficient knockout mice
Cln1/5 dko	*Cln1/d*-deficient double-knockout mice
CNPase	2',3'-cyclic nucleotide 3'-phosphohydrolase
CNS	central nervous system
COS-1 cells	African green monkey kidney cells
CSF	cerebrospinal fluid
DAB	3,3'-diaminobenzidine tetrahydrochloride HCl
DMEM	Dulbecco's modified Eagle's medium
DNA	deoxyribonucleic acid
DPX	p-xylene-bis(pyridinium bromide)
EB	embryoid body
ECL	enhanced chemiluminescence
EM	electron microscopy
EndoH	endoglycosidase H
ER	endoplasmic reticulum
FCS	fetal calf serum
FITC	fluorescein isothiocyanate
FP	fingerprint profile
GABA	gamma-aminobutyric acid
GalCer	galactosylceramide
GalNAc	N-acetylgalactosamine
GFAP	glial fibrillary acidic protein
GFP	green fluorescent protein
Glc	glucose
GROD	granular osmiophilic deposits
GSL	glycosphingolipid
HDL, LDL, VLDL	high, low, very low density lipoprotein
HeLa cells	human cervical tumour cells
IBA-1	ionised calcium adaptor protein 1
ic	internal capsule
if/IF	intermediate filament (if); immunofluorescence (IF)
iPS	induced pluripotent stem cells
kDa	kilodalton(s)
LAMP-1	lysosomal associated membrane protein
LCAT	lecithin:cholesterol acyltransferase

LDLR	LDL receptor superfamily
LFB	Luxol Fast Blue
LIMP-2	lysosomal integral membrane protein
LPS	*Escherichia coli* lipopolysaccharide
LSD	lysosomal storage disorder
M6P	mannose-6-phosphate
MAG	myelin associated glycoprotein
Man	mannose
MBP	myelin basic protein
MEF	mouse embryonic fibroblast
MOG	myelin-oligodendrocyte glycoprotein
MPR	mannose 6-phosphate receptors (MPR46 and MPR300)
MPR-/-	mannose-6-phosphate receptor deficient cell line
MPS	mucopolysaccharidoses
mRNA	messenger RNA
MS	multiple sclerosis
NCL	neuronal ceroid lipofuscinosis
NG-2	chondroitin sulphate proteoglycan
NPC1/2	Niemann-Pick type C1/2
OL	oligodendrocyte
OPC	oligodendrocyte precursor cell
PBS	phosphate buffered saline
PFA	paraformaldehyde
PL	phospholipids
PLP	proteolipid protein
PLTP	phospholipid transfer protein
PNGaseF	peptide N-glycosidase F
PPT1	palmitoyl protein thioesterase 1 (CLN1)
PS	penicillin/streptomycin
RNA	ribonucleic acid
ROI	region of interest
RT	room temperature
RT-PCR	real-time polymerase chain reaction
S1BF	somatosensory barrel field cortex
SAP	sphingolipid activator protein (saposin)
SDS-PAGE	sodium dodecyl sulphate polyacrylamide gel electrophoresis
SH-SY5Y	human neuroblastoma cells
SM	sphingomyelin
Snca	α-synuclein
SSEA-1	stage-specific embryonic antigen 1
TBS-(T)	tris buffered saline – (Tween)
TGN	*trans*-Golgi network
TIRF	total internal reflection fluorescence microscopy
TRITC	tetramethylrhodamine isothiocyanate
vLINCL$_{Fin}$	Finnish variant form of late infantile neuronal ceroid lipofuscinosis
VPM/VPL	ventral posterior nuclei of the thalamus
wt	wild type

Amino acid abbreviations that appear in this thesis work according to IUPAC nomenclature:

Amino acid	3-letter	1-letter	Amino acid	3-letter	1-letter
Arginine	**Arg**	**R**	**Proline**	**Pro**	**P**
Asparagine	**Asn**	**N**	**Serine**	**Ser**	**S**
Aspartic acid	**Asp**	**D**	**Threonine**	**Thr**	**T**
Histidine	**His**	**H**	**Tyrosine**	**Tyr**	**Y**

1 Introduction

Neurodegeneration is an umbrella term for progressive loss of neurons. Various acquired and inherited diseases of the central nervous system (CNS) are caused by neurodegenerative events, including e.g. Alzheimer's and Parkinson's diseases (AD, PD). Neurodegenerative disorders are usually incurable and are connected to high expenses for the health care system, dramatically diminished quality of life, infirmity and death. Regarding these aspects, development of treatments is of uttermost importance. The reasons for neuronal death are complex and often difficult to elaborate. Studies on monogenic diseases involving neurodegeneration, like neuronal ceroid lipofuscinoses (NCLs), may further the understanding of neuronal death in neurodenerative diseases and help to develop treatments.

NCLs comprise a group of recessively inherited neurodegenerative disorders affecting mainly children. The first clinical description of any NCL reaches back to 1826 by Dr. Otto Christian Stengel in Norway (Haltia, 2006). Hitherto, at least nine genes are known to underlie this group of disorders (Kousi *et al.*, 2012; Noskova *et al.*, 2011). Degeneration of nerve cells and accumulation of autofluorescent ceroid-lipopigment in neural and peripheral tissues are two histopathological characteristics of NCLs (Goebel, 1997). One form of NCLs is the CLN5 disease, late infantile variant form formerly known as Finnish variant late infantile neuronal ceroid lipofuscinosis, vLINCL$_{Fin}$. This type is caused by mutations in the *CLN5* gene and belongs to the Finnish disease heritage (Norio, 2003). As the numbers of diagnosed CLN5 patients other than of Finnish origin have been rising during the last few years, the original term vLINCL$_{Fin}$ is not appropriate anymore. Patients of various origins have been found all over the world: Columbian, Portuguese, French Canadian, Hispanic, Swedish, Chinese, Asian Indian, Egyptian and Pakistani ancestry (Bessa *et al.*, 2006; Pineda-Trujillo *et al.*, 2005; Xin *et al.*, 2010). To date, the functions of most NCL proteins remain unclear including CLN5. CLN5 shows no homology to any other known proteins and is evolutionary conserved only among vertebrates. However, interactions between NCL proteins, especially between CLN5 and other NCL proteins have been suggested by *in vitro* studies and comparative gene expression analysis (Lyly *et al.*, 2009; Vesa *et al.*, 2002; von Schantz *et al.*, 2008). Why defects in NCL proteins, which vary in function, cell location and solubility, lead to the similar pathological endpoint remains elusive. In this thesis, the aim was to elucidate the basic properties of the CLN5 protein, deeper analyse the impact of the loss of function in *Cln5*-deficient mice and study the affected pathways, when Cln5 and its predicted interaction partner Cln1/Ppt1 are both simultaneously not functional.

2 Review of the literature

2.1 Lysosomes and lysosomal storage disorders

2.1.1 Intracellular membrane trafficking pathways

All eukaryotic cells are surrounded by a membrane that functions as a barrier be-tween the inside cell components and its environment. The inside of a cell is further organised into compartments each surrounded by its own membrane. One way of communication between these compartments, also named organelles, is *via* traffick-ing vesicles which transport proteins and lipids. The main events of vesicular traf-ficking can be divided into several steps: sorting of the cargo, vesicle formation, subsequent transport along the cytoskeleton, detection of the target organelle, finally membrane fusion and release of the cargo (van Vliet *et al.*, 2003). In general, pro-teins contain signal sequences which determine their localisation within the cell (van Vliet *et al.*, 2003). Lipids are hypothesised to contain target information within their structure (Haucke and Di Paolo, 2007).

The endocytic and the secretory pathways are the two major routes of intracellular trafficking, which are interconnected *via* the Golgi complex and endocytic com-partments (Bonifacino and Rojas, 2006). The endocytic pathway describes an in-wards directed vesicle-mediated route from the environment into the cell, which is generally used for internalisation of extracellular macromolecules, such as lipids and proteins. After the cargo has entered the cell, it continues its journey to early endosomes from where it is either transported to multivesicular bodies (MVBs), late endosomes or lysosomes. Alternatively, it is recycled back to the cell sur-face/extracellular space *via* tubular recycling endosomes (Pryor and Luzio, 2009). In contrast, the secretory pathway is used to transport cargoes synthesised in the endo-plasmic reticulum (ER) and Golgi complex to the cell surface, to endosomes and/or lysosomes or to the extracellular space. Disturbances in the intracellular transport can lead to severe dysfunctions of tissue and organs. For example, about 50 lyso-somal diseases are known to be caused by dysfunctional cargo transport.

2.1.2 The lysosome and its function within the cell

Lysosomes embody one of the major degradative and catabolic compartments in eukaryotic cells. They are the so called waste disposal system of cells as they are able to degrade extracellular material that has been internalised (e.g. microbes) and recycle cellular molecules. 1955 Christian de Duve first described lysosomes as membrane-closed compartments with acid phosphatase activity (De Duve *et al.*,

1955). Alex Novikoff displayed the first morphological presentation of lysosomes by transmission electron microscopy (Novikoff *et al.*, 1956). The existence of a single phospholipid bilayer surrounding the lysosomes and globular and tubular shapes has been confirmed shortly after that. Lysosomes appear electron-dense in electron micrographs, often include irregularities and membrane sheets, and the content can highly vary (Saftig and Klumperman, 2009). The vacuolar H_1-ATPase, a large transmembrane multiprotein complex plays a key role in the maintenance of the acidic interior with a pH of 4.5–5 (Marshansky and Futai, 2008). Lysosomes contain more than 50 different acid hydrolases (e.g. proteases, phosphatases, glycosidases, lipases, nucleases, sulfatases) that are capable of degrading macromolecules and even membranes into their monomeric components in this acidic environment (Schröder *et al.*, 2010). Studies on lysosomal membrane proteins (LMPs) have been quite demanding due to the hydrophobic nature of LMPs. Currently, the number of predicted lysosomal membrane proteins range from hundred to several hundred (Lubke *et al.*, 2009; Schröder *et al.*, 2010). LMPs are involved in the establishment and maintenance of the pH gradient between cytoplasm and lysosomal lumen, hydrolase compartmentalisation, membrane fusion and transport (Saftig *et al.*, 2010). Additionally, lysosomes contain various transporters that are involved in the export of lysosomal catabolites from the lysosomal lumen to the cytosol or import macromolecules for degradation (Schröder *et al.*, 2010).

The biogenesis of lysosomes has been extensively studied and a number of models have been described: the maturation model (lysosomes mature from endosomes), the vesicular transport model (vesicles distribute cargo between endosomes and lysosomes), the kiss-and-run model (cargo is exchanged by transient contacts, "kisses", between endosomes and lysosomes and then disscociate "run" again), the direct fusion model (endosomes and lysosomes fuse to a hybrid organelle) and the fusion-fission model (a mixture between direct fusion and kiss-and-run: lysosomes and endosomes fuse permanently, form a hybrid organelle and subsequently lysosomes re-form from hybrid organelles again) (Luzio *et al.*, 2007) (**Figure 1**).

The capability of lysosomes to interact and fuse with other cell compartments like late endosomes, autophagosomes, phagosomes and even the plasma membrane has been well established (Luzio *et al.*, 2007). These events take place *via* complex protein-protein interactions and are highly dynamic (Saftig and Klumperman, 2009). For instance, endocytosed and newly synthesised macromolecules are transported to lysosomes by kissing events and direct fusion. The resulting hybrid organelles act as degradation compartments of endocytosed macromolecules and lysosomes are re-formed from the hybrid organelle by maturation (Luzio *et al.*, 2007). The basic characteristics of lysosome fusion with the plasma membrane and with late endosomes have been extensively studied, but how these processes are precisely regulated requires further investigation.
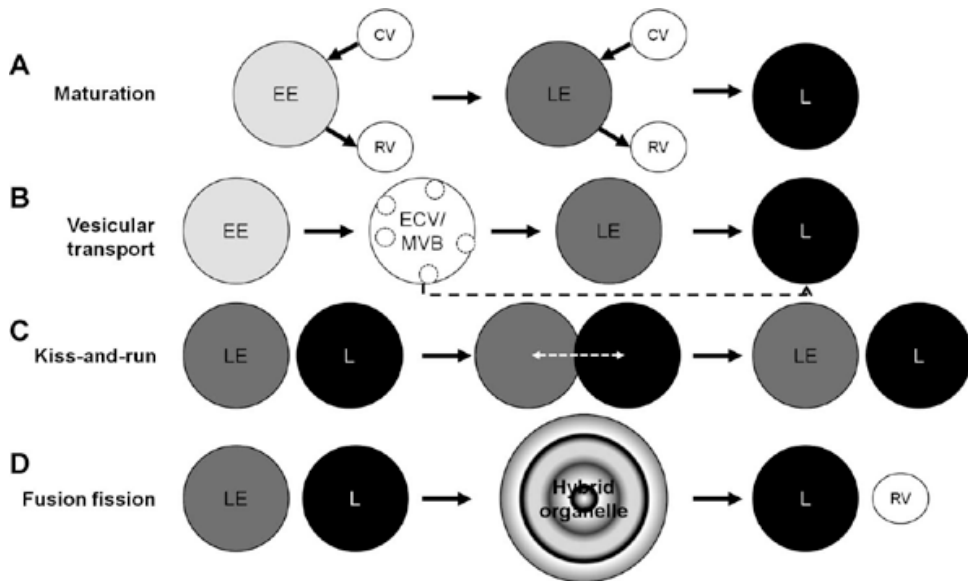
Figure 1: proposed models for biogenesis of lysosomes and how cargo is delivered to lysosomes. In the first step, endocytic cargo is internalised from the plasma membrane to early endosomes (EE) and then to late endosomes (LE). **A**. In the maturation model, endosomes mature into lysosomes (L) by gradual addition of lysosomal components. **B**. The second model postulates that EE, LE and lysosomes are separate and stable compartments and cargo is transferred through an endosomal carrier vesicle (ECV)/ multivesicular body (MVB). **C**. In the third model LE and lysosomes transiently fuse, exchange material and depart again. **D**. The fusion fission model is a mixture of kiss-and-run and direct fusion.
Abbreviations: CV, cargo vesicle; ECV, endosomal carrier vesicle; EE, early endosome; L, lysosome; LE, late endosome, MVB, multivesicular body; RV, recycling vesicle.
Adapted from Luzio *et al.*, 2007; Mullins and Bonifacino, 2001.

2.1.3 Lysosomal targeting of proteins

It is of great importance for the lysosomal function that lysosomal proteins are correctly targeted to their destination (Braulke and Bonifacino, 2009).

Soluble lysosomal proteins are synthesised as pre-pro-proteins with an N-terminal signal sequence (20-25 aa), which translocates the precursor protein into the lumen of the endoplasmic reticulum (ER) (Hasilik *et al.*, 2009). The signal peptides are removed and initial protein glycosylation takes place. The signal motif for N-glycosylation is Asn-X-Ser/Thr (x: any amino acid except proline) and is evolutionary conserved (Braulke and Bonifacino, 2009). The oligosaccharide branch $Glc_3Man_9(GlcNAc)_2$ is attached to the amino group of the asparagine side chain amide and processed and modified in the ER and Golgi apparatus. Mature glycopro-

teins can contain three different types of N-glycans: high mannose, complex and hybrid sugars. Another post-translational modification taking place in the Golgi complex is O-glycosylation, where sugar residues can be transferred to the OH-group of an amino acid side chain, mostly of serine or threonine. This type of glycosylation is a single monosaccharide transfer process initiated by specific GalNAc transferases (over 24 described). In contrast to N-glycosylation, O-glycosylation is not known to take place at a single consensus sequence. However, the various Gal-NAc transferases are highly specific and control the glycosylation process. Addition and modification of sugar residues also play an important role in protein folding, quality control and transport (Helenius and Aebi, 2001; Ruddock and Molinari, 2006).

In the Golgi apparatus, soluble lysosomal proteins usually undergo further modifications which are important for the lysosomal targeting (**Figure 2**). For example, most lysosomal hydrolases obtain mannose-6-phosphate (M6P) residues in their oligosaccharide chains by the sequential action of two enzymes, the GlcNac-1-phosphotransferase and N-acetylglucosamine-1-phosphodiester α-N-acetyl-glucosaminidase (uncovering enzyme, UCE) (Coutinho *et al.*, 2011). This is specific for N-glycans and has not been reported for O-glycans (Durand and Seta, 2000).

Soluble lysosomal proteins can later be recognised and bound by their M6P residues in the *trans*-Golgi network (TGN) by two type I transmembrane (single-pass transmembrane proteins with the N-terminus exposed to the extracellular or luminal space and the C-terminal part located on the cytoplasmic side) mannose-6-phosphate receptors of 46kD (MPR46, cation-dependent MPR, dimer) and 300kD (MPR300, cation-independent MPR, monomer) (**Figure 2**) (Ghosh *et al.*, 2003). The recognition of cargo (soluble lysosomal proteins) by the two MPRs is distinct but overlapping concerning intracellular targeting (Qian *et al.*, 2008). The soluble lysosomal protein-MPR complexes exit the TGN in clathrin coated vesicles associated either with GGA proteins (Golgi-localised, γ-ear-containing, Arf (ADP-ribosylation factor)-binding proteins) or AP-1 (adaptor protein-1), which recognise and select different cargoes and assist incorporation of targeting/fusion proteins to transport vesicles (Daboussi *et al.*, 2012). The transport vesicles then fuse with the endocytic system (**Figure 2**) (Doray *et al.*, 2002; Puertollano *et al.*, 2003). The low pH in endosomes leads to the dissociation of the soluble lysosomal protein-MPR complex and the receptors can be recycled and transferred back to the TGN *via* two predicted pathways involving a multiprotein complex (retromer) and Rab9-TIP47 (Rab9, small GTPase; TIP47, tail interacting protein of 47kD) (**Figure 2**). However, the involvement of TIP47 in the retrograde trafficking of MPRs from endosomes to the TGN is discussed controversially (Braulke and Bonifacino, 2009; Bulankina *et al.*, 2009). Lysosomes do not contain MPRs which differentiates these organelles from endosomal compartments. A fraction of the MPRs are located at the plasma mem-

brane, where they deliver enzymes from the extracellular space towards lysosomes (**Figure 2**) (Braulke and Bonifacino, 2009).

In the past years, more and more soluble lysosomal proteins have been described to traffic to lysosomes in an MPR-independent manner. One alternative route is *via* sortilin, a 95kD type I transmembrane protein, which is acting as a sorting receptor for sphingolipid activator proteins (SAPs), cathepsin D and H, acid sphingomyelinase and nerve growth factor precursor (pro-NGF) (Canuel *et al.*, 2008; Chen *et al.*, 2005; Lefrancois *et al.*, 2003; Ni and Morales, 2006). Sortilin is retrieved from endosomes to the TGN by the retrograde transport machinery (Kim *et al.*, 2010). Also, the lysosome-integral membrane protein 2 (LIMP-2), a type III (multipass) transmembrane protein, has been shown to mediate the lysosomal targeting of β-glucocerebrosidase (Reczek *et al.*, 2007). Whether LIMP-2 is recycled between endosomes and the TGN like MPRs is currently not known.

In contrast to soluble lysosomal proteins, lysosomal membrane proteins contain sorting signals in their sequence of the cytoplasmic tails and are independent from MPRs. The signals usually mediate both lysosomal destination and endocytosis from the extracellular space. Two pathways, the direct and indirect route, have been suggested for lysosomal membrane proteins (Braulke and Bonifacino, 2009). The direct route refers to trafficking of lysosomal membrane proteins from the TGN to early/late endosomes and then directly to lysosomes (**Figure 2**). In the indirect pathway, the lysosomal membrane proteins traffic constitutively from the TGN to the cell surface, and then are internalised into early endosomes and subsequently transported to late endosomes/lysosomes (**Figure 2**). Lipid modifications have also been suggested to contribute to lysosomal targeting (Braulke and Bonifacino, 2009). For example, C-terminal prenylation of the transmembrane NCL protein CLN3 has been shown to be involved in the sorting from endosomes to lysosomes (Storch *et al.*, 2007).

For internalised proteins, which are targeted to lysosomes for degradation, there are different routes to reach their destination. Some endocytosed proteins, like low-density lipoprotein, detach from their receptors in the early endosomes due to the acidic pH and are subsequently degraded in the lysosomes. The free receptors can then recycle back to the plasma membrane. Other ligands, like epidermal growth factor (EGF), do not dissociate from their receptors. The receptor-ligand-complexes, which are ubiquitinylated, are endocytosed from the cell surface and internalised into luminal vesicles. Subsequently, late endosomes which contain these vesicles fuse with lysosomes (Luzio *et al.*, 2007).
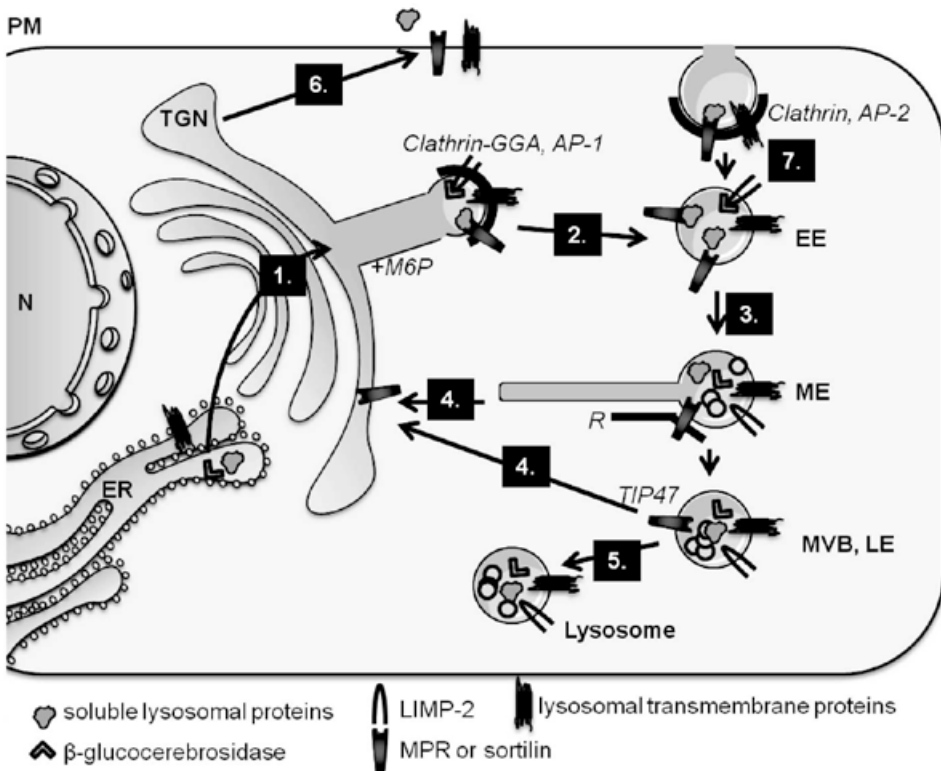
Figure 2: sorting of lysosomal proteins. **1.** Lysosomal proteins are synthesised at the endoplasmic reticulum (**ER**) and transported to the Golgi apparatus. At the *trans*-Golgi network (**TGN**), some soluble lysosomal proteins obtain a mannose-6-phosphate (**M6P**)-modification and bind to mannose-6-phosphate receptors (**MPRs**: MPR46 or MPR300), while others are recognised by sortilin or LIMP-2, like e.g. the β-glucocerebrosidase. **2.** The enzyme-receptor complexes and lysosomal transmembrane proteins concentrate in clathrin/GGA/AP-1-coated dense areas of the TGN, from where clathrin-coated carriers transport them to endosomes. **3.** Acidic pH induced dissociation of the enzyme-receptor complexes in the endosomes. **4.** MPR and sortilin are retrieved from endosomes to the TGN by retrograde transport machinery that, among various components, includes retromer and maybe **TIP47** (tail interacting protein of 47kD). **5**. LIMP-2 remains as a component of the lysosomal membrane. **6.** A part of the MPRs, and possibly some of the other receptors/lysosomal transmembrane proteins, are transferred from the TGN to the plasma membrane (**PM**). **7.** The cell surface located receptors deliver enzymes from the extracellular medium to endosomes and consequently to lysosomes.
AP-1/-2, adaptor-protein; **EE**, early endosome; **GGA**, Golgi-localised, γ-ear-containing, Arf (ADP-ribosylation factor)-binding proteins); **LE**, late endosome; **ME**, maturing endosome; **MVB**, multivesicular body; **N**, nucleus. Some elements of the figure were produced using Servier Medical Art (www.servier.com). Modified from Braulke and Bonifacino, 2009.

2.1.4 Lysosomal storage disorders

Lysosomal function and lysosomal turnover of macromolecules are of great importance for cellular homeostasis. Lysosomal storage disorders (LSDs) comprise a group of metabolic disorders caused by mutations in lysosomal enzymes, lysosomal integral membrane proteins, and proteins playing a role in the post-translational modification/trafficking to lysosomes (Schultz *et al.*, 2011). LSDs are recessively inherited, monogenic and the diseases are progressive (Futerman and van Meer, 2004). One hallmark of LSDs is the accumulation of un- or partially degraded catabolic macromolecules, leading to cellular dysfunction and consequently clinical symptoms. Age of onset and clinical manifestations can vary greatly among LSD patients with congenital, infantile, juvenile and adult forms, but most patients appear clinically normal at birth. Historically, the subtypes of LSDs were classified on the basis of the related accumulated substrate including sphingolipidoses, mucolipidoses, mucopolysaccharidoses (MPS), lipoprotein storage disorders, lysosomal transport defects, neuronal ceroid lipofuscinoses (NCLs) to list a few of them. Once the role of the affected protein is defined, the reason for the accumulated storage material often becomes apparent, e.g. defective proteins in Niemann-Pick type C1/2 (NPC1/2) diseases result in cholesterol accumulation as they are involved in cholesterol transport from the lysosome (Tang *et al.*, 2010). Another example are mucopolysaccharidoses (MPS), where proteoglycans are the accumulating storage material, being substrates for the defective proteins (Schultz *et al.*, 2011). In contrast, the cause of neuronal ceroid lipofuscinoses (NCLs) is still unclear, as it was not possible to find direct links between the defective proteins and the accumulating storage material as will be discussed in more detail later.

The clinical phenotype of LSD patients is very diverse ranging from severe neuropathology including dementia and seizures (NCLs) to symptoms confined to peripheral tissue (Fabry disease). The exact diagnosis can be challenging as genotype-phenotype correlations can be incorrect as in some cases the same genetic background and mutation can present a different clinical outcome. For example, only few Gaucher disease patients exhibit neurological symptoms which is surprising as this disease belongs to the sphingolipidoses and the levels of glycosphingolipids is enriched within the brain. The disease phenotype, severity and progression may be affected by secondary pathways, other genes or even environmental factors which complicate an exact prognosis and choice of treatment.

2.2 Key players of the central nervous system (CNS)

2.2.1 Cells of the CNS and their functions

The central nervous system is a very complex organ system containing a variety of cell types networking together to receive, process, integrate and react to the incoming information and to coordinate the activity of all body parts together with the peripheral nervous system (PNS). The so called neuronal doctrine was coined by Wilhelm von Waldeyer-Hartz based on the work of Ramón y Cajal and others in 1891 (Guillery, 2007). It places neurons at the centre of the CNS and considers glial cells such as oligodendrocytes, microglia and astrocytes to be passive supportive cells and not being involved in any informational exchange. The neuronal doctrine has been more and more questioned in the recent years (Bullock *et al.*, 2005). Today it is known that neurons are not the only functional units in the nervous system but glial cells, such as astrocytes, are also able to communicate with themselves and with neurons *via* gap junctions and chemical signalling (Giaume *et al.*, 2010).

2.2.1.1 Neurons

Neurons, also named nerve cells, are well studied cells, which transmit and process information by electrical and chemical signalling. They vary in shape, size and length, which determine their functions. In addition, their localisation within the brain is also important for their function. In general, neurons consist of a soma, the cell body; dendrites, which are thin structures that start from the soma and can be long and highly branched; and finally a single axon that extends from the soma at a special site, the axon hillock. There are many possible subclassifications of neurons based on the shape, number of neurites, dendrites, connections, axon length and neurotransmitters (described in Bear *et al.*, 2007).

During development of the mammalian CNS neural stem cells generate neurons and two types of glial cells (astrocytes and oligodendrocytes) (Gotz and Huttner, 2005), and the nervous system derives from the ectoderm, the outermost layer of the developing embryo. The neuroectoderm generates the neural plate along the dorsal side of the embryo, and the latter then creates a hollow neural tube. The telencephalon, the anterior part of the neural tube, proliferates and expands rapidly to finally give rise to the brain. Step by step the proliferating cells differentiate into neurons, astrocytes and oligodendrocytes, which then migrate to their final destinations. In the end, the neurons extend their axons and dendrites to setup the neuronal network. Neurogenesis has been shown to not be restricted to early development but also occurs in adult mammals, especially in the hippocampus and subventricular zone (Bonfanti and Peretto, 2011).

In neuronal signalling, dendrites receive signals which are integrated/processed at the soma. Further, the electric signal is transmitted down the axon to the presynaptic terminals, where the axon and dendrites of neighbour neurons form synapses. However, it has been reported that action potentials can also propagate back from the axon and soma regions to dendrites (Rapp *et al.*, 1996).

Most neurons in the nervous system form neuron-neuron connections and are therefore called interneurons. Neurons, which contain neurites in the sensory surfaces of the body, e.g. the skin or the retina of the eye, are classified as primary sensory neurons. Neurons that form synapses with muscles and transmit movement commands are called motor neurons (described in Bear *et al.*, 2007).

Neurons can also be classified on the basis of the cell shape and dendrites (described in Stahl, 2008): for instance, pyramidal cells have a soma shaped like a triangular pyramid, shorter basal dendrites, an extensively branched spiny apical dendrite and a single axon emerging from the basal pole of the soma (**Figure 3A**). Most neurons in the cerebral cortex are pyramidal neurons, especially in the prefrontal cortex. Purkinje cells are located in the cerebellum and contain extensive branched dendritic trees from an apical position and an axon from the basal poll (**Figure 3B**). Basket neurons have highly ramified dendritic trees, being cortical interneurons with axons spreading horizontally making inhibitory contacts with the soma of other neurons (**Figure 3C**). Double bouquet neurons are also inhibitory interneurons in the cortex, resembling two bouquets of flowers in appearance and contain a vertically oriented axon (**Figure 3D**). Spiny neurons have a long axon and dendrites pointing in all directions covered with numerous spines (**Figure 3E**). They are located in the striatum where they receive information from the cortex, thalamus and substantia nigra. Finally, chandelier neurons are named after their unique axonal structure resembling an old fashioned chandelier and are also inhibitory interneurons in the cortex (**Figure 3F**).

Further, neurons can be classified depending on the number of neurites as unipolar (one neurite), bipolar (two neurites) or multipolar (three or more; most neurons). Neurons with long axons extending from one part of the brain to another are projection neurons. Those with short axons, which do not extend the proximity of the soma are local circuit neurons. In addition, neurons can be classified based on their neurotransmitter chemistry, e.g. cholinergic (neurons that produce and release acetylcholine), noradrenergic (norepinephrine), glutamatergic (glutamate), GABAergic (GABA) and peptidergic (peptides) (described in Bear *et al.*, 2007).
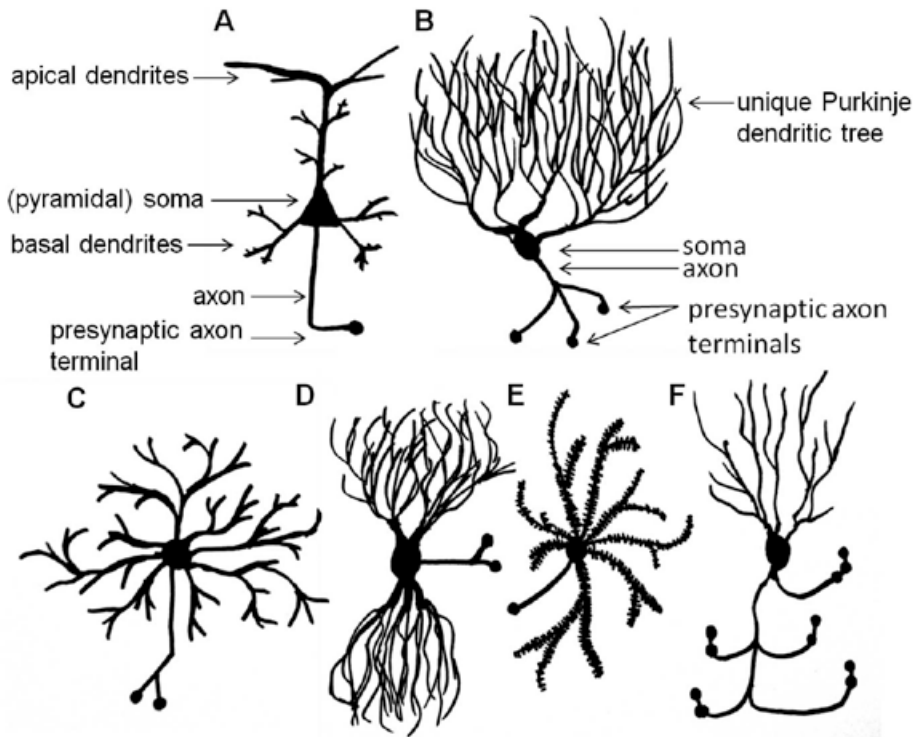
Figure 3: overview of some neurons types. (**A**) The soma of pyramidal cells is shaped like a pyramid. They have a branched spiny apical dendrite, shorter basal dendrites, and one axon. Pyramidal neurons constitute the majority of neurons in the cerebral cortex. (**B**) Cerebellar Purkinje cells have extensively ramified dendritic trees and a single axon. (**C**) Cortical basket neurons are inhibitory interneurons with widely ramified dendritic trees, which make many contacts with the soma of other neurons. (**D**) More cortical inhibitory interneurons are double bouquet cells. They look like two bouquets of flowers and contain a vertically oriented tight bundle of axons and innervate dendrites of other cortical neurons. (**E**) Spiny neurons have dendrites that radiate in all directions and are extensively covered with spines. They reside in the striatum and receive input from cortex, thalamus, and substantia nigra. Their axons are long and exit the striatum or return as recurrent collaterals to innervate adjacent spiny neurons. (**F**) Other inhibitory cortical interneurons are chandelier neurons. Their axons look like an old-fashioned chandelier with axon terminals shaped like vertically oriented cartridges. They inhibit pyramidal neuron. Modified from Stahl *et al.*, 2008.

2.2.1.2 Oligodendrocytes

The efficiency and speed of action potentials depend on the integrity of axons, which in turn is dependent on a specialised structure called myelin. Myelin is produced by oligodendrocytes, which wrap spirals of membrane around axons of multiple neurons in the CNS. Oligodendrocyte biology, myelination and maintenance of myelin sheaths are very complex and highly regulated processes (Simons and Trot-

ter, 2007). During development, oligodendrocyte precursor cells (OPCs) are generated at multiple foci along the neural tube and divide and migrate throughout the CNS. The migration of OPCs is mediated *via* contacts with extracellular matrix, cell surface molecules and secreted molecules. After reaching their final destination most oligodendrocytes differentiate into mature myelin-producing oligodendrocytes, going through morphological changes and formation of an extensive network of branching processes (**Figure 4**) (Zhang, 2001). However, some OPCs persist into adulthood.
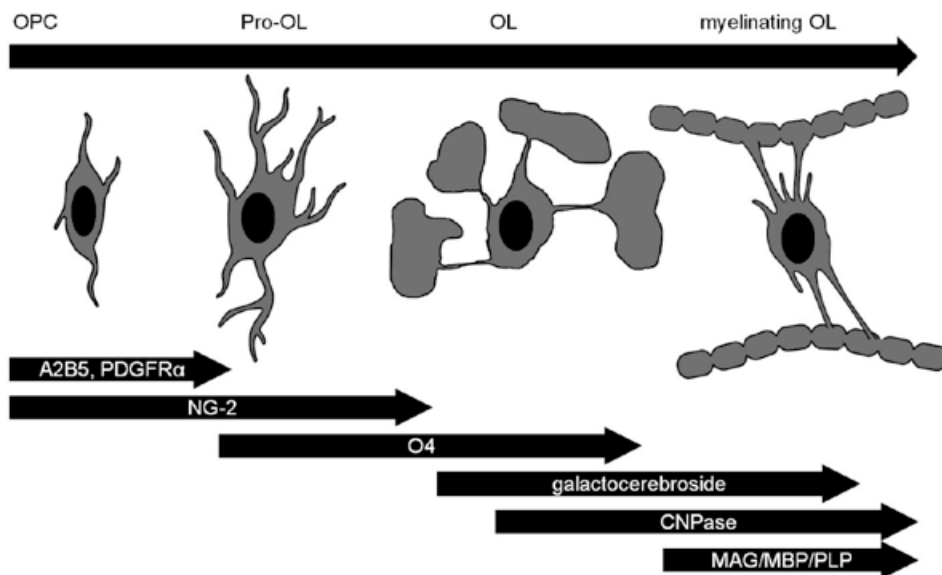
Figure 4: differentiation of oligodendrocytes. The oligodendrocyte differentiation is a gradual process of morphological changes. The transformation starts from a bipolar oligodendrocyte precursor cell (OPC), to an immature pro-oligodendrocyte (pro-OL) with multiple processes, to a mature oligodendrocyte (OL) with membrane-sheaths and last to a myelinating OL which can extend its processes to many axons. These transformation steps can be followed with molecular markers which are sequentially expressed: A2B5 antigen, platelet derived growth factor receptor α (PDGFRα) and chondroitin sulphate proteoglycan (NG-2) are good OPC and pro-OL markers; O4 antigen marks pro-OLs and mature OLs; galactocerebroside, 2',3'-cyclic nucleotide 3'-phosphohydrolase (CNPase) marks mature OLs; myelin associated glycoprotein (MAG), myelin basic protein (MBP) and proteolipid protein (PLP) are expressed in myelinating oligodendrocytes. Some elements of the figure were produced using Servier Medical Art (www.servier.com). Modified from Zhang, 2001.

Myelin of peripheral nerves consists of approximately 70-85% lipids and 15-30% proteins (Norton, 1981). There are no myelin-specific lipids but the glycosphingolipid galactosylceramide, also known as galactocerebroside, is the most characteristic for myelin (Aggarwal *et al.*, 2011). In the adult brain the galactosylceramide

content is proportional to the concentration of myelin. Other major lipids of myelin are cholesterol, sphingomyelin and ethanolamine-containing plasmalogens (Aggarwal *et al.*, 2011). Also the fatty acid composition of many lipids is characteristic in myelin. The proteolipid protein (PLP) and the myelin basic proteins (MBP) are the major protein components of the myelin sheath. Other less abundant proteins are e.g. the 2′-3′-cyclic nucleotide 3′-phosphohydrolase (CNPase), the myelin-associated glycoprotein (MAG) and the myelin-oligodendrocyte glycoprotein (MOG) (Baumann and Pham-Dinh, 2001). MBP is found throughout the thick membraneous processes and has been described to be a useful marker to examine myelination defects and differentiation of oligodendrocytes *in vivo* (Vincze *et al.*, 2008). Furthermore, MBP and CNPase have been predicted to participate in the formation of myelin membranes by interactions with the cytoskeleton. MBP is thought to serve as a microtubule-stabilising protein (Galiano *et al.*, 2006) and CNPase is suggested to induce microtubule assembly and process outgrowth *via* copolymerisation with tubulin (Lee *et al.*, 2005). CNPase is absent in compact myelin but is highly expressed at the cytoplasmic laminae of plasma membranes of myelinating oligodendrocytes and is connected to the cytoskeleton.

2.2.1.3 Microglia

Until 1991, the very existence of microglia was under debate. A leading textbook of neuropathology doubted this and suggested to abandon the term microglia (Dolman, 1991). About the same time the idea of a "microglial immune network" in the CNS was first proposed (Graeber and Streit, 1990). Nowadays, microglia are considered to be a key element in the CNS being involved in the brain and spinal cords innate immune system (Graeber and Streit, 2010). In contrast to other glial cells like astrocytes, oligodendrocytes and ependymal cells which are derived from the neuroepithilium forming the neuronal tube, microglial cells are of mesodermal origin (Chan *et al.*, 2007; Pont-Lezica *et al.*, 2011).

In the healthy brain microglia are widely distributed throughout all regions and reside closely with neurons and astrocytes (Lawson *et al.*, 1990; Nimmerjahn *et al.*, 2005; Tremblay *et al.*, 2010; Wake *et al.*, 2009). Microglia express receptors for all known neurotransmitters and are able to synthesise many neuroactive molecules (Kettenmann *et al.*, 2011; Lucin and Wyss-Coray, 2009).

Under healthy conditions microglia have a ramified/branched appearance with a small cell soma. Microglia with this appearance are also called resting microglia, which may be misleading as they are constantly and actively scanning the environment within the CNS with their ramified processes (Nimmerjahn *et al.*, 2005). Microglial cells have a very plastic phenotype and can change their morphological and functional spectrum depending on their so called state of activation (**Figure 5**).

Under certain conditions microglia have the capability to transform into macrophages but their functions differ from macrophages in other organs (Graeber and Streit, 2010).
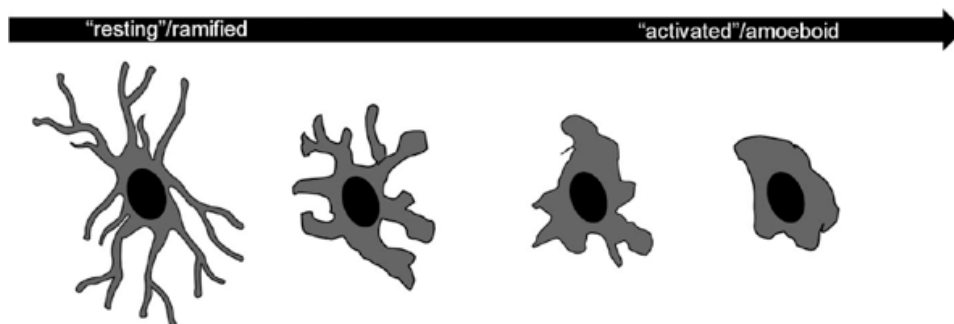
Figure 5: schematic illustration of the morphological change from resting ramified microglia towards activated microglia. Some elements of the figure were produced using Servier Medical Art (www.servier.com).

Microglia are suggested to have several functional phenotypes. In the healthy brain microglial cells do not remain silent but show high dynamic motility. During development neuronal synapses are being extensively formed, remodelled and a large number of immature synapses are again eliminated by a process called synaptic pruning (Hua and Smith, 2004). Recent *in vivo* imaging and high resolution EM studies have shown that microglia actively and transiently connect to dendritic spines in healthy mouse cortex (Tremblay *et al.*, 2010; Wake *et al.*, 2009). Therefore, microglia are suggested to monitor the functional status of synapses and thus the CNS circuitry (Tremblay *et al.*, 2011). In the adult brain, microglia can detect dysfunctional synapses and are also involved in a phenomenon called postlesional synaptic stripping. In this process, microglial cells remove branches from nerves near damaged tissue to promote neurogenesis and remapping of the CNS circuitry (Trapp *et al.*, 2007). Also, under disease conditions and in the removal of myelin debris they serve as macrophages and antigen-presenting cells of the brain (Graeber, 2010).

Further, microglia are suggested to play a role in neurotransmission and may act as an upstream partner for astrocytes (Pascual *et al.*, 2012; Tremblay *et al.*, 2011). It has been shown that activation of microglia involves ATP and the purinergic receptor $P2Y_1$ (Pascual *et al.*, 2012). This receptor is only expressed in neurons and astrocytes. Microglial activation results in microglial ATP production, which in turn activates astrocytic ATP production and leads to a $P2Y_1$ receptor mediated glutamate release (Pascual *et al.*, 2012; Tremblay *et al.*, 2011). Possible downstream effects might be glutamate binding to neuronal receptors (e.g. the metabotropic glutamate

receptor 5 (mGluR5)), which in turn then increases the excitatory postsynaptic current frequency (Pascual *et al.*, 2012; Tremblay *et al.*, 2011).

Microglia can be visualised in brain tissue and cell cultures. The number of markers for the identification of all microglial activation stages is still growing, but a molecular marker that does not also recognise peripheral macrophages remains unknown. Anyhow, the markers are cell-type specific and do not label other glia cell types or neurons in the CNS. *Griffonia simplicifolia* isolectin B$_4$ (ILB4) or tomato lectin has been proven to be useful in lectin-histochemical/antibody-based experiments (Kettenmann *et al.*, 2011). Blood vessels can be stained with this method as well but they can be easily distinguished by morphological criteria under the microscope. Other established antibody markers for microglia are e.g. CD11b (CD18, complement receptor 3), IBA-1 (ionised calcium adaptor protein 1), CD45 (leukocyte common antigen), CD68 (macrosialin), CD163 (scavenger receptor M130), CD169 (sialoadhesin, siglec-1), GLUT5 (glucose transporter 5) and F4/80 antigen (Kettenmann *et al.*, 2011). The expression levels of some of the molecules correlate with the state of microglial activation e.g. IBA-1, CD11b and CD68.

2.2.1.4 Astrocytes

The most abundant cells in the mammalian brain are astrocytes, named after their stellate shape, which are involved in various processes in the CNS. Astrocytes express high amounts of intermediate filaments (if), which build the cytoskeleton. The glial fibrillary acidic protein (GFAP) and vimentin are the two main types of IF proteins in astrocytes (Verkhratsky and Butt, 2007). GFAP is used as marker to detect astrocytes. Its expression levels are especially increased in reactive astrocytosis. Interestingly, in healthy adult mammals the GFAP expression varies within types of astrocyte as only 15-20% express it in the cortex and hippocampus, but almost all Bergmann glial cells in the cerebellum express GFAP (Verkhratsky and Butt, 2007). It has been shown that GFAP is not the best marker to study astrocyte morphology itself as it only stains the primary branches, which only represent about 15% of the total volume of an astrocytic cell (Bushong *et al.*, 2002). Remarkably, one astrocytic cell in rodents is capable to cover a spatial domain up to 80.000 μm^3, wrap multiple neuronal somata, associate with up to 600 neuronal dendrites, and contact up to 100.000 individual synapses (Freeman, 2010). These numbers increase considerably in humans. The volume of one astrocyte is almost 30 times higher than in rodents and can contact about 2.000.000 synapses (Freeman, 2010).

Classification of astrocytes is based on their morphology. The largest group, stellate-shaped astrocytes, include protoplasmic (grey matter) and fibrous (white matter) astrocytes (Kimelberg, 2010; Verkhratsky and Butt, 2007). Another large group of astrocytes are radial glia, bipolar cells with elongated processes and an ovoid cell body. Radial glia are common in the developing brain and are the first cells gener-

ated from neuronal progenitors. Later, this cell type disappears from many brain regions and converts to stellate-shaped astrocytes. In adults, radial glia are still present in the retina (Müller glia) and cerebellum (Bergmann glia) (Reichenbach *et al.*, 2010). Furthermore, smaller populations of astrocytes have been described, being localised to specific brain regions, called vellate (cerebellum), interlaminar (primate cortex), tanycytes (periventricular organs, hypophysis, raphe part of the spinal cord), pituicytes (neurohypophyse), perivascular and marginal astrocytes (Verkhratsky and Butt, 2007). Moreover, astrocytes that surround the ventricles or the subretinal regions are called ependymocytes, choroid plexus and retinal pigment epithelial cells (Verkhratsky and Butt, 2007).

Astrocytes in general serve developmental functions such as neuronal path finding and regulation of synaptogenesis (Slezak and Pfrieger, 2003). They are substantial for the formation and regulation of the blood-brain barrier (BBB) (Koehler *et al.*, 2009) and provide various nutrient and metabolic substrates for neurons. Astrocytes also participate in the control of ion concentrations and the pH of the extracellular spaces in the CNS (Maragakis and Rothstein, 2006), and are important for synaptic function and neurotransmitter synthesis (Perea *et al.*, 2009). They contain processes with end-feet which contact the brain vasculature and cover neuronal synapses and hence play a central role in modulating neuronal activity and the cerebral blood flow. Additionally, the cells are excitable, which is detectable by increased Ca^{2+} concentrations in the cytosol due to mobilisation of Ca^{2+} from the ER. The increased Ca^{2+} level can create a signal which can occur spontaneously in the absence of neuronal activity or be induced by neurotransmitters (Perea and Araque, 2005). The manifold functions of these extraordinary cells make it clear that dysfunctions of these cells can lead to drastic consequences.

2.2.2 Pathophysiology of neurons and glia in neurodegeneration

Neurodegeneration is characterised by progressive loss of neuron structure and function. This can be caused by defects in neurons themselves or can be a secondary effect due to dysfunctional glial cells. CNS insults lead to specific reactions of glial cells, known as reactive gliosis. These reactions include activation of microglia, reactive astrocytosis, and disturbed oligodendrocyte biology which are all fundamental in the progression of neural pathology.

2.2.2.1 Neurodegeneration

The hallmark of neurodegenerative diseases is the progressive loss of neurons. In most cases there is no cure, only symptoms can be treated to provide partial relief for the patients. Treatment of patients is often delayed due to the fact that many cells are already dead before symptoms occur. Neuronal activity can be disrupted at many stages: molecular pathways can be interrupted (Bossy-Wetzel *et al.*, 2004), synapses can be affected (Shankar and Walsh, 2009), neuronal subpopulations and local circuits in certain brain regions or even higher order neuronal networks can be damaged (Palop *et al.*, 2006).

Neurodegenerative diseases are often associated with intracellular and/or extracellular accumulation of misfolded proteins, like Creutzfeldt-Jacob, Parkinson's and Alzheimer's diseases (PD and AD). However, the underlying mechanisms why neurons die and the early steps of the disease are complex and poorly understood (Nakamura and Lipton, 2009). For instance, in PD patients accumulations of α-synuclein and synphilin aggregates are found, called Lewy bodies. In the brain of AD patients intracellular neurofibrillary tangles, containing hyperphosphorylated tau, and extracellular β-amyloid plaques are found (Nakamura and Lipton, 2009). Misfolded proteins cause continuous ER-stress, continued by disturbances in the protein folding and clearance machinery (Mukherjee *et al.*, 2011). ER-stress leads to the activation of the unfolded protein response (UPR). The purpose of UPR is the restoration of ER function. In order to achieve this, global protein synthesis is shut down to reduce the load and proteins that are important for the degradation of misfolded proteins (mutant/unfolded) are upregulated. However, if the ER function is too severely affected, cell death pathways are activated. ER-stress also leads to disruption of calcium homeostasis (Mukherjee *et al.*, 2011). This is deleterious especially for neurons as calcium is important in neuronal activity. Ca^{2+} acts as second messenger in various signaling pathways and is stored in the ER. Intracellular gradients are normally maintained by Ca^{2+} channels and ATP-driven Ca^{2+} pumps. In neurodegenerative diseases increased levels of Ca^{2+} in the cytoplasm have been reported, leading to disturbed intracellular signalling (Mukherjee *et al.*, 2011).

To study basic mechanisms of neurodegeneration inherited monogenetic neurode-generative disorders can serve as helpful models as the defective gene is usually known and subsequent pathways which lead to neurodegeneration can be analysed in detail.

2.2.2.2 Oligodendrocyte pathology

Oligodendrocytes are responsible for the myelination integrity and function of neu-rons. Disturbances in oligodendrocyte biology are associated with major diseases of the CNS and often have an impact on white matter structures. CNS white matter can be affected in many ways e.g. by disturbed myelination, loss of the myelin sheaths, gliosis, axonal damage which in turn has an impact on the myelin integrity or by permanent myelin deficiency. Some diseases with myelin defects due to mutations in myelin proteins are muscular dystrophies, mitochondrial or peroxisomal diseases, and many more.

Multiple sclerosis (MS) is an example for an immune-mediated demyelinating dis-ease. The trigger and primary cause of MS remains elusive. Genetic predisposition and environmental factors are suggested to be involved in the disease (Compston and Coles, 2008). Genetic involvement has been shown due to the high disease con-cordance in monozygotic twins (Handunnetthi *et al.*, 2010). However, it is not a single gene defect which leads to the disease. Involvement of environmental factors is supported due to the fact that MS is more frequent in northern than in southern regions in the world (Compston and Coles, 2008). In MS, lymphocytes and mono-cytes cross the blood-brain-barrier (BBB), and oligodendrocytes/myelin sheaths are destroyed due to inflammation, but interestingly rarely neurons directly (Nave, 2008). Another example where myelination is affected are leukodystrophies, a group of rare inherited dys-/demyelination diseases (Nave, 2008). In this case oligodendro-cytes are incapable to correctly assemble or maintain myelin and these patients usu-ally suffer from a severe delay in motor and cognitive development.

2.2.2.3 Microglial activation

Microglia serve protective and pathogenic functions. The recent view on microglia in disease suggests rather an active protective than an aggressive role (Graeber and Streit, 2010). Nevertheless, it is currently not clear how much chronic forms of in-flammation contribute to the pathogenesis in neurodegenerative diseases in general (Saijo and Glass, 2011). Microglia respond to inflammatory or injurious stimuli in the CNS in a pre-programmed manner that is designed to kill and to set the stage for repair and resolution of the disease. Activated microglia can be distinguished by combined immunophenotypic and morphological changes. They produce many pro-inflammatory mediators like reactive oxygen species (ROS), cytokines and chemokines, which are involved in the pathogen clearance (Saijo and Glass, 2011).

On the other hand, prolonged and excessive microglial activation can lead to pathological inflammation that may contribute to neurodegenerative diseases (Glass *et al.*, 2010; Perry *et al.*, 2010). Microglia are suggested to take part in the adaptive immunity by expressing MHC class II (major histocompatibility) in the active state, which in turn activates native T cells to differentiate into effector T cells but *in vivo* this hypothesis has not been proven yet (Saijo and Glass, 2011).

2.2.2.4 Reactive astrocytosis

All kinds of brain insults cause a complex astroglial response, which can be observed as astrocyte hypertrophy and proliferation. This is a defensive brain reaction with the goal to isolate the damaged area from the rest of the tissue, to rebuild the BBB and to help to remodel brain circuits surrounding the damaged areas. Hallmarks of reactive astrocytes are hypertrophy and a significant increase in the cytoskeleton production: the protein synthesis of intermediate filaments such as GFAP and vimentin is highly upregulated. GFAP and vimentin form the cytoskeleton together with actin and microtubules. It has also been reported that the crosstalk between activated microglia and astrocytes can amplify inflammatory responses and contribute to the release of neurotoxic factors (Saijo and Glass, 2011). Epilepsies are a group of disorders which are characterised by periodic seizures. Astrocytes are suggested to play a role in seizure generation and spread within the CNS as these cells are involved in the control of neuronal firing (Seifert *et al.*, 2010; Seifert and Steinhauser, 2011). In principal, a neuron operates by receiving signals from other neurons *via* its synapses. The combination of the incoming signals leads to an excess of a threshold, which in turn results in so called neuronal firing, meaning that the neuron is sending further signals to connective neurons. These signals can be either excitatory or inhibitory to a neuron. Astrocytes express transporters that take up glutamate to terminate the action of this neurotransmitter at synapses in the CNS (Seifert *et al.*, 2010). Changes in the activity of these transporters have been shown to be characteristic in temporal lobe epilepsy (TLE) and other brain disorders (Seifert *et al.*, 2010). Further, excessive extracellular glutamate has been detected in human epileptogenic tissue and was reported to stimulate recurrent seizures and neuronal cell death (Seifert *et al.*, 2010). Astrocytes are involved in the integrity. Therefore, it is logical that defects in the BBB has been suggested to play a role in seizure generation (Seifert *et al.*, 2010).

Although little is understood about the interplay and molecular pathways between neurons and glia in disease, it becomes more and more apparent that glial activation is not always bad. Astrocytes and microglia are important for the environmental homeostasis of neurons, clearance of debris and in general fulfil rather neuroprotective than destructive roles in the CNS.

2.3 Lipid metabolism

2.3.1 Cholesterol homeostasis and transport

Cholesterol and phospholipids are essential components of mammalian membranes. In mouse and human about one quarter of the total amount of cholesterol is found in the CNS. Mammals are able to absorb lipids *via* food intake but as basically every cell is also capable to synthesise cholesterol *de novo* from acetyl-CoA (AcCoA) this is not necessarily required (Dietschy, 2009) (**Figure 6**). Cholesterol transport is a highly regulated process. Cholesterol from food intake is absorbed in the intestinal lumen at the microvillus border *via* Niemann Pick type C like protein (NPC1L1) into the cytosolic compartment (Dietschy, 2009) (**Figure 6**). It is then esterified into cholesteryl ester (CE) and associated with chylomicron particles. Systemic tissues can produce cholesterol *de novo* and take up lipids from plasma lipoprotein complexes, chylomicrons, low-density or very-low-density lipoproteins (LDL, VLDL) (**Figure 6**). These complexes transport lipids from one organ to another and consequently provide peripheral cells with membrane components and precursors to generate steroids. High density lipoprotein (HDL) is important for reverse cholesterol transport from peripheral tissues to the liver since the liver is the only organ actively excreting cholesterol (**Figure 6**). In general, lipoprotein particles consist of triacylglycerols, unesterified and esterified cholesterol, phospholipids and apolipoproteins and their density decreases the more neutral lipids they contain. Lipoprotein particles in the blood are spherical and among the major structural apo lipoproteins apoA-I is linked to HDL, apoB-100 to LDL and VLDL and apoE to HDL and VLDL (Mahley *et al.*, 1984).

Liver and other tissues express the low density lipoprotein receptor (LDLR), which plays a key role in receptor-mediated endocytosis of cholesterol and CE that are associated with lipoproteins containing apoB-100 or apoE (**Figure 6**). Further, liver and endocrine glands are the main tissues expressing the transporter scavenger receptor class B type I (SR-BI). SR-BI selectively facilitates the uptake of CE from HDL into the cytosolic cell compartments (**Figure 6**). Also, LDL can bind to the SR-BI receptor in adrenocortical glands where corticoid biosynthesis takes place. Cholesterol and CE that were taken up *via* the LDLR or bulk-phase endocytosis pass through the late endosomal/lysosomal compartment of cells and sterols incorporated *via* SR-BI and NPC1L1 are moved directly into the metabolically active pool in the cytosol (Liu *et al.*, 2007; Xie *et al.*, 2000) (**Figure 6**). Niemann Pick type C1 (NPC1) is another sterol transporter which acts together with Niemann Pick type C2 (NPC2). CEs are hydrolysed in late endosomes/lysosomes by an enzyme called lysosomal acid lipase (LAL) and free cholesterol is transferred to NPC2, and further to NPC1. Cholesterol is transported to the luminal leaflet of the vesicles, flips to the cytosolic side and can be transported by cytosolic carriers to other destinations (Kwon *et al.*,

2009). Further, NPC1 plays a role in transporting cholesterol from the late endosomal/lysosomal compartment to the cytosolic metabolic active pool (Dietschy, 2009) (**Figure 6**). The metabolically active pool in the cytosol supports continuous turnover of cholesterol in the plasma membrane (Aqul *et al.*, 2011) (**Figure 6**). Lecithin:cholesterol acyltransferase (LCAT) in circulation is involved in the cholesterol conversion to CE and is essential for the formation of spherical HDL. Also in the brain LCAT is present, though at lower concentrations and is mainly expressed by astrocytes (Hirsch-Reinshagen *et al.*, 2009).

ABC (ATP-binding cassette) transporters are involved in the transport of lipids to the cell surface and facilitate further lipidation of HDL particles and subsequent reverse cholesterol transport (RCT) to the liver. These include especially ABCA1 and ABCG1 and 4 (van der Velde, 2010). Excessive cholesterol is either directly excreted in the feces or first converted to bile acids and subsequently excreted (Dietschy, 2009) (**Figure 6**). Reverse cholesterol transport from peripheral cells and the CNS to the liver for excretion or bile acid synthesis is mediated *via* circulating HDL (Ikonen, 2008).

In the CNS, lipids fulfil a wide range of physiological functions such as myelination, neurite outgrowth (Vance *et al.*, 2005), synaptogenesis (Slezak and Pfrieger, 2003) and can act as signalling molecules (Bazan, 2003). The unique composition of the brain and relative isolation from the rest of the body system affect the lipid composition in the CNS, which differs from the rest of the body. One difference is the distribution of cholesterol in the brain, where most of it is located in myelin formed by oligodendrocytes. Interestingly, cholesterol uptake across the blood-brain barrier (BBB) is not detectable neither in newborn nor adult rodents or humans and therefore the plasma cholesterol supplies are blocked by the BBB (Hayashi, 2011). Hence, high rates of *de novo* cholesterol synthesis in neurons and glial cells e.g. astrocytes provide the essential amounts of cholesterol during development. The rates of cholesterol synthesis are in line with myelin production, being highest during the first four weeks after birth in mice (Hayashi, 2011). Oligodendrocytes produce the myelin sheaths, which are rich in cholesterol, galactosphingolipids and saturated long-chain fatty acids. Surrounding the axons with these thick hydrophobic membranes increases the velocity of electrical conduction along neurons (Dietschy and Turley, 2004). In adult rodents and humans the cholesterol synthesis still continues, but at lower rates (Dietschy, 2009). After the myelination process of oligodendrocytes, astrocytes are the key players for cholesterol synthesis and supply for neurons (Hayashi, 2011) (**Figure 6**). Neurons do not synthesise sufficient amounts of cholesterol and depend on external supply by e.g. astrocytes (Nieweg *et al.*, 2009).

In the brain the main lipoprotein particles are called HDL-like particles and are disc-oidal and smaller than in plasma (Koch *et al.*, 2001; Legleiter *et al.*, 2004). Several of the proteins involved in cholesterol transport in the circulation are also present in the cerebrospinal fluid (CSF) of the CNS. The major CNS apolipoprotein is apoE and plays the central role in lipid metabolism in the brain with a concentration of 5-15% of that in plasma (Hayashi, 2011). Other apo lipoproteins such as apoA-I, A-II, CI-III, D and J are also present in the CSF (Hayashi, 2011). It has been shown that mouse primary astrocyte cultures secrete apoE, J and D but not apoA-I (DeMattos *et al.*, 2001). ApoA-I, the major HDL apolipoprotein in the blood is not synthesised in the brain and thought to be either able to cross the BBB (Kratzer *et al.*, 2007) or may be synthesised by capillary endothelial cells (Panzenboeck *et al.*, 2002).

Under normal conditions, HDL-like particles are secreted mostly from astrocytes and microglia, and can be secreted from neurons under certain conditions (Hayashi, 2011). For example, apoE synthesis is known to take place in astrocytes (Pitas *et al.*, 1987), microglia (Nakai *et al.*, 1996) and at low levels in neurons (Brecht *et al.*, 2004). Glial cells secrete apoE, phospholipids and cholesterol which form HDL-like particles. These particles can then bind to apoE receptors on neurons (**Figure 6**). Neurons express several members of lipoprotein receptors from the large class of the LDL receptor superfamily (LDLR), which bind to apoE and are involved in choles-terol transport amongst other functions (Hayashi, 2011; Vance and Hayashi, 2010) (**Figure 6**). Neurons have been reported to express the LDL receptor, the LDL re-ceptor related (LRP1), the VLDL receptor and the apoE receptor-2 (apoER2). Many are also expressed in microglia, astrocytes and oligodendrocytes (Vance and Haya-shi, 2010).

In the CNS the ABC transporters are key players in the transport of lipids to the cell surface and facilitate the lipidation to lipoparticles, especially ABCA1, ABCA2, ABCG1 and ABCG4 (Kim *et al.*, 2008). The plasma membrane ABCA1 transporter is important for the phospholipid and cholesterol efflux from neurons to apoE. The endo/lysosomal ABCA2 mediates intracellular sphingolipid transport and myelin maturation and is highly expressed in oligodendrocytes. The vesicular ABCG1/4 transporters mediate intracellular cholesterol transport and efflux in neurons and astrocytes. ABCG1 is also highly expressed in microglia (Kim *et al.*, 2008). The sterol synthesis is balanced by metabolising excessive cholesterol to 24(S)-hydroxycholesterol, which is able to cross the BBB and thereby is eliminated from the CNS (Lutjohann *et al.*, 1996) (**Figure 6**).
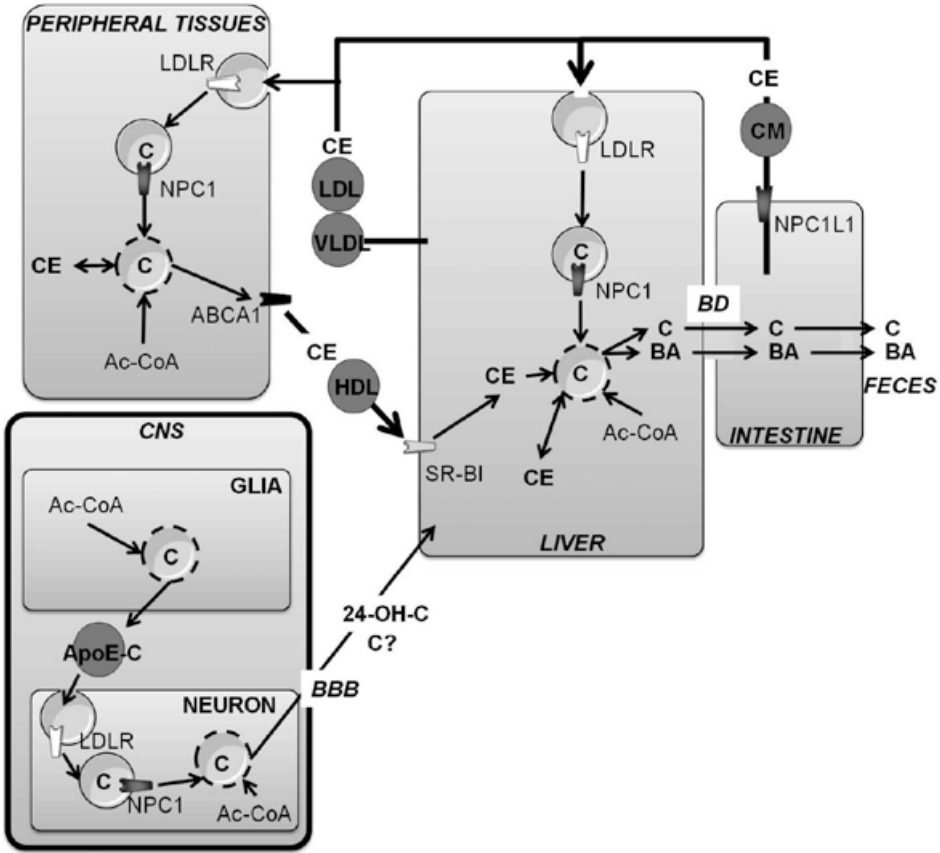
Figure 6: simplified scheme of the cholesterol flow through the major tissue compartments. The body is divided into four tissue compartments intestine, liver, central nervous system (CNS) and remaining peripheral tissues. The thick black arrows represent the cholesterol flow through plasma carried in CM, VLDL/LDL and HDL. The specific cholesterol transporters LDLR (white), NPC1 (dark grey), ABCA1 (black), SR-BI (light grey), and NPC1L1 (grey) are shown. Two intracellular cholesterol pools are indicated within each compartment: one is located in the late endosomal/lysosomal compartment (solid circle) and the other is the metabolically active pool of unesterified cholesterol in the membranes of the cytosolic compartment (dashed circle). Cholesterol transport from the lysosomal to the metabolically active pool requires NPC1. NPC2 (not shown), acts together with NPC1 to promote cholesterol flow out of the lysosome. ApoE is expressed in astrocytes and assembled with unesterified cholesterol (C) in order to build apoE lipoproteins (apoE-C). ApoE-C binds to receptors on the cell surface of neurons. In the CNS, excessive cholesterol is oxidised to 24-hydroxycholesterol (24-OH chol). 24-OH chol is then transported *via* the blood-brain-barrier (BBB) and blood plasma to the liver, where it is excreted into bile for elimination. Abbreviations: Ac-CoA, Acetyl-CoA; BBB, blood brain barrier; BD, bile duct; C, unesterified cholesterol; CE, cholesteryl ester; BA, bile acid; 24-OH-C, hydroxylated cholesterol. Modified from Dietschy, 2009.

2.3.2 Sphingolipid metabolism

Sphingolipids present essential components of cell membranes and comprise a large family of glycolipids and phospholipids sharing a sphingoid base backbone. Synthesis takes place in the ER and Golgi compartment and the sphingolipids can be subsequently delivered to the plasma membrane (Chatterjee, 1998; Simons and Vaz, 2004). Ceramide is a component of most sphingolipids and acts as an anchor for lipid-bound carbohydrates (Kolter and Sandhoff, 1999). Sphingolipids that do not contain carbohydrate residues also exist, like ceramide itself, sphingomyelin or sphingolipid metabolism intermediates such as sphingosine (Young *et al.*, 2012). Lactosylceramide is the common precursor of various glycosphingolipids (GSLs) and synthesised by the enzyme galactosyltransferase I, which transfers a galactose moiety from UDPgalactose to glucosylceramide (Kolter and Sandhoff, 1999). Sugar residues are added stepwise in the Golgi compartment by membrane bound glycosyltransferases (Kolter and Sandhoff, 1999). In the plasma membrane, sphingolipids, especially sphingomyelin, are suggested to concentrate in pre-existing microdomains called lipid rafts (Kolter and Sandhoff, 2006). Lipid rafts are reported to contain higher levels of glycosylphosphatidylinositol-anchored proteins, sphingomyelin, and cholesterol (Kolter and Sandhoff, 2006). Further, cholesterol/sterols and sphingolipids have been reported to interact and to be co-regulated (Mukherjee and Maxfield, 2004; Puri *et al.*, 2003). Sphingolipids have been shown to play a role in a wide range of functions like in cell recognition, apoptosis, cell growth, proliferation, inflammation, autophagy and differentiation (Bartke and Hannun, 2009).

2.3.3 Cholesterol and sphingolipids in neurodegeneration

The brain consists of ~2% cholesterol that is mainly generated *via de novo* synthesis (Zipp *et al.*, 2007). Hence, factors affecting cholesterol metabolism could have a significant impact on CNS function. Defective cholesterol metabolism has been linked to several neurological disorders e.g. AD, NPC disease and NCLs (the latter to be discussed later in more details). ApoJ and apoE isoforms, particularly *APOε4* allele, have been connected to AD as genetic risk factors, but the underlying mechanisms triggering the disease have not been clarified (Vance and Hayashi, 2010). Extracellular β-amyloid plaques and intracellular neurofibrillary tangles are characteristic for AD. ApoE has been shown to co-localise with these hallmarks in AD patients (Namba *et al.*, 1991). Recently, a study has shown that induced expression of apoE increased the clearance of β-amyloid plaques in AD mouse models (Cramer *et al.*, 2012). Another example, where cholesterol trafficking is affected, is NPC disease belonging to the group of lysosomal storage disorders. Mutations in either NPC1 or NPC2 cause accumulation of the lipids cholesterol, sphingomyelin (SM), multiple GSLs and the catabolic product of sphingolipids sphingosine in lysosomal

storage compartments (Lloyd-Evans *et al.*, 2008). NPC1 and NPC2 are involved in cholesterol efflux from late endosomes/lysosomes (Rosenbaum and Maxfield, 2011) (**see 2.3.1**). Sphingolipidoses comprise a group of inherited diseases and belong to the LSDs (**see 2.1.4**), caused by defects in genes encoding proteins involved in the lysosomal degradation of sphingolipids. The degradation pathway of glycosphingolipids in humans is strictly sequential and defects for nearly every step have been reported except for the degradation of lactosylceramide (Kolter and Sandhoff, 2006). Lactosylceramide can be degraded by two different enzyme/activator systems and no single enzyme defect has been described to cause isolated lactosylceramide storage (Zschoche *et al.*, 1994). However, in combination with other sphingolipids, lactosylceramide accumulates when various cofactors are absent, as e.g. in prosaposin deficiency (Kolter and Sandhoff, 2006).

2.4 Neuronal Ceroid Lipofuscinoses (NCL)

2.4.1 Common clinical and pathological features

Neuronal ceroid lipofuscinosis (NCL) is a collective term for a group of rare and severe autosomal recessive inherited diseases belonging to the superior group of lysosomal storage disorders. In Finland the number of new NCL diagnoses is 2-3 per year and the estimated NCL incidence per 100.000 live births is 4.82 (Mole *et al.*, 2011). The estimated prevalence per million population is 9.4 (Mole *et al.*, 2011). Hallmarks of NCLs are degeneration of the brain and often the retina, the accumulation of autofluorescent lipofuscin-like lipopigments in the lysosomes of neuronal and extraneuronal tissues (Goebel, 1997). NCLs are considered to be the most common neurodegenerative disorders of childhood. Patients are found worldwide and so far almost 365 mutations causing NCLs have been described occurring in 9 genes, *CLN1, CLN2, CLN3, CLN4, CLN5, CLN6, CLN7, CLN8* and *CLN10* (NCL mutation data base, http://www.ucl.ac.uk/ncl) (Kousi *et al.*, 2012). The age of onset in NCLs varies from newborn to adult, but clinical features are quite similar to each other, including motor disturbances, progressive blindness, epilepsy and eventually premature death (Haltia, 2003; Jalanko and Braulke, 2009).

The storage materials in cells of NCL patients show various ultrastructures that correlate with the underlying mutated gene and type of NCL. The shape of the ultrastructures can vary from granular osmiophilic deposits (GRODs) to fingerprint (FP), curvilinear (CL) or rectilinear (RL) profiles (Elleder *et al.*, 1999). An overview of the classic clinical phenotypes and their variations associated with the NCL genes, the major components of the storage material and ultrastructural phenotype, are presented in **Table 1**. However, the storage material in NCL patients is not considered to be disease-specific and consists mostly of sphingolipid activator proteins,

also known as saposins A and D (SAPs A and D) or the subunit c of the mitochondrial ATP synthase (Mole *et al.*, 2011).

To date, NCLs are divided into ten forms according to the mutated genes *CLN1* to *CLN10*, even though not all genes have been identified (**Table 1**). Originally, the classification was based on clinical and phenotypical characteristics. Different mutations within one gene may result in varying phenotypes and age of onset, which makes diagnosis complicated on the basis of clinical or phenotypical features. Recently, a new nomenclature system has been proposed, which includes the NCL subtypes (Kousi *et al.*, 2012). This intends to provide better understanding for clinicians, scientists, patients and affected families. The new system derives from the genetic defect and takes the varying phenotype into account, e.g. CLN5 disease, late infantile variant (Kousi *et al.*, 2012).

2.4.2 NCLs and disturbed lipid metabolism

Several NCLs have been linked to disturbed lipid metabolism. Human patients of CLN1 and CLN3 diseases display abnormal molecular phospholipid species in cerebral cortex measured by normal phase high performance liquid chromatography (HPLC) and on-line electrospray ionisation ion-trap mass spectrometric detection (LC–ESI–MS) (Käkelä *et al.*, 2003). Further, 1 month old *Cln1* ko mice have been shown to present reduced levels of total cholesterol and apoA-I and attenuated phospholipid transfer protein (PLTP) activity in serum lipid analyses (Lyly *et al.*, 2008). PLTP has been shown to be involved in the transfer process of cholesterol to HDL through the ABCA1-mediated pathway (Oram *et al.*, 2003).

Two NCL proteins, the palmitoyl protein thioesterase (PPT1/CLN1) and CLN5 have been shown to interact in *in vitro* pulldown assays with the mitochondrial F_1-ATP synthase (Lyly *et al.*, 2008; Lyly *et al.*, 2009). The mitochondrial F_1-ATP synthase has been reported to act as a receptor for apoA-I (Martinez *et al.*, 2003). The ectopic α- and β-subunits of the ATP synthase were found to be enriched at the plasma membrane in *Cln1* ko neurons by total internal reflection fluorescence (TIRF) microscopy and radiolabelled apoA-I uptake was increased in *Cln1* ko glial cells and neurons (Lyly *et al.*, 2008). CLN8 contains domains which are suggested to play roles in ceramide synthesis, lipid regulation and protein translocation in the ER (Winter and Ponting, 2002). Further, NCL disease models, as for *Cln6* and *Cln10* (Cathepsin D knockout), have been shown to contain increased amounts of complex glycosphingolipids (Jabs *et al.*, 2008). Finally, CLN10/Cathepsin D has been suggested to regulate ABCA1-mediated phospholipid and cholesterol efflux (Haidar *et al.*, 2006).

GENE	PROTEIN	CELLULAR LOCALISATION	MAJOR STORAGE COMPONENTS	ULTRASTRUCTURE	CLINICAL PHENOTYPE
CLN1 (PPT1)	PPT1	lysosomes	SAPs A and D	GROD	Infantile classic, late infantile, juvenile, adult
CLN2 (TPP1)	TPP1	lysosomes	SCMAS	CL, FP	Classic late infantile, juvenile
CLN3	CLN3	endo-lysosomal	SCMAS	CL, FP	Juvenile, classic
CLN4 (DNAJC5)	CSPα	synaptic/clathrin-coated vesicles	SAPs A and D	GROD	Adult (Parry disease)
CLN5	CLN5	lysosomes	SCMAS	CL, FP, RL	Late infantile variant, juvenile, adult
CLN6	CLN6	ER	SCMAS	CL, FP, (Kufs type A: FP, GROD)	Early juvenile variant, (late infantile variant)
CLN7 (MFSD8)	MFSD8	endo-lysosomal	n.d.	FP, RL	Late infantile variant, juvenile-adult
CLN8	CLN8	ER/ER-Golgi	SCMAS	CL, CL-like, FP	EPMR, late infantile variant
CLN9 (n.d.)	n.d.	n.d.	SCMAS	CL, FP, GROD	Early juvenile variant
CLN10 (CTSD)	cathepsin D	lysosomes	SAP D[1]	GROD	Congenital classic, late infantile, adult

Table 1: classification of NCLs on the basis of the affected gene. The genes, encoded proteins, their cellular localisation, ultrastructural findings, as well as clinical phenotypes are presented. The different intracellular localisations are highlighted in different grey shades. Abbreviations: **CL**, curvilinear profiles; **CLN1** etc, ceroid lipofuscinosis, neuronal 1 etc; **CSPα**, cystein spring protein; **DNAJC5**, DnaJ (Hsp40) homolog, subfamily C, member 5; **EPMR**, epilepsy, progressive with mental retardation; **ER**, endoplasmic reticulum; **FP**, finger-print profile; **GROD**, granular osmiophilic deposits; **MFSD8**, major facilitator superfamily domain containing 8; **n.d.**, not determined; **PPT1**, palmitoyl protein thioesterase 1; **RL**, rectilinear profile; **SAP**, saposin; **SCMAS**, subunit c of the mitochondrial ATP synthase; **TM**, transmembrane; **TPP1**, tripeptidyl peptidase 1. [1] testing of SAP A has not been reported. Modified from Mole *et al.*, 2011.

2.4.3 Common pathways behind NCLs

Originally, Zhong and co-workers hypothesised that NCL proteins do not interact with each other, based on yeast two–hybrid studies between PPT1, 2 and 3 (Zhong *et al.*, 2000). A few years later protein-protein interactions among NCL proteins have been described by *in vitro* experiments using co-immunoprecipitation, GST-pulldown assays and by an experiment, which showed that defective cell growth of patient cell lines could be reversed by transfecting NCL proteins (Lyly *et al.*, 2009; Persaud-Sawin *et al.*, 2007; Vesa *et al.*, 2002). Lyly *et al.* suggested that CLN5 interacts with most of the other NCL proteins like PPT1/CLN1, TPP1/CLN2, CLN3, CLN6 and CLN8 (CLN7 and CLN10/Cathepsin D have not been tested). The other NCL proteins are also suggested to interact with each other. On gene level common pathways have been suggested for *Cln1* and *Cln5* by comparative gene array studies on knockout mouse brains (von Schantz *et al.*, 2008). The F_1-ATPase has been shown to bind to both, PPT1/CLN1 and CLN5, in GST pulldown assays (Lyly *et al.*, 2009). **Figure 7** summarises the suggested NCL protein-protein interactions.
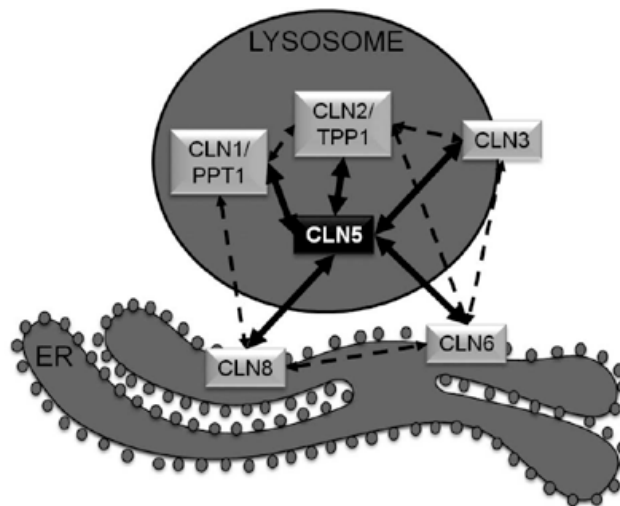
Figure 7: s**cheme of NCL protein-protein interactions *in vitro*.** Proteins are represented in the cellular compartment in which they are localised. Arrows with continuous lines indicate reported CLN5 interactions (Lyly *et al.*, 2009; Vesa *et al.*, 2002; von Schantz *et al.*, 2008). Dashed arrows indicate other suggested protein-protein interactions within the NCL proteins (Persaud-Sawin *et al.*, 2007).
Abbreviations: **CLN**, ceroid lipofuscinosis, neuronal; **ER**, endoplasmic reticulum; **PPT1**, palmitoyl protein thioesterase 1; **TPP1**, tripeptidyl peptidase 1. Some elements of the figure were produced using Servier Medical Art (www.servier.com).

2.4.4 CLN5 disease, late infantile variant NCL

Originally, CLN5 disease, late infantile variant phenotype was thought to be confined to Finland, and therefore was known as Finnish variant late infantile NCL (vLINCL$_{Fin}$). The prevalence of CLN5 disease in Finland is 2.6 per million inhabitants but even higher in the Southern Ostrobothnia area with a prevalence of 1:5000 within the local child population of 15 years of age or younger (Uvebrant and Hagberg, 1997). Within the last couple of years it has become more and more evident that CLN5 disease is not confined to the Finnish population but found all over the world in a variety of different ethnic groups (Bessa *et al.*, 2006; Cannelli *et al.*, 2007; Cismondi *et al.*, 2008; Holmberg *et al.*, 2000; Kousi *et al.*, 2009; Lebrun *et al.*, 2009; Pineda-Trujillo *et al.*, 2005; Sleat *et al.*, 2009; Xin *et al.*, 2010; and unpublished). Patients have been found in Europe (Italy, Portugal, Sweden, the Czech Republic, the Netherlands, UK), in North (USA, Canada) and South (Argentina, Columbia) America and many other countries such as Afghanistan, China, Egypt or Pakistan or with Arabian, Asian or Hispanic origin (NCL mutation data base, http://www.ucl.ac.uk/ncl).

The majority of patients carry a 2.0-bp deletion of the CLN5 coding region at the end of the sequence which leads to an early stop codon in CLN5 protein sequence (Holmberg *et al.*, 2000; Savukoski *et al.*, 1998). In addition 27 mutations and 9 polymorphisms have been characterised (NCL Mutation Database: http://www.ucl.ac.uk/ncl).

First clinical symptoms of CLN5 disease include motor disturbances and loss of vision usually at the age 4-7 years (Holmberg *et al.*, 2000; Santavuori *et al.*, 1991; Santavuori *et al.*, 1982; Xin *et al.*, 2010). The disease progresses with motor and mental deterioration, myoclonia, seizures and ultimately leads to death in most cases at the age of 12-23 years of age. However, two adult onset patients have been reported with a delay of 6 to 8 years between the onset of the disease and disease progression (Xin *et al.*, 2010).

Neuropathological features are generalised cerebral and extreme cerebellar atrophy (Autti *et al.*, 1992; Tyynelä *et al.*, 1997). In the late stage of disease, Purkinje cells in the cerebellum and thalamic neurons are almost completely lost, and cortical neurons, often in a laminar pattern involving laminae III and V, are mildly to moderately obliterated, but present moderate to pronounced enlargement of cells, called ballooning (Tyynelä *et al.*, 1997). White matter edema (spongiosis) may be also observed (Cannelli *et al.*, 2007). Widespread extensive astrocytosis in the cortex and cerebellum has been reported in patients and *Cln5$^{-/-}$* mice (Tyynelä *et al.*, 2004; von Schantz *et al.*, 2009). Moreover, mild microglial activation in patients has been shown by the marker CD68, presenting enlarged cells with autofluorescent material (Tyynelä *et al.*, 2004). In addition, myelin loss is a clinical feature in patients (Autti

et al., 1997). The storage material mainly consists of the subunit c of the mitochondrial ATP synthase, but also small amounts of SAPs A and D have been detected (Tyynelä *et al.*, 1997). The ultrastructure of the cytoplasmic inclusion storage bodies can range from FP, CL to RL profiles (Tyynelä *et al.*, 1997).

CLN5 shows no homology to other proteins making it impossible to deduce its function from known proteins with comparable structures. The gene is only conserved in vertebrates. CLN5 consists of 407 aa with a predicted size of about 46 kDa (Savukoski *et al.*, 1998). In contrast to other vertebrates, CLN5 in humans contains four possible initiator methionines. Consequently, the synthesis of wt CLN5 in a cell-free system resulted in four CLN5 proteins ranging from 39-47 kDa (Isosomppi *et al.*, 2002). The CLN5 protein contains eight predicted N-glycosylation sites and is highly glycosylated with high mannose and complex-type sugars leading to higher observed molecular weights in Western Blot analysis ranging from 52-75 kDa (Isosomppi *et al.*, 2002; Vesa *et al.*, 2002). Moreover, CLN5 contains three M6P moieties connected to Asn320/330/401, pinpointing that CLN5 is a soluble lysosomal protein (Sleat *et al.*, 2006). Prior to this study, the localisation and solubility of the CLN5 protein was debated (Bessa *et al.*, 2006; Isosomppi *et al.*, 2002; Savukoski *et al.*, 1998; Vesa *et al.*, 2002). Overexpression experiments have presented both ER (Vesa *et al.*, 2002) and lysosomal localisation for CLN5 (Isosomppi *et al.*, 2002; Vesa *et al.*, 2002). Mouse Cln5 has been shown to be a soluble, lysosomal protein by immunofluorescence studies and a triton X-114 phase separation assay of transiently transfected COS-1 cells (Holmberg *et al.*, 2004).

2.4.5 CLN1 disease, classic infantile NCL

CLN1 disease, classic infantile NCL (formerly known as infantile NCL (INCL) or Santavuori-Haltia disease) is caused by mutations in the *CLN1* gene, which encodes for a lysosomal enzyme, the palmitoyl protein thioesterase 1 (CLN1/PPT1) (Hellsten *et al.*, 1996; Lehtovirta *et al.*, 2001; Salonen *et al.*, 2001; Vesa *et al.*, 1995). PPT1 cleaves palmitate from H-ras *in vitro* (Camp and Hofmann, 1993) but *in vivo* substrates remain elusive. The patients develop symptoms typically by the age of 6-12 months and then progressively suffer from mental, cognitive and motor decline, severe microcephaly, myoclonus and loss of vision (Haltia *et al.*, 1973b; Santavuori *et al.*, 1973). By the age of 3 years the electroencephalogram (EEG) becomes usually iso electric, indicating a complete lack of brain activity. Death occurs early around 9-13 years of age (Santavuori, 1988). The storage material mainly consists of SAPs A and D (Tyynelä *et al.*, 1993). The ultrastructures of the cytosolic inclusion bodies are granular osmiophilic deposits (GRODs) (Haltia *et al.*, 1973a; Haltia *et al.*, 1973b).

To date, 48 mutations have been defined in *CLN1* gene (NCL mutation data base, http://www.ucl.ac.uk/ncl). CLN1/PPT1 consists of 306 aa, has an N-terminal signal sequence of 26 aa, which is co-translationally cleaved, and has three Asn linked glycosylation sites, which are endoH sensitive (Bellizzi *et al.*, 2000). CLN1/PPT1 has been shown to use the MPR-dependent route to lysosomes (Hellsten *et al.*, 1996; Sleat *et al.*, 2005; Verkruyse and Hofmann, 1996).

2.4.6 Cln1 and Cln5 animal models

Animal model systems are invaluable tools to gain new insights into the molecular mechanisms underlying NCLs. NCLs are not restricted to humans and also occur in other vertebrates such as e.g. cattle, sheep, dog and mouse (NCL mutation data base, http://www.ucl.ac.uk/ncl). Small vertebrate models, like e.g. mouse and zebrafish, are useful animal models to investigate the mechanisms underlying this devastating disease and they are known to contain orthologues of NCL genes. In this thesis project NCL mouse models lacking the *Cln1*, the *Cln5* or both genes have been used.

Two *Cln1* knockout mouse models have been generated using different targeting strategies, leading to the deletion of exon 4 ($Ppt1^{\Delta ex4}$) or exon 9 ($Cln1^{-/-}$) (Gupta *et al.*, 2001; Jalanko *et al.*, 2005). Both knockout mouse models present a severe infantile NCL phenotype including profound brain atrophy, localised reactive gliosis and neurodegeneration. The defects are first detected in the thalamus and subsequently in the cortex (Bible *et al.*, 2004; Kielar *et al.*, 2007). Astrocytosis is first observed in individual thalamic nuclei, cortical laminae and cerebellum before the onset of neuronal loss (Kielar *et al.*, 2007; Macauley *et al.*, 2009). $Ppt1^{\Delta ex4}$ mice have also been linked to disturbed lipid metabolism (Lyly *et al.*, 2008).

A knockout mouse model for Cln5 disease has also been generated by targeted deletion of exon 3 of the *Cln5* gene ($Cln5^{-/-}$) (Kopra *et al.*, 2004). Naturally occurring defects in *Cln5* have been found in cattle, canine and sheep (Frugier *et al.*, 2008; Houweling *et al.*, 2006; Melville *et al.*, 2005). $Cln5^{-/-}$ mice display a relatively slow disease progression with disturbed vision from 5 months onwards and relatively mild brain atrophy even in old mice (Kopra *et al.*, 2004). Progressive loss of neurons within the thalamocortical system with a different timing compared to other NCL mouse models has been recently shown in $Cln5^{-/-}$ mice (von Schantz *et al.*, 2009). Neuron loss in these mice occurs first in the cortex and subsequently in thalamic relay nuclei. To date, no therapeutic attempts have been made on these mice. Pronounced astrocytosis has been detected in these mice at 4 months of age and microglial activation rather late at 12 months of age (von Schantz *et al.*, 2009). Gene expression profiling has pinpointed to early upregulation of immune response genes (Kopra *et al.*, 2004).

In this thesis project a mouse model lacking both genes was generated and is described in the Material and Methods section. The neuropathological features in the two knockout mouse models, which have been reported prior to this thesis work are summarised in **Table 2**.

MOUSE MODEL	*Cln1* ko	*Cln5* ko
Onset of symptoms	>5 months	> 8 months
Phenotype	Seizures and motor disturbances[a]	Seizures and motor disturbances[b]
Ultrastructure of storage material	GROD[a]	RL, FP, CL[b]
Onset of neuron loss	Thalamus (4months)[c]	Cortex lam IV and V (4months)[c]
Reactive astrocytosis (GFAP)	Cortex and thalamus (3months)[a]	Cortex and thalamus (3months)[c]
Microglial activation (F4/80)	Cortex and thalamus (3months)[a]	Cortex and thalamus (12 months)[c]

Table 2: overview of neuropathological changes reported prior to this thesis work in NCL knockout mouse models used in this thesis. *Ppt1*$^{\Delta ex4}$ equates *Cln1* ko and *Cln5*$^{-/-}$ equates *Cln5* ko (the nomenclature used throughout this thesis work).
Abbreviations: **CL**, curvilinear profile; **FP**, fingerprint profile; **GFAP**, glial fibrillary acidic protein; **GROD**, granular osmiophilic deposits; **RL**, rectilinear profile. [a]Jalanko *et al.*, 2005 and unpublished; [b]Kopra *et al.*, 2004 and unpublished; [c]von Schantz *et al.*, 2008

3 Aims of the present study

Prior to this study, the *Cln5* gene, defective in CLN5 disease, late infantile variant NCL, has been identified and knockout mouse models for *Cln1* and *Cln5* were available. Following aims were addressed in this study:

- Characterisation of the basic properties of the CLN5 protein in more detail with focus on processing, localisation and trafficking within the cell.

- Analysis of the consequences of mutations in the *CLN5* gene on its localisation in the cell.

- Analysis of the *Cln5* expression in the mouse brain.

- Verification of the impact of *Cln5*-deficiency in the mouse brain, focusing on microglial activation and myelination defects.

- Analysis of the functional importance of *Cln5* in lipid homeostasis.

- Investigation of possible links between Cln5 and its suggested interaction partner Cln1/Ppt1 by characterising a *Cln1/5* double-knockout mouse model.

4 Materials and Methods

4.1 Materials and methods

An overview of the methods used in this thesis is given in Table 3. Brief general descriptions of the techniques are also described here. More details are available in the original publications.

Table 3: list of methods used during this thesis.

METHODS	ORIGINAL PUBLICATION	CHAPTER
Analysis of protein maturation and glycosylation	I	4.1.10
Basic staining techniques of mouse tissue: LFB, Nissl	II+III	4.1.13
Cell culturing of SH-SY5Y, COS-1, HeLa, MPR$^{-/-}$ cells	I	4.1.3
Efflux studies of [^{3}H] cholesterol to apoA-I	II	4.1.18
Gene expression profiling	III	4.1.7
Generation of Cln1/5 double-knockout mice	III	4.1.1
Generation of iPS cells and embryoid body formation	III	4.1.5
Image thresholding analysis	II	4.1.17
Immunofluorescence staining	I+II	4.1.9
Immunohistochemical staining and analysis of paraffin and free floating mouse brain sections	II+III	4.1.16
In vitro LPS stimulation of mouse primary microglia and mouse cytokine array	II	4.1.12
Light, confocal, fluorescence, electron microscopy	I-III	4.1.9; 4.1.13
Measurements of thickness and regional volume of mouse brain	II+III	4.1.14
Mouse brain isolation and histological processing	II+III	4.1.13
Neuron cell counts	III	4.1.15
Primary cells: isolation and culture of neurons, oligodendrocytes, microglia, astrocytes and peritoneal macrophages	II	4.1.4
Pulse-chase analysis with [^{35}S] and immunoprecipitation	I	4.1.10
Pulse-chase of BODIPY-LacCer	II	4.1.18
Quantitative real-time PCR	II	4.1.6
Recombinant DNA techniques and site-directed mutagenesis	I	4.1.2
Reverse transcriptase PCR	II+III	4.1.6
RNA extraction from mouse brain and cell cultures	II+III	4.1.6
SDS-PAGE and Western Blot analysis	I+III	4.1.11
Serum lipid analysis	II+III	4.1.18
Transient and stable transfections of cell lines	I	4.1.3

4.1.1 *Cln1* ko, *Cln5* ko mice and generation of *Cln1/5* double-knockout mice (II+III)

Homozygous *Cln1* ko and *Cln5* ko mice, maintained on the *C57BL/6JRcc* background have been developed prior to this study and were available for further studies (Jalanko *et al.*, 2005; Kopra *et al.*, 2004). We crossed these mice to generate first heterozygous and later *Cln1/Cln5*-double-knockout (*Cln1/5* dko) offspring. The *Cln1/5* dko offspring were viable and fertile. *C57BL/6JRcc* wild-type (wt) mice served as a control strain. The genotypes of all mice were verified by polymerase chain reaction (PCR) of DNA from tail biopsies (Jalanko *et al.*, 2005; Kopra *et al.*, 2004).

4.1.2 Expression constructs and site-directed mutagenesis (I+unpubl.)

Human wild-type CLN5–pCMV5 (aa 1–407) and CLN5–pCMV5 carrying the different disease causing mutations p.Y392X, p.E253X, p.D279N were available prior to the studies (described by Isosomppi *et al.*, 2002; Vesa *et al.*, 2002). CLN5 constructs carrying the mutations p.R112P and p.R112H mutations were generated into CLN5–pCMV5 construct by site-directed *in vitro* mutagenesis, using the Quick-Change mutagenesis kit from Stratagene. All used expression constructs of mutated CLN5 start from the first methionine (M1). GFP–CLN5 constructs starting from methionines M1-M4 were cloned in frame with an N-terminal GFP-tag in vector pEGFP-C1. Full-length mouse Cln5 cDNA (aa 1–341) with a C-terminal myc/his-tag, was developed by cloning the Cln5cDNA into pcDNA3.1A/myc–his expression vector. The construction of CLN1–pCMV5 and CLN3-pCM5 were described earlier (Järvelä *et al.*, 1998; Salonen *et al.*, 2000). All constructs were verified by sequencing.

4.1.3 Cell culturing and transfections (I + unpublished)

Human cervical cancer cells (HeLa) and African green monkey kidney cells (COS-1) were cultured in Dulbecco's modified Eagle´s medium (DMEM) (+10% fetal calf serum (FCS), 1% penicillin/streptomycin (PS)). Human neuroblastoma cells (SH-SY5Y) were maintained in DMEM:Ham's F12 medium (+10% FCS, PS, 0.1% non-essential amino acids). Transient transfections were done with Fugene HD transfection reagent. A stable cell line expressing CLN5 was established (CLN5-SH-SY5Y) by co-transfecting cells with human CLN5–pCMV5 and pREP4 vector (hygromycin B resistance). Mannose-6-phosphate-receptor double-deficient mouse fibroblasts (MPR$^{-/-}$, MPR46- and MPR300-deficient) were provided by Thomas Braulke (Germany) (Pohlmann *et al.*, 1995). The MPR$^{-/-}$ cells were cultured in DMEM (+20% FCS, 1% PS). Transient transfection of MPR$^{-/-}$ cells was done with Lipofectamine 2000 transfection reagent.

4.1.4 Cell culture of mouse primary neurons, glial cells and peritoneal macrophages (II)

Mouse embryonic fibroblasts (MEFs) from E16.5 old mice were cultivated in DMEM (+20% FCS, 1% PS). Peritoneal macrophages were obtained from 2-6 month old mice into phosphate buffered-saline (PBS) (+Ca^{2+}, Mg^{2+})/0.1% BSA (bovine serum albumin) (see publication II for further details). Mouse cortical neurons were prepared from mouse embryos 14.5-16.5 days post-fertilisation. Cerebral hemispheres were removed and placed in ice-cold 20 mM glucose/PBS. The meninges and blood vessels were carefully removed and cortical tissues were separated. Individual cells were isolated by trituration in 1 ml PBS, and incubated in trypsin-EDTA/DNaseI (0.1%/0.4 mM/10 mg/ml) for 5 min at 37°C. Trypsin was inactivated by FCS. The cells were centrifuged at 1000 rpm for 2 min and resuspended in Neurobasal media (+B-27, 0.5 mM L-glutamine and 1% PS). Two hemispheres were plated per poly-D-lysine hydrobromide (PDL)-coated 6-well plate. Two-thirds of the culture medium were replaced every fourth day. Mouse oligodendroglial cultures were prepared from mouse embryos E16.5 days post-fertilisation. The preparation steps were essentially the same as for the cortical neurons until after the centrifugation step. The cells were then resuspended in DMEM/F-12 media (+B-27, 40 ng/ml fibroblast growth factor (FGF; Sigma-Aldrich), 20 ng/ml epidermal growth factor (EGF), 1% PS). 50000 cells/ml were transferred to an uncoated 12-well plate. After 3-6 days the cells were triturated and transferred to oligosphere medium (DMEM/F-12 + B27, 10 ng/ml FGF, 10ng/ml platelet derived growth factor (PDGF), 1% PS). The cells were passaged every 3 days. After 1-2 passages cells were mechanically triturated, centrifuged at 1000 rpm for 2 min and the resuspended in fresh medium. 100.000-150000 cells/well were placed to a poly-L-ornithine hydrochloride (PO)-coated 6-well plate. After 3-4 days the medium was replaced by DMEM (+B27, 3% FCS, 1% PS). OLs were fixed with 4% PFA/PBS at different time points post-differentiation. Primary cultures of purified microglia and astrocytes were obtained from 3day old mice. Following decapitation, the brains were isolated and washed in ice-cold 20 mM glucose/PBS. Cerebral hemispheres were dissected and the meninges removed. The hemispheres were trypsinised in 1 ml PBS + trypsin-EDTA/DNaseI for 20 min at 37°C. Trypsin was inactivated by FCS, cells were centrifuged for 5min at 1000 rpm and resuspended in DMEM (+1% PS, 10% FCS). One hemisphere was plated per PO-coated T-75 cell culture flask two-thirds of the culture medium were replaced every third day. After 10-14 days the microglial cells were selectively detached from the flasks by shaking (2 h, 37°C, 225 rpm) on a rotary shaker. Suspended microglia were seeded and after 2h medium was replaced to remove loosely adhered cells (Eagle-MEM, 2mM L-glutamine, 1% PS, 10% FCS, 5ng/ml mouse macrophage-colony stimulating factor (M-CSF). Purified astrocytes were obtained by adding fresh medium to the cells which were still attached after the

primary shaking and a following shaking for 16-18 hours at 300 rpm. The suspended cells were transferred to an uncoated cell culture dish and after 1h the medium replaced.

4.1.5 iPS (induced pluripotent stem) cell studies (III)

The experiments and protocols of iPS cell studies are described in detail in publication **III** and therefore only shortly described here. In brief, MEFs were reprogrammed by retrovirus-mediated delivery of the four Yamanaka factors (Oct3/4, Sox2, Klf4 and c-myc) (Takahashi *et al.*, 2007). iPS cell clones were grown on LIF-producing SNL-feeder cells*,* collected on the basis of colony morphology, expanded and purified by MACS anti-stage-specific embryonic antigen 1 (SSEA-1) MicroBeads (Miltenyi Biotech). The clones were analysed with an ES cell characterisation kit (Millipore) and by RT-PCR (for more details see publication **III**).

Embryoid bodies (EB) were grown in suspension in ES medium. On day seven, the size of the EBs was determined by a microscopic analysis. Pluripotency of the produced iPS cell clones was analysed by staining the spontaneously differentiated cells with anti-FoxA2 anti-β-III tubulin or anti-desmin antibodies (**Table 4**) to stain endoderm, ectoderm and mesoderm.

4.1.6 RNA extraction and real-time PCR (II+III)

In short, for real-time PCR RNA of mouse brain hemispheres or cells was extracted and quantified by NanoDrop. Genomic DNA was removed with DNAseI. TaqMan Reverse transcription kit with Random hexamer primers was used for the reverse transcription reactions. The mRNA expression levels were measured with real-time PCR analysis on an ABI prism 7700 sequence detection system. The detailed parameters can be seen in study **II + III**. Relative levels of the selected genes were calculated using the $\Delta\Delta C_T$ method (Livak and Schmittgen, 2001).

4.1.7 Gene expression profiling (III)

In brief, RNA was isolated from mouse cortices and its purity determined by Agilent 2100 Bioanalyzer. Its concentration was measured with NanoDrop, labelled and fragmented; followed by hybridisation, post-hybridization washes, staining and scanning. Gene expression profiles were determined with the Illumina MouseWG-6 v2.0 Expression BeadChip and Genome Studio Data Analysis Software. Chipster v1.4.7 analysis software was used for gene expression analyses. Pathway analyses were done with DAVID Bioinformatics Resources 6.7 software. For further details see study **III**.

4.1.8 Used antibodies (I-III)

Table 4: overview of primary antibodies used in this thesis.

antibody	organism	dilution	company/reference	target	study
Immunofluorescence experiments					
1D3	mouse	1:50	Stressgen	ER marker (PDI)	**I**
1D4B	rat	1:100	Developmental studies Hybri-doma bank	Mouse lysosomal marker (LAMP-1)	**I**
1GmII-3	guinea pig	1:100	(Holmberg *et al.*, 2004)	Cln5	**I**
1RmI-4	rabbit	1:500	(Holmberg *et al.*, 2004)	Cln5	**I**
AB5320	rabbit	1:200	Millipore	OPC marker (NG-2)	**II**
β-III tubulin	rabbit	1:1000	Covance	ectoderm	**III**
Desmin	rabbit	1:500	Epitomics	mesoderm	**III**
FoxA2	goat	1:1000	Santa Cruz	endoderm	**III**
H4A3	mouse	1:100	Developmental studies Hybri-doma bank	Human lysosomal marker (LAMP-1)	**I**
m385	rabbit	1:300	(Luiro *et al.*, 2001)	CLN3 aa242-258	**I**
MAB 386	rat	1:100	Millipore	Differentiated OLs (MBP)	**II**
SMI91R	mouse	1:200	Covance	OLs (CNPase)	**II**
Western Blot analysis					
GFP	mouse	1:2000	Santa Cruz	GFP	**I**
CLN5-C/32	rabbit	1:300-1:500	(Schmiedt *et al.*, 2010)	Human CLN5 aa392-407	**I**
β-tubilin	mouse	1:1000	Chemicon	β-tubilin (loading control)	**III**
α-syn.	mouse	1:1000	BD Biosciences	α -synuclein	**III**
Immunohistochemistry					
CD68	Rat	1:1000	Serotec	Activated microglia	**II+III**
GFAP	rabbit	1:4000	DAKO	astrocytosis	**III**
IBA-1	rabbit	1:100	Menarini	Microglia	**II**
MBP	Rat	1:500	Millipore	OLs	**II+III**
α-syn. &#945	rabbit	1:1000	gift by prof. M.G. Schlossmacher	α-synuclein, raised and affinity-purified at Open Biosystems	**III**

Table 5: overview of secondary antibodies used in this thesis.

Antibody	organism	dilution	Company/reference	Conjugated to	study
Immunofluorescence experiments					
a-guinea pig	goat	1:200	Jackson Immu-noResearch	TRITC	**I**
a-rabbit	Goat or donkey	1:200	Jackson Immu-noResearch	Cy5, TR	**II+III**
a-mouse	goat or donkey	1:200	Jackson Immu-noResearch	Cy5, TR, FITC	**I+III**
a-rat	Goat or donkey	1:200	Jackson Immu-noResearch	Cy5	**I+II**
Western Blot analysis					
a-rabbit	swine	1:10000	DAKO	HRP	**I**
a-mouse	goat	1:5000	DAKO	HRP	**I+III**
Immunohistochemistry					
a-rat	Rabbit	1:1000	Vector laboratories	biotinylated	**II+III**
a-mouse	goat	1:200	Vector laboratories	biotinylated	**III**
a-rabbit	goat	1:1000	Vector laboratories	biotinylated	**II**

4.1.9 Immunofluorescence (IF) staining and microscopy (I+II)

For IF analysis, cells were fixed in ice cold methanol or 4% paraformaldehyde/PBS (PFA). After fixation cells were blocked by incubating them with 0.5% BSA in PBS or in case of PFA fixation in PBS supplemented with 0.2% saponin and 0.5% BSA. Primary antibodies (**Table 4**) were diluted in PBS (0.5% BSA or 0.5% BSA/0.2% saponin) and incubated for 1 h. Excess antibodies were removed by washing the cells three times with PBS (0.5% BSA or 0.5% BSA/0.2 % saponin). Secondary antibodies (**Table 5**) were also diluted in PBS (0.5% BSA or 0.5% BSA/0.2% saponin) and the cells incubated for 1h. After washing the cells three times with PBS the labelled coverslips were mounted with GelMount and visualised with a Leica DMR confocal microscope or with an Axio Imager.Z1 microscope.

4.1.10 Analysis of CLN5 protein maturation and glycosylation (I)

Many tools are available to analyse intracellular trafficking and maturation in cell culture systems. It is important to keep in mind that there are no absolutely fixed resident components of compartments but proteins/lipids are continually moving between different compartments. The balance of traffic between the compartments determines the steady-state localisation (Watson *et al.*, 2005). Pulse-chase experiments are powerful tools to analyse e.g. biosynthesis, protein maturation and protein degradation. Metabolic labelling with low energy ß-emitting isotopes radioisotopes

like [35S] methionine is widely used as it is incorporated into newly synthesised proteins and relatively stable. The actual experiment can be divided into three steps: the pulse-chase, immunoprecipitation of the protein of interest and finally SDS-PAGE and detection of the signal. However, results using this method should be verified by a second method as this type of labelling inhibits cell proliferation, induces cell cycle arrest and may alter the cell morphology (Hu and Heikka, 2000). CLN5-SH-SY5Y cells were metabolically labelled by starving them in methionine-free DMEM and thereafter labelling with [35S] methionine. Not internalised label was removed and the cells were chased in medium. Cell lysates were immunoprecipitated with CLN5-C/32 antibody (**Table 4**) and A/G sepharose beads. The samples were separated by SDS-PAGE and the gel was fixed. The radioactive signal was intensified with sodium salicylate. The dried gel was exposed to an autoradiographic film.

To verify the pulse-chase results protein synthesis was blocked by treating the cells with 50 µg/ml cycloheximide (CHX) up to 24 h. Anterograde trafficking between the ER and Golgi apparatus was analysed by cell treatment with 2.5 µg/ml brefeldin A (BFA), which blocks the anterograde trafficking. Protein N-glycosylation was studied by cell treatment with a dolichol pyrophosphate-N-acetylglucosamine inhibitor 10 µg/ml tunicamycin. To deglycosylate proteins to analyse their posttranslational modifications peptide N-glycosidase F (PNGaseF) was used. PNGaseF cleaves between the innermost GlcNAc and asparagine residues of high mannose, hybrid, and complex oligosaccharides from N-linked glycoproteins. Also, endoglycosidase H (EndoH) was used that removes Asn-linked mannose-rich N-glycans, but not complex type sugars (see publication **I** for further details). Samples were separated by SDS-PAGE, immunoblotted and then probed for CLN5.

4.1.11 SDS-PAGE and Western Blot analysis (I+III)

Protein concentration of the samples (study **I**: cell lysates or study **III**: mouse brain extracts) was determined with a DC protein assay and equalised amounts of total protein were analysed. The samples were denaturised at 95°C with Laemmli buffer containing 2% β-mercaptoethanol for 5 min, samples were loaded and separated on 10-14% SDS-PAGE gels. Proteins were transferred to nitrocellulose membranes (Amersham Biosciences) by electroblotting at 400 mA for 1 h. Afterwards Ponceau protein stain was used to confirm protein loading and even transfer. Skimmed milk powder (5%) in tris buffered saline–tween (TBS-T) was used for blocking and as dilution buffer for primary antibodies (**Table 4**), TBS-T for the secondary horseradish peroxidase (HRP)-conjugated antibodies (**Table 5**). For the detection of antigens enhanced chemiluminescence (ECL) was used as HRP substrate.

4.1.12 Mouse cytokine array (II)

Briefly, mouse primary microglia were treated with *Escherichia coli* lipopolysaccha-ride (LPS) or no stimulant. 24 h later media was changed to medium without any supplements. 48 h later the supernatant was collected and cells were harvested for determination of protein concentration. The cytokine levels in the culture media were determined using the mouse cytokine array panel A (Proteome Profiler[TM] Ar-ray). Data was captured by exposure to Fuji medical x-ray films. Arrays were scanned and optical densities were determined with imageJ.

4.1.13 Mouse brain preparation, electron microscopy (EM), autofluorescence detection and basic stainings of mouse brain tissue (II+III)

For EM analyses (**III**), bisected brains were immersion fixed in 0.1 M phosphate buffer pH 7.4/4% PFA/2.5% glutaraldehyde, incubated in fresh fix solution, and stored in 10mM phosphate buffer. Cortical and thalamic pieces were osmicated, dehydrated and embedded in epoxy resin. Ultra thin sections were contrasted with uranyl acetate and lead citrate. The sections were viewed and analysed with a JEOL 1400 Transmission Electron Microscope, and images were taken using a Digital Camera Olympus-SIS Morada, 36 x 24 mm CCD, 11 Mega pixels, pixel size: 9 µm. For Nissl (**II+III**), Luxol Fast Blue (LFB) (**II**), autofluorescence detection (**III**) and most immunohistochemical stainings (**II+III**) mice were deeply anesthetised with Ketalar®/Rompun® vet (2:1) and transcardially perfused with vascular rinse PBS and by a fresh solution of 4% PFA. Brains were isolated and postfixed in 4% PFA. The brain samples were cryoprotected in a solution of 30% sucrose/TBS containing 0.05% NaN$_3$ for a minimum of 48 h, then frozen and stored at −70°C. Next, for further preparation brains were bisected along the midline, and 40µm frozen coronal sections were cut with a sliding microtome through the rostrocaudal extent of the cortical mantle (**Figure 8**). Sections were collected into 96-well plates containing cryoprotectant solution.

Figure 8: schematic sagital view of an adult mouse brain. For immunohistochemical analysis coronal sections were cut through one hemisphere of a mouse brain. Modified from The Mouse Brain in Stereotaxic Coordinates (Paxinos and Franklin, 2001).

For some immunohistochemical stainings, mouse brains were fixed in 4% PFA, embedded in paraffin and sectioned at 5 μm (**III**). Sections were deparaffinised, rehydrated in alcohol series, incubated in 5% H_2O_2, and rinsed with TBS. The sections were boiled in Na-citrate buffer (pH 6.0), blocked and incubated with primary antibody (**Table 4**). Next, samples were rinsed with TBS-T and incubated with secondary antibody (**Table 5**). The sections were treated with avidin-biotinylated HRP complex, washed with TBS and treated with 3,3′-diaminobenzidine tetrahydrochloride HCl (DAB). Subsequently, sections were counterstained with haematoxylin. After dehydration, the sections were cleared in xylene, air-dried and coverslipped with p-xylene-bis(pyridinium bromide) DPX. To analyse the extent of endogenous autofluorescence mouse brain sections were mounted onto chrome-gelatine coated slides and coverslipped with Vectashield. Images from each section were captured using a Leica SP5 confocal microscope and a 488 nm excitation laser. For Nissl staining, a classic nucleic acid staining traditionally used on nervous tissue sections (**II + III**), the mounted brain slices were incubated with 0.05% cresyl fast violet/ 0.05% acetic acid in water, rinsed in distilled water and differentiated through an ascending series of ethanol, cleared in xylene, and finally coverslipped with DPX. LFB staining was used to stain myelin (**II**). The sections were first rinsed in deionised water, then in 70% ethanol, then in 95% ethanol, followed by the staining step overnight with 0.1% LFB in 95% ethanol at 60°C. Unbound stain was removed by a washing step in deionised water. The LFB stain was differentiated by a brief rinse in 0.05% lithium carbonate followed by 70% ethanol. The sections were rinsed in deionised water and counterstained in 0.05% Cresyl Fast Violet solution for 20 min at 60°C. Sections were rinsed in deionised water, 70% ethanol and dehydrated through increasing ethanol concentrations, cleared in xylene and coverslipped with DPX.

4.1.14 Thickness and regional volume measurements (II+III)

Stereological estimates were obtained with *StereoInvestigator* software (Micro-brightfield Inc). First, a one in six series of mouse brain sections were Nissl stained (**see 4.1.13**). Regions of interest (ROI) were defined by referring to the neuroanatomical landmarks as described in Paxinos and Franklin, 2001. A sampling grid was superimposed over the ROI and the number of points covering the area was assessed. The volume in μm^3 was estimated from a series of sections through each ROI (for further details see original publication **II** and **III**). Analyses were carried out on an Olympus BX50 microscope linked to a DAGE-MTI CCD-100 camera. The mean coefficient of error for all Cavalieri estimates was determined using the method of Gundersen and Jensen (1987) and was less than 0.05. For thickness measurements of brain regions ten perpendicular lines were traced from the pial surface of the cortex to the white matter of the corpus callosum (**III**). The mean length was taken as a measure of thickness and this was determined in three consecutive sections from a defined rostrocaudal level for each analysed region (Bible *et al.*, 2004; Kielar *et al.*, 2007).

4.1.15 Neuron counts (III)

For the quantification of the neuronal cell number Nissl-stained mouse brain sections were used from a 1:6 series and a design-based optical fractionator probe was utilised. A ROI was determined, a grid superimposed and cells were counted with a 100x objective within a series of dissector frames. Grid and dissector sizes were chosen according to each brain region using a coefficient of error (CE) value of ≤ 0.1 to indicate sampling efficiency. All neuron counts were done with a Zeiss, Axioskop 2 MOT microscope linked to a DAGE-MTI CCD-100 camera.

4.1.16 Immunohistochemistry (II+III)

One in six series of brain sections were treated with 1% H_2O_2 in TBS for 20 min to quench endogenous peroxidase activity. Next, the sections were washed in TBS, blocked with 15% serum/TBS for 40 min and then incubated with specific primary antibodies (**Table 4**), which were diluted in TBS (+0.3% Triton X-100, 10% goat/rabbit serum). Next, the sections were rinsed with TBS and subsequently incubated in the according biotinylated secondary antisera (**Table 5**) in TBS (+0.3% Triton X-100, 10% normal serum). The sections were rinsed in TBS, incubated with an avidin–biotinylated peroxidase complex in TBS, rinsed in TBS, and immunoreactivity was detected by incubation in 0.05% DAB and 0.001% H_2O_2 in TBS. Ice-cold TBS was added to the sections which were then rinsed, mounted, air-dried, cleared in xylene, and coverslipped with DPX.

4.1.17 Image thresholding analysis (II)

The optical densities were obtained by semi-automated thresholding image analysis (Bible *et al.*, 2004). Thirty non-overlapping images were taken from 3 consecutive brain sections starting from a defined anatomical landmark. The area of immuno-reactivity was determined with Image Pro Plus image analysis software. Thereby, a threshold that discriminated staining from background in each image was applied. Data were plotted as the mean percentage area of immunoreactivity per field for each region.

4.1.18 Lipid metabolism studies (II+III)

To study systemic lipid disturbances blood for serum lipid and lipoprotein analysis was collected from mice (see studies **II**+**III**). Total cholesterol was determined en-zymatically in mouse serum *via* a series of coupled reactions that hydrolyse cho-lesteryl esters and oxidise the 3-OH group of cholesterol (CHOD-PAP 1489232 kit, Roche Diagnostics). The reaction byproduct hydrogen peroxide was measured quan-titatively in a peroxidase catalysed reaction that produced a colour. The colour in-tensity is proportional to the cholesterol concentration and therefore the absorbance was measured at 500 nm. Also, triglycerides were measured enzymatically in mouse serum using a series of coupled reactions in which triglycerides were hydrolysed to produce glycerol (GPO-PAP 1488872 kit, Roche Diagnostics). Glycerol then in turn was oxidised using glycerol oxidase, and hydrogen peroxide one of the reaction products, was measured as described for cholesterol. PLTP activity was determined with a radiometric assay (Jauhiainen and Ehnholm, 2005). In short, the activity is detected as transfer of radioactively labelled phospholipids from donor liposomes to acceptor HDL particles. Radioactivity was measured from supernatants, which con-tain the loaded HDL particles and PLTP with a liquid scintillation counter. Mouse apoA-I was quantified using a sandwich enzyme-linked immunosorbent assay (ELISA) with use of a polyclonal rabbit anti-mouse apoA-I IgG, performed in 96-well plates coated with this antibody. Purified mouse apoA-I was used as a primary standard. Serum samples were diluted in PBS-Tween 20 (0.1%) + 0.5% BSA. Bound apoA-I was detected by the addition of polyclonal rabbit anti-mouse apoA-I, conjugated to HRP. The assay was linear in the range of 6.5-420 ng/ml. In the paraoxonase-1 (PON-1) activity assay, paraoxon (diethyl-p-nitrophenylphosphate) was used as a substrate (Gan *et al.*, 1991). Briefly, 20 µl serum was added to buffer-substrate solution (100 mM Tris-HCl, pH 8.0, 1 mM $CaCl_2$, 1.2 mM paraoxon) and incubated at 37°C for 10 min. PON converts paraoxon to p-nitrophenol, a yellow compound that is measured at 405 nm. The activity unit is µmol/min. For the lipo-protein analysis, serum samples were fractionated by fast-performance liquid chro-matography (FPLC).

For cholesterol uptake and efflux analyses, peritoneal macrophages were incubated with [^{3}H]cholesterol-LDL. Unattached LDL particles were removed by a washing step. To evaluate the uptake, cells were scraped and scintillation counted. To measure the efflux, the macrophages were washed with PBS after labelling, incubated with apoA-I, the medium collected and the cells washed with PBS. The medium and cell lysates scintillation counted. To study the fluorescent sphingolipid transport, peritoneal macrophages were incubated with EMEM + boron dipyrromethene (BODIPY) FLC$_5$-lactosylceramide (BODIPY-LacCer). BODIPY is an effective biological label since it has been reported to have a superior photostability compared to fluorescein and is relatively insensitive to changes in polarity and pH values (Ulrich *et al.*, 2008). Fluorescent sphingolipids can be used as fluorescent structural markers for the Golgi compartment, as tracers of lipid metabolism and trafficking of lipid endocytosis pathways can be followed (Pagano and Chen, 1998; Pagano *et al.*, 1991). BODIPY-LacCer is known to be internalised *via* caveolae and reaches early lysosomes within few minutes from where it either recycles back to the cell surface or *via* late endosomes to the Golgi compartment (Choudhury *et al.*, 2002; Choudhury *et al.*, 2004; Sharma *et al.*, 2003). Further, cellular identification of lysosomal lipid storage disorder phenotypes is possible with BODIPY-LacCer as the trafficking towards the Golgi compartment is disturbed in these diseases (Puri *et al.*, 1999). In the experiments, the PM labelling was assessed in the beginning and the label was chased for several time-points. The BODIPY-LacCer internalisation was imaged with fluorescence microscopy (for details see study **II**).

4.2 Ethical aspects

The studies were performed in accordance with approved animal policies of the National Institute for Health and Welfare and the University of Helsinki and the State Provincial offices of Finland (agreement numbers ESLH 2009-05074/STH 415, KEK09-058 and KEK09-060). The work has been carried out following good practise in laboratory animal handling and the regulations for handling genetically modified organisms.

5 Results and discussion

5.1 The CLN5 protein (I+II)

5.1.1 *Cln5* expression in the brain and cells of the CNS (II)

It has been reported earlier that *Cln5* is expressed in mouse brain and all other peripheral organs (heart, kidney, lung, liver, skeletal muscle, spleen, testis) tested by Northern Blot analysis (Holmberg *et al.*, 2004). Further, *Cln5* expression in mouse brain has been detected at embryonic stage E13 and was shown to be elevated at the age of 1 month also by Northern hybridisation (Holmberg *et al.*, 2004). Reverse transcriptase PCR studies detected *Cln5* in cell cultures representing different cell populations of the embryonic mouse brain (mixed glial cells, hippocampus, cortex, total brain) (Holmberg *et al.*, 2004). *In situ* hybridisation analysis of *Cln5* mRNA showed widespread expression in E15 old mice being more abundant in the developing cerebellar cortex, cerebellum and the ganglionic eminence (Holmberg *et al.*, 2004). Immunohistochemical staining of Cln5 in mouse brain sections of postnatal mice detected immunoreactivity in Purkinje cells, diverse cortical neurons, hippocampal pyramidal cells and glia (not further specified) in P7 up to 2 month old mice (Holmberg *et al.*, 2004).

One aim of this thesis was to elucidate the *Cln5* gene expression among the different cell types in the mouse CNS by qPCR analyses. Therefore, mRNA was extracted from separately cultured neurons, astrocytes, oligodendrocytes and microglia from wt mice (*C57BL/6JRccHsd*). RT-PCR indicated that *Cln5* expression levels among cells of the CNS were highest in microglia, followed by astrocytes, oligodendrocytes and neurons in descending order (**Table 6 and II; Figure 1B**). Additionally, *Cln5* expression levels were significantly increased in microglia (three-fold) after stimulating cells with LPS, which causes immune responses and activates microglial cells. This indicates a possible role for Cln5 in immune response (**II; Figure 1C**). Moreover, the gene expression was analysed over life time in mouse brain. The overall expression levels of *Cln5* increased gradually in mice from 3 days up to 3 months of age, where it then reached a plateau (**II; Figure 1A**). This indicates that Cln5 expression may play a role in brain development. Interestingly, distinct differences in the gene expression patterns of NCL types have have been reported. For example, gene expression of *Cln1* and *Cln5* has been suggested to be under developmental control, whereas the expression levels for *Cln2* and *Cln10* have been shown to remain constant during development (Holmberg *et al.*, 2004; Suopanki *et al.*, 2000).

Interestingly, the expression levels of NCL genes vary highly between neurons and different types of glial cells in rodents (rats, mice, **see Table 6**) although neuron-

The CLN5 disease - protein
maturation, trafficking and pathology

specific death is a hallmark in all forms of NCL. However, it is noteworthy that these findings of gene expression levels in different cell types may not reflect the protein expression levels and consequently, the function of NCL proteins. Only analyses on protein level can verify these findings. Also, human *CLN5* expression needs to be verified over life-time to see at which age CLN5 protein reaches its plateau in healthy humans.

GENE	neurons	astrocytes	microglia	OLs
Cln1				n.d.
Cln2				n.d.
Cln3				n.d.
Cln5				
Cln7				n.d.
Cln10				n.d.

Table 6: gene expression levels of NCL genes in different cell types of the CNS from mice (*Cln5*) and rats (*Cln1-3, 7, 10*) cell cultures. Black filling indicates the highest gene expression; followed by dark grey, light grey and white. Same colours within one row indicate similar expression levels (e.g. for *Cln1* neurons ≈ astrocytes > microglia). Abbreviations: n.d., not determined; OLs, oligodendrocytes. The table was assembled using data from Sharifi *et al.*, 2010 and **study II**.

The finding that expression of NCL genes is distributed differently between the various CNS cells is supported by the different pathological profiles of the NCL mouse models, when all events like neuronal loss, astrocytosis and microglial activation are taken into consideration (Cooper, 2010). However, it is remarkable that different gene products lead to a similar pathological endpoint. It remains to be clarified if NCLs are truly connected on protein level *in vivo*, like it has been indicated by *in vitro* studies (Lyly *et al.*, 2009; Vesa *et al.*, 2002).

5.1.2 Maturation and trafficking to the lysosomes (I)

Prior to this study, controversial characteristics about the CLN5 protein maturation, localisation and solubility have been published (Bessa *et al.*, 2006; Holmberg *et al.*, 2004; Isosomppi *et al.*, 2002; Savukoski *et al.*, 1998; Vesa *et al.*, 2002). In cell culture based transient overexpression analyses CLN5 protein has been suggested to be an ER resident (Vesa *et al.*, 2002) and a lysosomal protein (Isosomppi *et al.*, 2002; Vesa *et al.*, 2002). Further, it was under debate whether CLN5 is a transmembrane protein (Bessa *et al.*, 2006; Savukoski *et al.*, 1998; Vesa *et al.*, 2002) or a soluble protein (Holmberg *et al.*, 2004). However, the fact that CLN5 contains M6P residues on high mannose-type sugars that are connected to Asn320/330 and 401 pinpoint to a soluble CLN5 protein (Sleat *et al.*, 2006). One goal of this thesis work was to shed light onto these controversies about the CLN5 protein.

Earlier theoretical prediction studies did not suggest an ER signal peptide to be present in the *CLN5* sequence. However, only the sequence starting from M1 was taken into consideration although the Cln5 sequence in mouse starts from methionine corresponding to M4 in humans (Savukoski *et al.*, 1998). Simulations for all four M1-M4 sequences presented herein (**I**; **Supp. Table S1**), predicted the existence of a signal peptide for the sequences starting from M2-M4 with different probabilities (SignalP). In accordance, it was shown earlier that four forms of CLN5 were translated in a cell-free system *in vitro* (Isosomppi *et al.*, 2002).

To address the question if all or only some of the methionines can be used as initiation points and if CLN5 may be cleaved, COS-1 and HeLa cells were transiently transfected with several constructs. The constructs contained GFP-tags introduced at the 5' end of each initiation methionine of the human CLN5 sequence (**Figure 9A and I; Figure 1A**). The expressed proteins were analysed by immunofluorescence and SDS-PAGE, followed by Western Blotting. GFP and a novel human specific C-terminal CLN5 antibody were utilised to detect both extremities of the overexpressed protein constructs. The novel antibody was raised against a synthetic peptide against the very C-terminal end of CLN5. As it detected the CLN5 protein in Western Blotting analyses, this indicated that CLN5 is not trimmed at the C-terminus. Further, the novel CLN5 antibody recognised a single 60 kDa protein for all M1-M4 constructs, whereas the GFP antibody detected proteins of variable molecular weights (**Figure 9B and I; Figure 1B-C**). The molecular weights correlated well with the estimated N-terminal fragment sizes assuming a signal peptide cleavage at the same site in all constructs. Based on the topology programmes this cleavage would occur at the amino acid position 96. Immunofluorescence observations supported the hypothesis of an N-terminal signal cleavage site regardless of the initiation methionine used. Cleavage was also supported by the immunofluorescense analyses showing that the signals of GFP and the C-terminal CLN5 antibody did not co-localise (**Figure 9D and I; Figure 1D-E**). GFP was always located in the ER whereas CLN5 was detected in the lysosomes in all M1-M4 constructs. Under endogenous circumstances signal sequences are rapidly degraded and therefore would be hard to detect. One possibility, why the sequence was detectable in the ER might be the GFP tag and/or the use of a transient overexpression system.

The result that all M1-M4 CLN5 constructs are cleaved and result in the same size proteins is an important starting point for future studies. This needs to be taken into consideration e.g. when developing antibodies, probes etc. If only one or all of the 4 possible initiation methionines are used *in vivo* remains elusive.
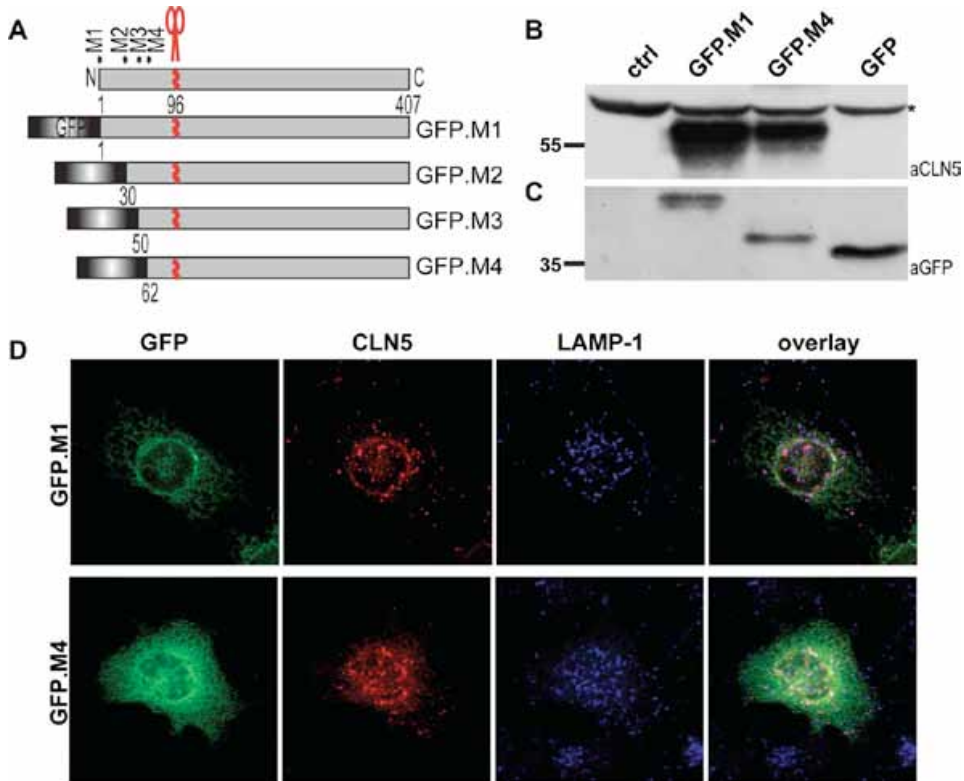
Figure 9: processing of human CLN5. (A) The human CLN5 protein contains four possible initiation methionines (M1-M4) at the following amino acid (aa) positions: 1, 30, 50 and 62. A predicted cleavage site is at position 96. A GFP-tag was introduced in front of all possible initiation methionines M1-M4. The constructs were transiently transfected into HeLa and COS-1 cells. COS-1 lysates were analysed by SDS-PAGE followed by Western Blotting using **(B)** the novel C-terminal CLN5 antibody and **(C)** GFP antibody. **(D)** Transfected HeLa cells were immunostained with a CLN5 antibody (red) and LAMP-1 (blue) was used as a lysosomal marker. As examples, the constructs GFP.M1 and GFP.M4 are presented here. *unspecific band

One pitfall is that the currently available antibodies against the CLN5 sequence do not recognise endogenous protein. Therefore, to study the maturation of the protein a stably human CLN5 expressing cell line starting from M1 (CLN5-SH-SY5Y) was established. Pulse-chase experiments and treatments of the stable cell line with reagents that affect normal protein transport namely cycloheximide (chx), tunicamycin and brefeldin A (BFA) revealed the existence of a 60 kDa pro- and a 50 kDa mature form of CLN5 (**I; Figure 2 A-C, F**). Chx blocks the *de novo* protein synthesis inhibiting translation elongation through binding to the E-site of the 60S ribosome and then blocks eEF2-mediated tRNA translocation (Schneider-Poetsch *et al.*, 2010). Occupation of the E-site by CHX and deacetylated tRNA causes an arrest of the ribosome on the second codon. BFA inhibits anterograde trafficking between the ER

and Golgi apparatus. This compound is often used to study protein trafficking in the endomembrane system of mammalian cells and it intervenes with the recruitment of coat proteins (COPI), which are important for certain vesicle formations (Nebenfuhr *et al.*, 2002). Treatment of cells with BFA leads to loss of COPI coats from the Golgi apparatus and subsequently anterograde vesicles are not longer able to fuse with the maturing *cis* cisterna of the Golgi. Tunicamycin is commonly used to study protein N-glycosylation, which blocks the synthesis of dolichol pyrophosphate-N-acetylglucosamine, a key enzyme in glycoprotein biosynthesis in the ER from the start (Elbein, 1987).

Moreover, the glycosylation status of CLN5 was verified and validated that it is highly glycosylated containing high mannose and complex type sugars (**I; Figure 2 D-F**). BFA treatment and subsequent analysis by Western Blotting indicated that the mature 50 kDa form of CLN5 derives from the 60 kDa proform by trimming of the carbohydrate trees. This possibly takes place in the TGN or post-Golgi (**see over-view Figure 10**).

The most common route for soluble lysosomal proteins to lysosomes is the MPR-mediated pathway, which has also been suggested for CLN5 by proteomic analyses (Kollmann *et al.*, 2005; Sleat *et al.*, 2006). Biochemical testing if CLN5 comes in the cytosolic or membrane fraction from human patient fibroblasts has been performed with the use of an antibody which was thought to detect endogenous CLN5 protein (Bessa *et al.*, 2006). However, the same antibody was tested in this study and previous results were not reproducible in our cell systems, indicating either that the antibody was unspecific for CLN5 in Western Blot analysis or detected yet unknown splice variants. Cell biological experiments to analyse the trafficking of CLN5 has not been performed prior to this study. Transient transfections of MPR-deficient fibroblasts indicated that CLN5 is also able to use an alternative route as immunofluorescence studies revealed lysosomal distribution within these cells (**I; Figure 3**). Which alternative route this may be, needs to be studied further, e.g. through LIMP-2 or sortilin. Interestingly, another NCL member CLN10/Cathepsin D has been described to be able to use the classical MPR-dependent pathway and also the sortilin mediated route to traffic to lysosomes (Canuel *et al.*, 2008). The finding that CLN5 is highly N-glycosylated and also secreted into the culture medium further pinpoints to a soluble protein (Isosomppi *et al.*, 2002; unpublished).

In summary, this study was important to elucidate some basic information about the CLN5 protein (**see overview Figure 9**). The earlier discrepancies, whether CLN5 is an ER or a lysosomal protein, could be clarified.

5.1.3 Consequences of mutations on the cellular localisation of CLN5 (I)

Next, it was of interest how different disease-causing mutations may affect the trafficking of CLN5 towards lysosomes. To investigate this, several cell lines as HeLa (for IF studies) and COS-1 (for Western Blot analyses) cells were each transiently transfected with constructs carrying five different mutations (**see Table 7**).

Amino acid change	Mutation	Steady-state localisation	Localisation after 5h of chx treatment
p.R112P	missense	ER	ER
p.R112H	missense	ER	ER
p.E253X	early stop	ER	unstable
p.D279N	missense	ER	ER, partly lysosomal
p.Y392X	2-bp deletion	ER	unstable

Table 7: list of CLN5 mutations analysed in transiently transfected cell lines and their intracellular localisation at steady-state and after treatment with cycloheximide (chx) for 6h.

The intracellular localisation of mutated constructs carrying p.R112P and p.R112H has not been characterised prior to this thesis project. The amino acid 112 has been found to be mutated in a Portuguese family (p.R112P) and a Colombian patient (p.R112H). The Colombian patient presented a juvenile onset of the CLN5 disease at the age of nine years with visual loss and fast disease progression (Pineda-Trujillo *et al.*, 2005). The Portuguese patient is a compound heterozygous (null mutation p.Q189X in one allele, mutations p.D279N and p.R112P in the other allele) presenting late infantile onset (Bessa *et al.*, 2006). The mutations p.E253X and p.D279N have been reported prior to this study but the intracellular localisation of mutated protein containing the p.E253X mutation has not been examined (Holmberg *et al.*, 2000; Savukoski *et al.*, 1998; Vesa *et al.*, 2002). The mutation p.Y392X was included because the localisation of the mutated protein remained controversial (Isosomppi *et al.*, 2002; Savukoski *et al.*, 1998; Vesa *et al.*, 2002).

At steady-state, all mutations lead to ER retention of the expressed CLN5 in HeLa cells (**I; Figure 4, Supp. Figure S2**). It has been published earlier that constructs carrying the mutations p.D279N and the most common mutation in Finland p.Y392X were able to reach the Golgi and even lysosomes (Isosomppi *et al.*, 2002; Vesa *et al.*, 2002). Therefore, the transiently transfected HeLa cells were treated with chx, to block the protein synthesis and chased the mutated CLN5 proteins up to 5h (**I; Figure 5**). Under these conditions, proteins with the missense mutations p.R112H and p.R112P did not leave the ER and were stably detected in the ER. The ER retention is probably due to folding defects caused by the mutations. It would be

important to investigate the role of CLN5 mutations in ER-stress mediated apoptotic cell death and ER-quality control. ER-stress responses have been shown to contribute to the disease progression in other NCLs, like CLN1/PPT1, CLN6 and CLN8 (Galizzi *et al.*, 2011; Oresic *et al.*, 2009; Wei *et al.*, 2008).

As expected, proteins carrying the mutation p.D279N were able to reach lysosomes. This construct contained a mutation that resulted in an additional N-glycosylation site.The proteins with an early stop (p.Y392X, p.E253X) were unstable and not detectable after 5h chx treatment. At shorter incubation times (1h) the mutated proteins were mostly detectable in the ER and in few cells detectable in vesicular structures, which however did not co-localise with the lysosomal marker LAMP-1. Isosomppi *et al.* utilised transiently transfected BHK-21 cells with CLN5 construct carrying the mutation p.Y392X and reported co-localisation with the medial Golgi marker CTR433 in most cells, partly ER and some vesicular-like staining (not co-localising with a lysosomal marker lgp120) at steady-state (Isosomppi *et al.*, 2002). The slight differences in detected localisation of the same mutant protein are potentially explainable by the use of different cell lines. Consistent with the data presented in this thesis work it was reported that 1 h chx treatment of transiently transfected BHK-21 cells resulted in decreased staining. Only minor vesicular staining was observed, which did not co-localise with lysosomal markers. Also, longer chx treatments led to total loss of staining, indicating instability of the mutated protein (Isosomppi *et al.*, 2002).

To assess whether the glycosylation status of the mutated CLN5 constructs p.R112H, p.R112P and p.D279N support the detected localisation, transiently transfected COS-1 cell lysates were treated with EndoH and PNGaseF, digesting the high mannose and complex type sugars, respectively. Interestingly, Western Blot analysis revealed that the CLN5 proteins carrying the mutations p.R112H and p.R112P contained both high mannose and complex type sugars even though immunofluorescence studies pinpointed to stable ER retention. This lead us to the conclusion that the CLN5 protein is able to traffic to the Golgi, where complex type sugars are added, and return to the ER after maturation and possibly interact with other proteins. This might be important since i*n vitro* studies have shown that CLN5 interacts with other NCL proteins such as CLN1-3, 6 and 8 (Lyly *et al.*, 2009; Vesa *et al.*, 2002). CLN6 and CLN8 are ER-resident proteins and it has been previously reported that CLN8 can recycle between ER and the ER-Golgi intermediate compartment (Lonka *et al.*, 2000). Therefore, CLN8 might interact with CLN5 within the pathway either from the ER towards the Golgi or in the recycling pathway from the Golgi towards the ER.

The majority of *CLN5* mutations cause a late infantile variant phenotype with very small variation in the clinical phenotype. For example, patients with *CLN5* muta-

tions carrying p.Y392X, p.Y75X, p.D279N and p.W224LfsX30 present the typical disease progression, even though the consequences on protein level have been shown to be very different *in vitro* (ER retention and lysosomal distribution, **see Table 7**). Also, the Portuguese patient carrying two *CLN5* mutations (p.D279N and p.R112P) presented classical disease onset and progression. As CLN5 carrying p.D279N alone was capable to rearch lysosomes at some point, it is likely that p.R112P affects the protein more severely. However, the Colombian patient with the mutation p.R112H presented a milder phenotype, which might indicate that the change from arginine to histidine may disrupt the function to a lesser extent than the change to proline. Nevertheless, this cannot be stated for sure as the Portuguese also carried the p.D279N mutation in one allele. It has been shown that Cln1 expression is increased in Cln5 ko mice and that CLN1 wt protein was able to rescue the lysosomal trafficking of CLN5 carrying different disease mutations in overexpression studies *in vitro*. This indicates a compensatory role of CLN1/PPT1 in *Cln5*-deficiency. This might be the reason why p.R112H mutated proteins were restricted to the ER in transient overexpression studies as endogenous CLN1/PPT1 expression may not be able to compensate the overexpressed levels (will be discussed later).

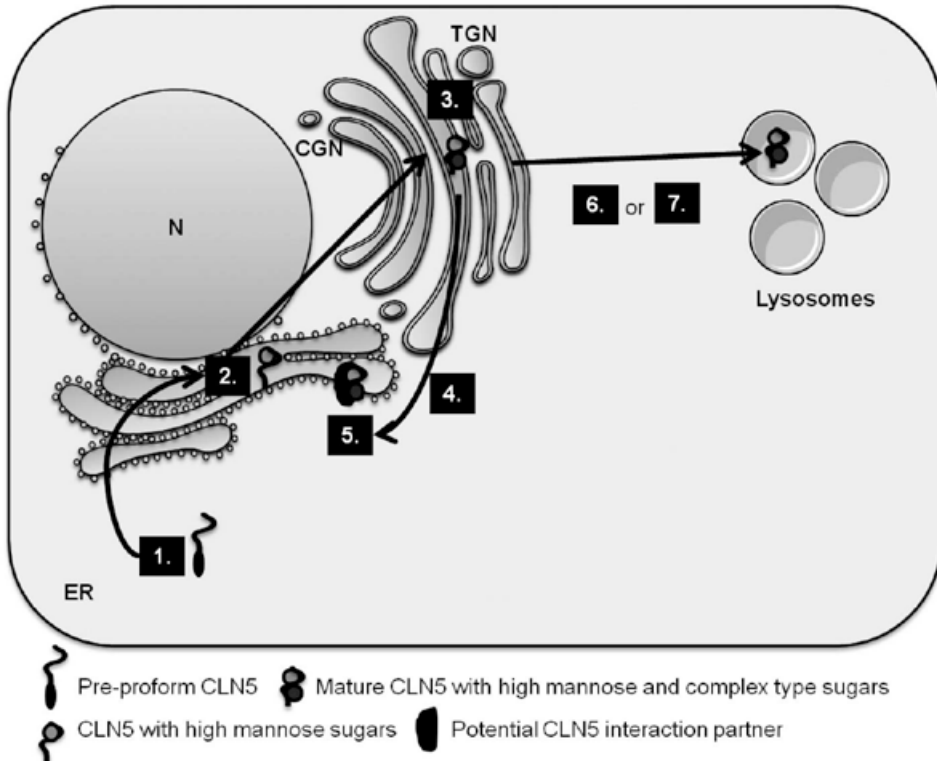Overall, **Figure 10** summarises the suggested maturation of the CLN5 protein (5.1.1-5.1.3).

Figure 10: summary of the predicted maturation of the CLN5 protein: 1. In the ER the signal peptide is removed from the pre-proform of CLN5. **2.** Next, high mannose-type residues are added. **3.** CLN5 continues to the Golgi where complex-type sugars are added. **4.** Possible retrograde transport back to the ER. **5.** CLN5 may interact with other proteins such as CLN6, 8 and 1. **6.** CLN5 continues through the early secretory pathway and traffics to the lysosomes *via* MPRs or **7.** uses an alternative unknown route to the lysosomes.
Abbreviations: CGN, *cis* Golgi network; ER, endoplasmic reticulum, N, nucleus; TGN, *trans* Golgi network. Some elements of the figure were produced using Servier Medical Art (www.servier.com).

5.2 Pathology of *Cln5* in mice (II)

5.2.1 Loss of *Cln5* leads to early inflammation and defective myelination in the mouse brain (II)

Preceding this thesis, *Cln5* ko mice had been generated and some basic characteristics have been studied (Kopra *et al.*, 2004; von Schantz *et al.*, 2009; von Schantz *et al.*, 2008). It has been reported that in *Cln5* ko mice cortical neuron loss was present at the age of 4 months, reactive astrocytosis at 1 month and microglial activation at 12 months (von Schantz *et al.*, 2009). Myelination defects in these mice were suggested due to findings of gene expression arrays but this has not been verified fur-

ther prior to this thesis work (Kopra *et al.*, 2004; von Schantz *et al.*, 2008). One aim of this thesis project was to further characterise the pathology of *Cln5* ko mice focusing on the early stage of the disease. Hence, 1 and 3 months old *Cln5* ko mice were used in our studies. Two regions were exemplarily examined, the ventral posterior nuclei of the thalamus (VPM/VPL) and the somatosensory barrel field cortex (S1BF; sends and receives information from the VPM/VPL region), as these are regions known to be affected in *Cln5* ko mice in general (von Schantz *et al.*, 2009). Furthermore, as representative white matter structures the corpus callosum (cc) and internal capsule (ic) were analysed (**Figure 11**).
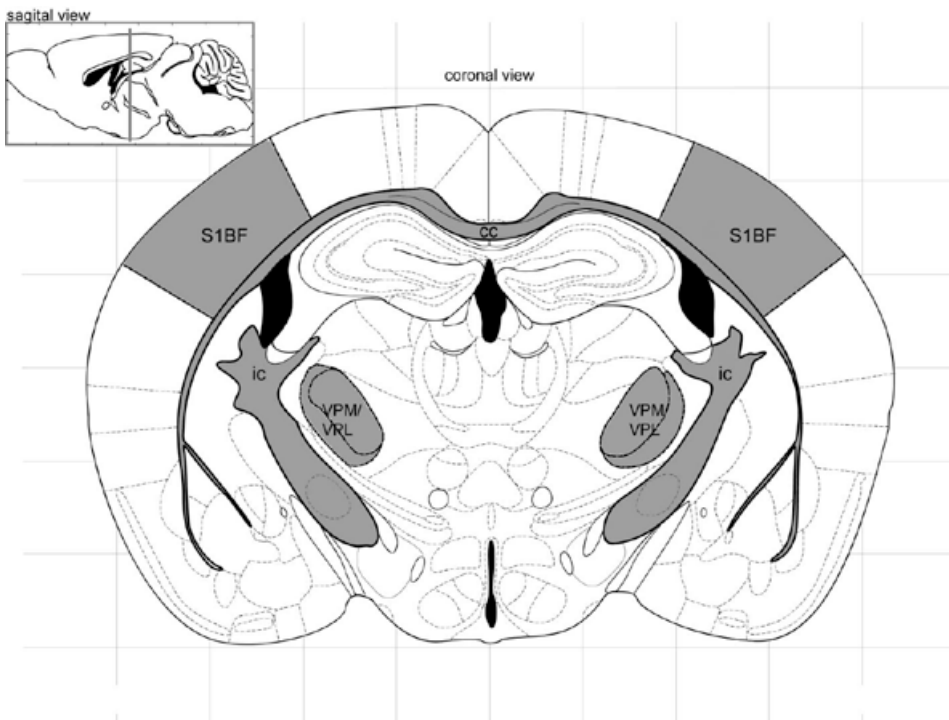
Figure 11: schematic coronal view of the mouse brain regions focused on in study II + III. The brain regions which were analysed the most are highlighted in grey. White matter structures: corpus callosum (**cc**) and internal capsule (**ic**). Somatosensory barrel field cortex (**S1BF**) sends/receives information to/from the ventral posterior nuclei of the thalamus (**VPM/VPL**). Modified from The Mouse Brain in Stereotaxic Coordinates (Paxinos and Franklin, 2001).

The finding that the highest *Cln5* expression levels were found in microglia indicated a possible important role for *Cln5* in these cells, which are important key players of the immune system in the CNS. The study of the microglial activation marker F4/80 indicated earlier that microglial activation would not take place before 12 months of age (von Schantz *et al.*, 2009). In contrast, in this thesis project the

microglial markers CD68 and IBA-1 indicated significant activation already at the age of 3 months in the studied regions S1BF and VPM/VPL (**Figure 12 and II; Figure 2**). Microglial activation in 1 month old mice was not significant yet but showed trends towards activation. IBA-1 stained cells also presented changes in morphology from the branched resting state towards an amoeboid active state in 3 months old *Cln5* ko mice compared to wt controls (**Figure 5 and II; Figure 2**). Unbiased thresholding image analysis of CD68 stained mouse brain sections verified the observations (**II; Figure 3**). The microglial activation was not confined to these regions but was widespread throughout the CNS, being most evident in other thalamic relay nuclei and cortical regions (somatosensory and auditory) as well as in the subiculum and substantia nigra. This, together with the finding that *Cln5* expression was enhanced in primary cultured microglia upon LPS induction, encouraged us to assess whether the immune response is altered in primary cultured microglia. LPS has been shown to trigger the expression of inflammatory mediators like interleukin 1 (IL-1), IL-6, reactive oxygen species (ROS), nitric oxide (NO) and tumor necrosis factor α (TNFα) in several cell types including microglia (Block *et al.*, 2007; Suzumura *et al.*, 2006). Therefore, the cytokine secretion from *Cln5* ko microglia was measured with and without LPS stimulation and compared to wt secretion profiles. However, no significant changes were detected between *Cln5* ko and wt microglia when 40 different cytokines were analysed (**II; suppl. Figure 1**). These results suggest that *Cln5* expression is upregulated in response to inflammatory stimuli (**II; Figure 1C**) but has no influence on the inflammatory response itself. However, further studies are required to assess whether the upregulated *Cln5* gene expression reflects Cln5 protein levels. Further, it would be of interest to analyse if purified Cln5 protein has an effect on microglial cells.

The circumstances defining whether microglial activation is harmful or beneficial to neuronal survival remain largely unclear. Microglial activation seems to be crucial for host defence and neuron survival, but overactivation of microglia causes destructive and neurotoxic consequences (Block *et al.*, 2007). The link between LPS stimulation and enhanced *Cln5* expression remains to be solved.

Next, possible myelination defects suggested by previous gene expression analyses and MRI studies in patients were investigated (Holmberg *et al.*, 2000; Kopra *et al.*, 2004; Rapola *et al.*, 1999; von Schantz *et al.*, 2008). Therefore, the volumes of white matter structures of the corpus callosum (cc) and internal capsule (ic) from Nissl stained brain sections from 1 and 3 month old *Cln5* ko and wt mice were quantified but did not indicate any significant changes at these ages. Myelin basic protein (MBP) was used as a marker to investigate the overall myelination within the brain. No alterations in white matter structures were observed but clearly disturbances in the myelination in the superficial laminae of the cortical region S1BF at the age 1 and 3 months of age were observed (**Figure 12 and II; Figure 4, suppl. Figure 2**).

Unexpectedly, LFB staining showed less staining in white matter structures in *Cln5* ko mice, but this could reflect the lipid metabolism changes in the knockout mice (discussed in detail later) as LFB is bound by lipids (**II; suppl. Figure 3)**.
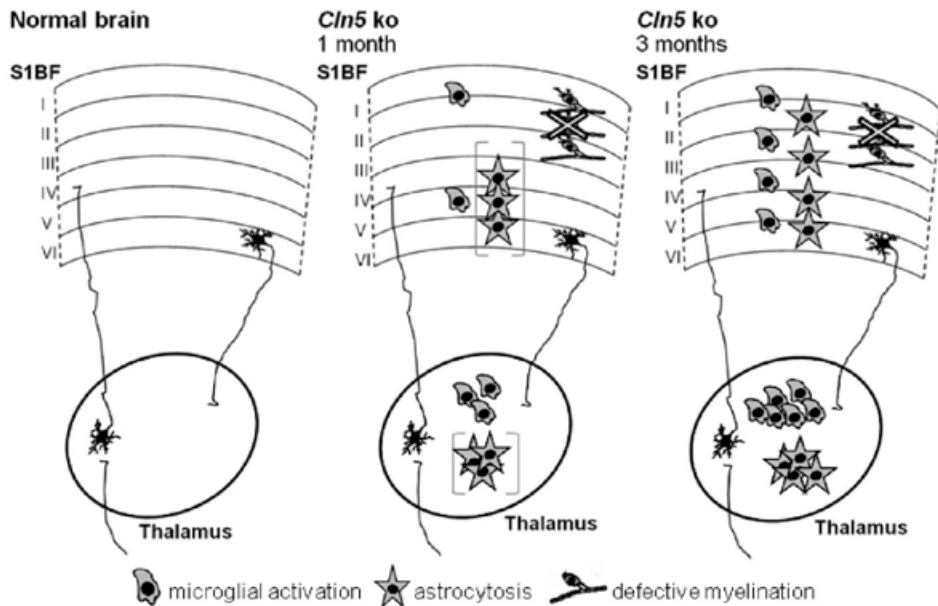

Figure 12: overview of the pathologic patterns taking place in young *Cln5* ko mice at 1 and 3 months of age. On the left a simplified normal organisation of thalamocortical pathways between the S1BF and VPM/VPL regions are presented. Sensory afferents reach thalamic relay neurons, which project mainly to lamina IV granule neurons. In turn, cortico-thalamic feedback neurons are mostly located in lamina VI. No neuron loss was detected in 3 month old in *Cln5* ko mice (**III**) and therefore no loss is predicted for 1 month old *Cln5* ko mice. Microglial activation is slightly elevated in 1 month old *Cln5* ko mice and is significant at 3 months of age (**II**). Activated microglia are found more prominent in the thalamic region at these age points compared to the cortex. Reactive astrocytosis has been detected in both regions of 1 month old *Cln5* ko mice, but these mice were in a different background (in brakets; von Schantz *et al.*, 2009). Herein, 3 month old *Cln5* ko mice were tested and presented reactive astrocytosis in the S1BF and VPM/VPL region (**III**). Significant defective myelination was detected in both age points in the superficial laminae of the S1BF region, but not in white matter structures (**II**).

In vitro differentiation studies of neurospheres towards mature oligodendrocytes by growth factors revealed a clearly delayed differention in *Cln5* ko cells supporting the suggestion of defective myelination in oligodendrocytes (**II, Figure 5**). Oligodendrocyte precursor cells (OPCs) were proliferated and differentiated towards mature myelinating oligodendrocytes (**see Figure 4**). In the early stages (4 days differentiation conditions) no differences in the morphology of NG-2 positive cells were observed in *Cln5* ko cells compared to wt OPCs. At later stages (7-10 days differenti-

ation conditions) MBP immunostaining presented differences in morphology. MBP specifically stains differentiated oligodendrocytes, but in contrast to the large flattened shape in wt OLs, *Cln5* ko OLs displayed numerous ramified processes and a small cell soma (**II; Figure 5**).

In the light of these results it is likely that the decreased MBP staining in the cortex of *Cln5* ko mice is due to a defective myelination process or is reflecting loss of pre-existing myelin. The number of neurons is not affected in 3 month old *Cln5* ko mice in the S1BF and VPM/VPL region (**Figure 12 and III; Figure 5**) supporting the hypothesis that there may be a defect in OLs themselves as lack of MBP staining does not reflect neuron loss. Also, the *in vitro* studies pinpoint towards defects in the OLs. Prior to this thesis, reactive astrocytosis has been detected in 1 month old *Cln5* ko mice of different background than studied here (von Schantz *et al.*, 2009). Herein, 3 month old *Cln5* ko mice were analysed and reactive astrocytosis was also detected at this age point (**Figure 12 and III; Figure 3**). Therefore, it will be interesting to examine if these two events are linked to each other as reactive astrocytosis has been connected to support remyelination (Shields *et al.*, 2000; Talbott *et al.*, 2005). Astrocytes secrete various factors which have been shown to coordinate complex responses by other cell types (Moore *et al.*, 2010). Among these secreted factors are platelet-derived growth factors (PDGF), which have been reported to influence oligodendrogenesis as the PDGF-α receptor is a phenotypic marker for OPCs (Moore *et al.*, 2010). PDGF-α expression has been presented to lead to increased OPC proliferation following focal demyelinating lesions (Vana *et al.*, 2007; Woodruff *et al.*, 2004). Also, conditioned media of astrocytes has been shown to increase oligodendrocyte differentiation (Moore *et al.*, 2010). Hence, astrocytes may promote myelin repair by e.g. PDGF-related signalling in the early stages of CLN5 disease, and possibly other NCL diseases until the capacity to repair the damages is reduced by time. Another interesting aspect for future studies is the interplay between microglia and astrocytes. Pro-inflammatory factors released by activated microglia have been shown to trigger reactive astrocytosis and inhibition of microglia resulted in suppressed reactive astrocytosis (Zhang *et al.*, 2010). Therefore, it would be interesting to study whether the inhibition of microglia has an effect on the pathology of *Cln5* ko mice.

In conclusion, loss of functional Cln5 leads to widespread early inflammation in the CNS (microglial activation and reactive astrocytosis) and defective myelination preceding neuronal degeneration. These findings give valuable information about the timing of pathological events in *Cln5* ko mice and point out the necessity to study the interplay between different cell types of the CNS in CLN5 disease.

5.2.2 *Cln5* ko mice present disturbances in systemic lipid metabolism (II)

Alterations in lipid metabolism has been linked to many neurodegenerative diseases, including NCLs (Ahtiainen *et al.*, 2007; Haidar *et al.*, 2006; Jalanko *et al.*, 2006; Lyly *et al.*, 2008; Lyly *et al.*, 2009; Narayan *et al.*, 2006; Winter and Ponting, 2002) (**see 2.4.2**). Dysregulated cholesterol metabolism has been linked to *Cln1* ko mice (Lyly *et al.*, 2008) (**see 2.4.2**). Further, sphingolipid metabolism was shown to be affected in NCLs. It was demonstrated that *Cln10* ko mice displayed increased levels of several gangliosides, molecules composed of a glycosphingolipid containing one or more sialic acids connected to the sugar chain, especially monosialogangliosides (GM2, GM3 and GD3) and bis(monoacylglycero)-phosphate (BMP) in the mouse brain were increased (Jabs *et al.*, 2008). It was further specified that GM2 was mainly accumulated in neurons and GM3 increased in glial cells (Jabs *et al.*, 2008). Recently, a review pointed out that human CLN9-deficient fibroblasts [the putative gene affected in CLN9 disease] contained lower amounts of ceramide and decreased ceramide synthase activity (Ben-David and Futerman, 2010). Overexpression of ceramide synthase was shown to partially rescue the phenotype, suggesting a possible regulative role of CLN9 for the ceramide synthase (Ben-David and Futerman, 2010).

To obtain insights whether the lipid homeostasis might be altered in general in *Cln5* ko mice, major lipid parameters from mouse serum derived from 1 month old mice were studied and the transport of cholesterol and sphingolipids in macrophages was analysed (**II; Figure 6-7**). Total cholesterol levels and phospholipid transfer protein (PLTP) activity were significantly increased in *Cln5* ko mice compared to wt mice, whereas no differences in triglyceride and apoA-I levels were observed (**see 4.1.18 and II for methods and Figure 6**). Further, fractionation by FPLC revealed that cholesterol was mainly found in HDL particles (**II; Figure 6**). Increased PLTP activity in *Cln5* ko serum supported this finding since PLTP has been reported to play a role in the transfer of cholesterol and phospholipids from cells to lipoprotein particles by interaction with ABCA1 (Oram *et al.*, 2003). Further, increased cholesterol transfer to apolipoproteins was verified by cell studies. Cholesterol efflux from peritoneal macrophages towards the major apolipoprotein of HDL, apoA-I, was significantly increased in *Cln5* ko compared to wt cells (**II; Figure 7**), whereas the uptake of cholesterol was similar in *Cln5* ko and wt peritoneal macrophages.

It has been reported earlier that CLN1/PPT1, CLN5 and the mitochondrial F_1-ATPase synthase interact *in vitro* (Lyly *et al.*, 2008; Lyly *et al.*, 2009) and the latter has been shown to act as a receptor for apoA-I (Martinez *et al.*, 2003). Further, some NCL models display mitochondrial alterations (Das *et al.*, 1999; Fossale *et al.*, 2004; Lyly *et al.*, 2008; Siakotos *et al.*, 1998). The cell surface distribution of the α- and β-subunits of the mitochondrial ATP synthase has been shown to be increased in *Cln1*

ko neurons detected by total internal reflection fluorescence (TIRF) microscopy (Lyly *et al.*, 2008). Correspondingly, apoA-1 uptake has been presented to be increased in *Cln1* ko neurons. Herein, the cell surface distribution of α- and β-subunits of the mitochondrial ATP synthase was also analysed by TIRF analysis in *Cln5* ko neurons but no changes were detected compared to wt neurons. This indicates that the possible defect in CLN5, linked to ATP synthase is not analogous to CLN1 disease. In conclusion, serum lipid analyses pinpoint to opposite roles in lipid metabolism for Cln1 and Cln5. **Table 8** summarises the general findings in *Cln1* ko and *Cln5* ko mice.

Wt vs. Mouse model	*Cln1* ko	*Cln5* ko
PLTP activity	↓	↑
Total cholesterol	↓	↑
ApoA-I	↓	-
Cell surface distribution of the α/β SU of the mF$_1$-ATPase in neurons	↑	-
Triglycerides	-	-
ApoA-I uptake	↑ (in neurons+glia)	- (in macrophages)
ApoA-I efflux	n.d.	↑ (in macrophages)
Cholesterol increased in	n.d.	HDL

Table 8: overview of the detected changes in serum lipid analyses and cell studies in *Cln1* ko (Lyly *et al.*, 2008) and in *Cln5* ko mouse (study II) models compared to wt mice. Abbreviations: n.d., not determined; α/β SU of mF$_1$-ATPase, α/β subunits of the mitochondrial F$_1$-ATPase.

In this study, sphingolipid transport was also shown to be affected in peritoneal macrophages and MEFs of *Cln5* ko mice. Fluorescent glycosphingolipid BODIPY-Lactoceramide was transported slower from endo-lysosomes to the Golgi apparatus compared to wt cells (**see 4.1.18 and II; Figure 8**). This is characteristic for sphingolipid storage diseases and therefore indicates that CLN5 disease may also display features of sphingolipidoses. It is noteworthy that sphingolipids are especially enriched in the myelin sheath and important for maintaining myelin in the CNS (Piccinini *et al.*, 2010). Hence, the altered sphingolipid transport and the defective myelination may be connected, which will be interesting to study in the future. This finding also suggests that CLN5 protein may be involved in lipid transport or their signalling pathways. As described in the literature review in chapter 2.3.1 ABC transporters are important key players in cholesterol efflux to the extracellular space and have been reported to be connected to another NCL protein, namely CLN10/Cathepsin D (Haidar *et al.*, 2006). The study of Haidar *et al.*, reported that reduction of CLN10/Cathepsin D leads to reduced ABCA1 levels and consequently

to decreased cholesterol efflux. In addition, ABCA1 is known to be higly expressed in microglia and ABCA2 has been reported to mediate intracellular shingolipid transport and myelin maturation (Kim *et al.*, 2008). It would be of high interest to investigate whether these transporters are also affected in CLN5 disease.

5.3 CLN5 and its interaction partner CLN1/PPT1 (III + unpubl.)

5.3.1 CLN1/PPT1 rescues the trafficking of mutated CLN5 to the lysosomes (unpublished)

Interactions between CLN5 and other NCL proteins have been suggested previously *in vitro*, including CLN1/PPT1, CLN2/TPP1, CLN3, 6 and 8 (Lyly *et al.*, 2009; Vesa *et al.*, 2002). Our group has previously shown that the lysosomal localisation of CLN5 carrying the most common disease-causing mutation, p.Y392X, can be restored by co-expressing wt CLN1/PPT1 supporting interactions between these two proteins (Lyly *et al.*, 2009). In contrast, co-expression of the mutated CLN5 protein with other NCL proteins did not result in correction of the lysosomal trafficking (Lyly *et al.*, 2009). Based on this finding, the study of this interaction was expanded in order to investigate whether PPT1 could restore the trafficking of CLN5 proteins carrying different disease-causing mutations. Therefore, PPT1 was transiently over-expressed with mutated CLN5 constructs carrying p.D279N or p.E253X in SH-SY5Y cells. The impact of PPT1 on the trafficking of the mutated CLN5 proteins was analysed by confocal microscopy and LAMP-1 was used as a lysosomal marker (**Figure 13 C,G,K,O,S,W**). Single transfection of the mutated CLN5 constructs lead to ER retention in SH-SY5Y cells (**Figure 13 I-L, Q-T**), but co-transfection with wt PPT1 dramatically changed the intracellular localisation of the mutated CLN5 proteins from ER retention towards vesicular distribution and co-localised with PPT1 and the lysosomal marker LAMP-1. It is noteworthy that mutated CLN5 had no effect on the intracellular localisation of PPT1.

These results indicate that the folding of the analysed mutated CLN5 proteins is probably not that severely affected due to the fact that PPT1 is still able to bind to the mutated CLN5 proteins and they can traffic to the lysosomes. The mutations possibly hit amino acids important for the function of CLN5 or disturbing other important interactions of the protein. However, the molecular basis of the interaction between these two NCL proteins remains elusive at this point. It could be speculated that PPT1 might act as a chaperone or is somehow facilitating the trafficking of CLN5 protein. This is interesting in particular as CLN5 was still able to traffic to lysosomes in MPR-deficient cells, indicating that CLN5 can utilise MPR-independent routes to reach lysosomes (**I; Figure 3**). It has been reported earlier that also PPT1 itself behaved differently from classical soluble lysosomal enzymes which utilise the MPR-dependent pathway (Lyly *et al.*, 2007). Mutating the glycosy-

lation site that was mostly involved in the MPR receptor binding did not affect the localisation of PPT1 *in vitro*.
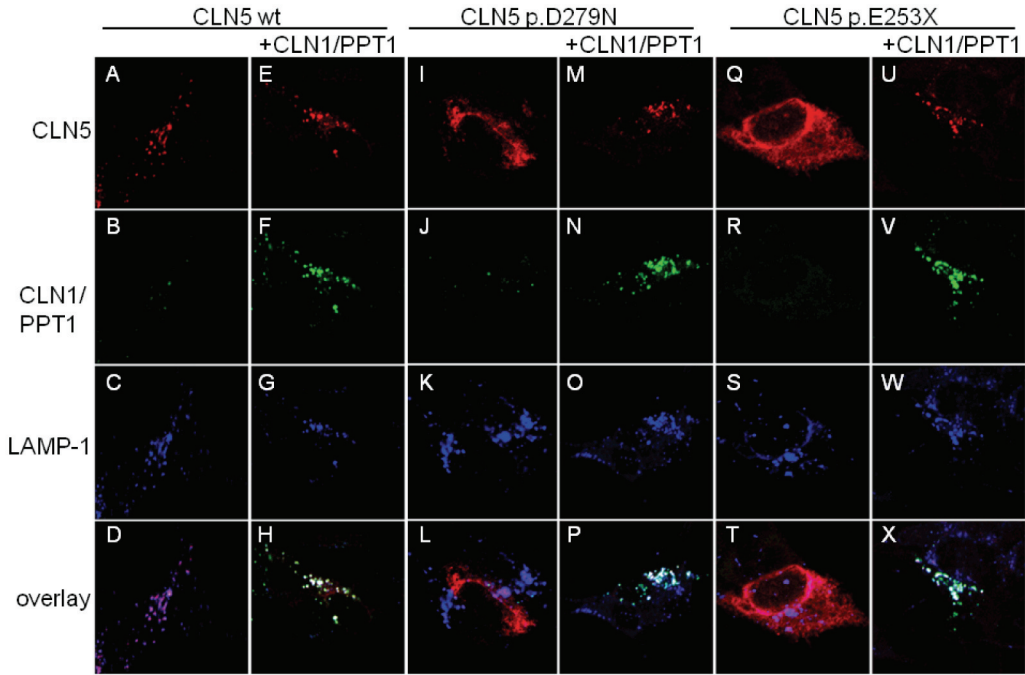

Figure 13: Rescued trafficking of mutant CLN5 by co-expression with wild-type (wt) CLN1/PPT1. SH-SY5Y cells were either transiently transfected alone with wt CLN5 (A-H), CLN5 carrying the p.D279N (I-P), p.E253X (Q-X) mutations or co-transfected with wt CLN1/PPT1 (E-H, M-P, U-X). Localisation of wt and mutant CLN5 protein was accessed through immunofluorescence with triple-staining for CLN5 (A,E,I,M,Q,U), CLN1/PPT1 (B,F,J,N,R,V), and lysosomal marker LAMP-1 (C,G,K,O,S,W). Stained cells were analysed by confocal microscopy and co-localisation is indicated by: CLN5 and LAMP-1 – pink; CLN5 and CLN1/PPT1 - yellow; CLN5, CLN1/PPT1 and LAMP-1 –white

5.3.2 Basic characterisation of *Cln1/5* dko mice (III)

Since *in vitro* studies and gene expression profiling of knockout mouse models have linked the NCL proteins PPT1 and CLN5 and suggest common pathogenic mechanisms, our aim was to further study the putative common pathways by generating a *Cln1/5* double knockout (*Cln1/5* dko) mouse (**see 4.1.1**) and to analyse its basic pathology. It could be expected that if *CLN1* and *CLN5* share common pathways, a knockout of both genes would result in a very severe disease. The double knockout mice were fertile but displayed a slight reduction in Mendelian breeding ratios (**III; suppl. Table 1**). The decreased number of expected offspring indicated possible defects in breeding or early development of *Cln1/5* dko mice. Previous studies with lysosomal storage disorders have indicated dysregulated formation of embryoid bodies from induced pluripotent stem cells (iPS-cells) (Meng *et al.*, 2010) and, therefore, iPS cells of wt and *Cln1/5* dko MEFs were generated. Morphologically selected clones, which also expressed the ES cell-specific markers SSEA-1; Nanog, Rex1, E-ras, Esg-1 and Fgf-4 (**III; suppl. Figure 2**) were chosen for embryoid body (EB) formation and further experiments. Microscopic follow up and diameter measurements revealed significantly smaller and irregular formed *Cln1/5* dko EBs compared to wt EBs up to 7 days (**III; Figure 2**). After 7 days *Cln1/5* dko EBs seemed to catch up and differences became less prominent pinpointing to defects in early development of EBs. In addition, spontaneous differentiation was also delayed in *Cln1/5* dko EBs (**III; Figure 2**).

At the age of 3 months the *Cln1/5* dko mice showed severe symptoms with balance problems and seizures (**described in III**) and the body weight was significantly lower compared to wt mice (**III; suppl. Figure 1**). The onset of symptoms was way earlier than in the single knockout mice. For *Cln1* ko mice, the onset of symptoms has been reported to be from 5 months onwards and for *Cln5 ko* mice only after 8 months (Jalanko *et al.*, 2005; Kopra *et al.*, 2004). The accumulation of autofluorescent storage material of 3 month old mice was studied in wt, *Cln1ko*, *Cln5 ko* and *Cln1/5* dko brains. It was highly prominent in *Cln1/5* dko, a bit less in *Cln1* ko mice and almost absent in *Cln5* ko and wt mice (**III; Figure 1**). The ultrastructure of the storage material in 3 month old *Cln1/5* dko mice was analysed by electron microscopy and displayed mainly GRODs and few rectilinear-like membranous ultrastructures (**III; Figure 1**). Further, periodic acid Schiff (PAS) staining revealed storage material in cortical neurons and glia in *Cln1/5* dko mice, but not in single-knockout or wt mice (**described in III; data not shown**).

5.3.3 Glial activation and defective myelination precedes neuron loss
   Cln1/5 dko mice (III)

Since early immune activation, such as microglial activation and astrocytosis has been observed in *Cln1* ko and *Cln5* ko mice (Bible *et al.*, 2004; von Schantz *et al.*, 2009) (**see 5.2.1**), the glial activation was also studied in *Cln1/5* dko mice and was compared to the single-knockout and wt mouse brains focusing on the S1BF and VPM/VPL as representative regions (**see Figure 11**).

The extent of microglial activation was detected with a CD68 marker in immunohistochemical analyses. CD68 detected significant microglial activation in *Cln5* ko mice at the age of 3 months (**II; Figure 2+3**). Therefore, 3 month old mice were selected for the analyses. Importantly, the CD68 marker had not been used in immunohistochemical studies for *Cln1* ko mice so far. At the age of 3 months all three knockout mouse models presented widespread immunoreactivity, most prominent again in *Cln1/5* dko mice, then *Cln1* ko and less in *Cln5* ko (**Figure 14 and III; Figure 3**). As the extent of immunoreactivity was very intense in 3 months old *Cln1/5* dko mice, 1 month old *Cln1/5* dko mouse brains were also stained and compared to wt mice revealing increased reactivity at this young age and further supporting the early microglial activation as an important phenotypic outcome of NCL (**III; suppl. Figure 4**).

GFAP was used to detect the extent of reactive astrocytosis and immunohistochemical staining revealed very intense immunoreactivity in *Cln1/5* dko mice, strong in *Cln1* ko, a few GFAP positive cells in *Cln5* ko mice and almost none in wt mouse brains at the age of 3 months (**Figure 14 and III; Figure 3**). As the astrocytosis has been previously detected in the single ko mice already at 1 month, it is very likely that also *Cln1/5* dko mice display significant astrocytosis earlier than 3 months.

In this study, defective myelination was presented to be a phenomenon linked to *Cln5* ko mice (**II; see 5.2.1**), but this has not been previously studied in *Cln1* ko mice, although human studies have earlier implicated demyelination in CLN1 disease (Haltia *et al.*, 1973a). As in study II, MBP was used to detect possible myelination defects. As previously seen in *Cln5* ko mice, there were no clear differences in the MBP immunoreactivity in white matter structures. However, all three mouse models presented less MBP positive fibres (dorsoventrally and horizontally) through the superficial laminae of S1BF, most prominently again in the *Cln1/5* dko mouse brains, followed by *Cln1* ko and *Cln5* ko mouse models (**Figure 14 and III; Figure 4**). Our studies thus implicate that cortical loss of MBP positive fibres is a prominent pathological feature of two NCL models and it will be interesting to investigate whether this is a common feature in NCLs.

Neuronal loss and brain atrophy was studied from Nissl stained sections. Thickness and volume measurements of various brain regions were carried out to determine possible mouse brain atrophies. No cortical thinning or volume alterations were detected in *Cln1/5* dko *or Cln1* ko mice compared to wt control in 3 months old mice, but a slight increase in thickness of the S1BF, M1 and V1 region and cortical volume in *Cln5* ko mice was measured (**III; suppl. Figure 5**). This supports earlier findings, where mice increased cortical thickness measures have also been reported in 12 month old *Cln5* ko mice (von Schantz *et al.*, 2009). This finding may be comparable to the hydrocephalus which has been observed in some NCL patients (Lee *et al.*, 2003).

Neuronal loss was determined by stereological measurements in Nissl stained sections of thalamic VPM/VPL and neuron populations in three cortical laminae of the S1BF region. Lamina IV granule neurons receive thalamic innervations, and lamina V and lamina VI contain projection neurons which provide important feedback to the thalamus. Significant cortical neuron loss in the S1BF region was only detected in lamina VI in 3 month old *Cln1/5* dko mice, but not in the thalamic VPM/VPL regions (**Figure 14 and III; Figure 5**). In single-knockout mice the findings were different. In *Cln1* ko mice, significant neuron loss was observed in thalamic VPM/VPL at the age of 5 months, and in cortical S1BF lamina IV at the age of 7 months (Kielar *et al.*, 2007). In *Cln5* ko mice, significant neuron loss was detected in cortical S1BF lamina V at the age of 4 months, and in both thalamic VPM/VPL and cortical S1BF laminae IV and V at the age of 12 months, but no significant loss of neurons was observed in S1BF lamina VI (von Schantz *et al.*, 2009). Neuron loss in *Cln1* ko mice begins in the thalamus and subsequently occurs in the cortical region, whereas the sequence is opposite in *Cln5* ko mice and starts in the cortex. Therefore, neuron loss in *Cln1/5* dko resembles more the *Cln5* deficiency in a way that the loss starts from cortex. However, in *Cln1/5* dko mice the neuronal loss starts from S1BF lamina VI and in Cln5 in lamina V.

Pathological findings in *Cln1/5* dko compared to *Cln1* ko and *Cln5* ko mice at the age of 3 months are summarised in **Figure 14**. The main result from these analyses is the conclusion that glial activation and defective myelination precede neuronal loss in these NCL mouse models, which has also been observed in *Cln3* ko mice and *Cln6* ko sheep and may a common feature in NCLs (Oswald *et al.*, 2005; Pontikis *et al.*, 2004; Pontikis *et al.*, 2005).
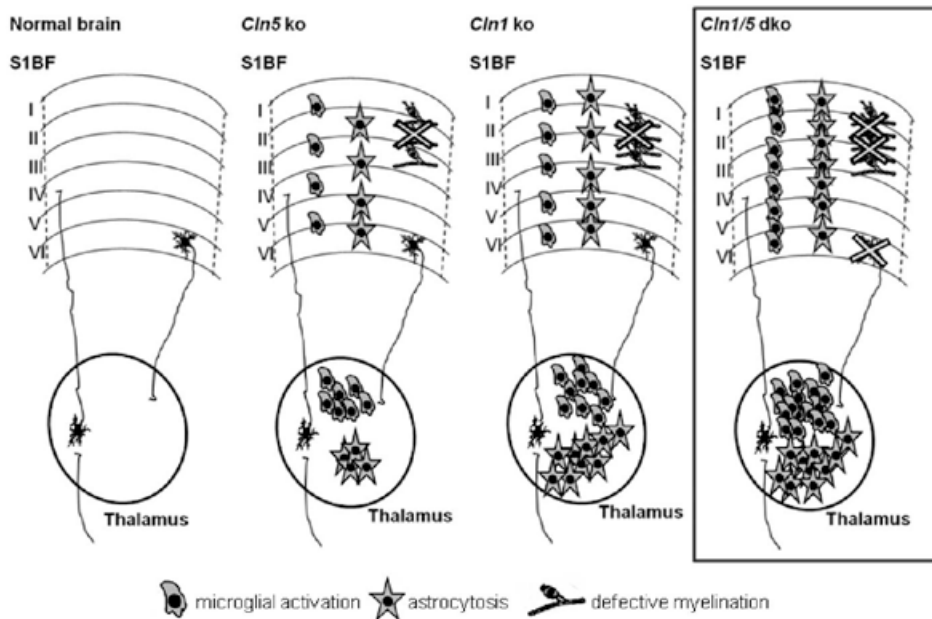
Figure 14: overview of the pathologic patterns in 3 month old *Cln5* ko, *Cln1* ko and *Cln1/5* dko mice. The schemes of the different mouse models are displayed from left to right according to the severity of pathologic findings. A simplified organisation of thalamocortical pathways between the S1BF and VPM/VPL regions is displayed. Sensory afferents extend to thalamic relay neurons, which project mainly to lamina IV granule neurons. In turn, cortical feedback neurons are found in lamina VI and project towards the thalamus. No neuron loss was detected in 3 month old neither in *Cln5* ko nor *Cln1* ko mice. In contrast, Lamina VI presented significant neuron loss in 3 month old *Cln1/5* dko mice. Microglial activation is present in all knockout models and most prominent in *Cln1/5* dko mice. In *Cln5* ko mice activated microglia are more prominent in the thalamus than in the cortex, which is also the case for *Cln1* ko mice. Reactive astrocytosis is present in all knockout mouse models and highly pronounced in the thalamus in *Cln1* ko and *Cln1/5* dko mice. Further, significant defective myelination was detected in the superficial laminae of the S1BF region in all knockout mouse models again being most prominent in *Cln1/5* dko mice.

5.3.4 Dysfunctional lipid metabolism is a common feature in *Cln1* ko, *Cln5* ko and *Cln1/5* dko mice (I+III)

Disturbed systemic lipid metabolism has been detected for both single knockout mouse models, *Cln1* ko (Lyly *et al.*, 2008) and *Cln5* ko (**II; Figure 6-8; see chapter 5.2.2**). Therefore, one aim of this thesis was to examine how the systemic lipid metabolism changes when both genes *Cln1* and *Cln5* are simultaneously deleted. The levels of total cholesterol, phospholipids, apoA-1, triglycerides, and PLTP activity in 1 month old female mouse serum were analysed (**Table 9**). The amounts of phospholipid and triglycerides in *Cln1/5* dko mice were significantly increased compared to the wt control (**III; Figure 6**). Interestingly, PLTP activity was highly and significantly elevated in *Cln1/5* dko mice compared to wt mice (**Table 9 and III; Figure 6**), exceeding the previously observed increase in *Cln5* ko serum (**Table 8 and II; Figure 6; see chapter 5.2.2**). Total cholesterol levels were slightly increased but not significantly unlike in *Cln5* ko samples. The detected changes in phospholipid and cholesterol levels can be linked to the increased PLTP activity, as PLTP has been shown to maintain HDL cholesterol levels in serum (Zannis *et al.*, 2008). Therefore, the distribution of lipids and apoA-1 in lipoprotein fractions was analysed in *Cln1/5* dko and wt serum. As previously shown herein, cholesterol was found to be clearly increased in HDL particles in *Cln1/5* dko serum (**Table 9 and III; suppl. Figure 6**). In addition, cholesterol levels were slightly decreased in VLDL particles (**III; suppl. Figure 6**). Also, the amount of phospholipids and apoA-1 were clearly elevated in both small and large HDL particles (**Table 9 and III; suppl. Figure 6**). These findings might relate to the increased PLTP activity seen in *Cln1/5* dko mice, as PLTP induces the formation of lipid-poor pre-β-migrating HDL particles (Vikstedt *et al.*, 2007). Further, elevated triglyceride levels were found in VLDL particles (**Table 9 and III; suppl. Figure 6**).

Wt vs. mouse model	*Cln1* ko	*Cln5* ko	*Cln1/5 dko*
PLTP activity	↓	↑	↑↑
Total cholesterol	↓	↑	-
ApoA-I	↓	-	-
Triglycerides	-	-	↑
Phospholipids	n.d.	n.d.	↑
Cholesterol increased in	n.d.	HDL	HDL
ApoA-I increased in	n.d.	n.d.	HDL
Triglycerides increased in	n.d.	n.d.	VLDL
Phospholipids increased in	n.d.	-	HDL

Table 9: overview of the detected changes in serum lipid analyses of 1 month old *Cln1* ko, *Cln5* ko and *Cln1/5* dko mice compared to wt.

In summary, these results verify that lipid homeostasis is disturbed in NCL mouse models outside the CNS. It is most likely that this is also the case in the CNS, as disturbed lipid metabolism has been linked to neurodegeneration in general. Cholesterol is known to be present in the myelin sheath and, therefore disturbed cholesterol metabolism might have an impact on the myelin assembly and contribute to the loss of myelin seen in *Cln1* ko, *Cln5* ko and *Cln1/5* dko mice. Further studies are required to clarify the signalling pathway connections and possible interaction partners related in lipid metabolism. Also, lipid trafficking studies focusing on cells of the CNS may give further insights into the basic mechanisms underlying these devastating diseases.

5.3.5 Gene expression profiling of *Cln1/5* dko mouse brain (III)

To detect changed gene expression levels in 1 month old *Cln1/5* dko mice, global gene expression of about 45 000 genes was analysed from cortex samples. Statistically significant upregulation of 24 genes and downregulation of 31 genes were detected (**III; suppl. Table 2**). Cyclase-associated protein 1 (*Cap1*, 1.9-fold) was found to be the most prominently upregulated gene, and other upregulated genes included complement subcomponents C1qb (*C1qb*, 1.6-fold) and C1qc (*C1qc*, 1.4-fold), Fc receptor homolog S (*Fcrls*, 1.6-fold) and glial fibrillary acidic protein (*GFAP,* 1.5-fold). The most downregulated gene was α-synuclein (*Snca*, -177.2-fold) and downregulation of oligodendrocytic myelin paranodal and inner loop protein (*Opalin*, -1.8-fold) and other myelin related genes (myelin and lymphocyte protein *Mal*, -1.6-fold, myelin associated glycoprotein *Mag*, -1.6-fold, myelin oligodendrocyte glycoprotein *Mog*, -1.5-fold,

proteolipid protein Plp1, -1.2-fold and myelin basic protein *Mbp*, -1.2-fold) were also detected.

DAVID Functional Annotation Clustering was used to study the affected pathways in 1 month old *Cln1/5* dko mice. Pathways linked to immune response were upregulated, and pathways linked to myelin ensheathment and nerve impulse transmission were downregulated (**III; suppl. Table 3**). These findings are consistent with detected changes in nerve ensheathment and myelination, and upregulation of inflammation associated pathways in *Cln1* ko mouse brain and neuron cultures (Ahtiainen *et al.*, 2007; von Schantz *et al.*, 2008). The *Cap1* is a gene, which is upregulated in all three mouse models (*Cln1* ko, *Cln5* ko and *Cln1/5* dko) plays an important role in neuronal growth cone-cytoskeletal dynamics (Ahtiainen *et al.*, 2007; von Schantz *et al.*, 2008; **III**). The gene expression analysis data is in line with the results from immunohistochemical studies, which revealed glial activation and loss of cortical myelin in *Cln1/5* dko mouse brains (**III; Figure 3-4; see 5.3.3**). Hence, these findings seem to be accurate and relate to the disease progression.

The downregulation of the α-synuclein gene expression in *Cln1/5* dko mouse cortex was not detected in single knockout mouse models previously. To analyse if the α-synuclein is downregulated at the protein level as well, immunohistochemical staining of α-synuclein in wt, *Cln1* ko, *Cln5* ko and *Cln1/5* dko brain sections were performed. Reduced α-synuclein staining in the cortical neuropil of *Cln1/5* dko mice was observed, but not in thalamic regions (**III; Figure 7**). Western blotting of whole brain lysates from 1 month old mice showed highly reduced α-synuclein protein expression in three out of five *Cln1/5* dko brain lysates, but was always present in wt and the single knockout mouse brain samples (**III; Figure 7**). This variation might reflect the decreased α-synuclein expression detected in the cortex, but probably not in the thalamus. α-synuclein has been reported to be upregulated in many neurodegenerative diseases (Vekrellis *et al.*, 2011) and was shown to be upregulated in cultured neurons of previously reported *Cln1* ko mouse model (Ahtiainen *et al.*, 2007). However, this model was in a different background than the one used in study III and cultured neurons instead of mouse cortex were studied. It has been reported that α-synuclein is a presynaptic protein, which plays a role in the regulation of dopaminergic transmission, synaptic plasticity, and vesicle trafficking (Ruiperez *et al.*, 2010; Uversky, 2008). Mice lacking α-synuclein display neurochemical, electrophysiological, and behavioural defects (Abeliovich *et al.*, 2000). Lipid-binding was suggested for α-synuclein as another function (Chua and Tang, 2011). Hence, α-synuclein and lipid metabolism might be involved in NCL pathology in general.

In summary, the findings of the gene expression analysis supply additional information about the pathways affected in the early stages of NCL diseases. Overall, NCL proteins may be involved in the development of the nervous system.

6 Conclusions and future prospects

In the past 10 years the pathology and molecular biology of the proteins behind CLN1 and CLN5 diseases have been studied using mouse and cell models and have furthered our understanding of these devastating diseases. When this PhD project was initiated, the *in vitro* function and 3D structure of CLN1/PPT1 had been described and the pathology of *Cln1* ko mice had been extensively studied. In contrast, less was known about the CLN5 protein. For example, localisation and solubility was discussed controversially. This project was initiated to clarify the maturation and localisation in the cell of normal and mutated CLN5 protein, to further characterise the pathology of *Cln5* ko mice and to analyse the *Cln1/5* dko mouse model in order to gain new insights behind NCLs in general.

One major finding of this project was on the maturation of the CLN5 protein. It was shown that the four pre-proforms of CLN5 undergo N-terminal signal peptide cleavage in the ER. All constructs resulted in one proform independent of the position of the starting methionine (M1-M4). The proform of CLN5 then acquires high mannose sugars in the ER, traffics further to the TGN, where complex type sugars are added. Finally the protein traffics to the lysosomes *via* MPR-dependent or independent pathways. These results lead to further questions which need to be clarified: for example, which is the MPR-independent route to the lysosomes? Also, the structure and function of the CLN5 protein remain unknown. Further, the gene expression levels of *Cln5* in cells of the CNS were measured. It was found that *Cln5* expression levels were highest in cultured microglia from *C57BL/6JRcc* mice. Also, it was shown that *Cln5* expression rises gradually in these mice up to 3 months of age and then reaches a plateau. However, the question remains if the mRNA levels reflect the protein levels. Further, it would be interesting to study if *Cln5* expression decreases at older age points than 5 months. If there is any functional defect in microglia caused by loss of functional Cln5, also needs to be assessed in the future.

Another major finding was the link between Cln5 and lipid metabolism. First evidence was provided that *Cln5*-deficiency leads to disturbed systemic cholesterol and BODIPY-Lactoceramide transport. It remains to be studied whether this defect is a direct or secondary effect and if the lipid transport within the CNS is affected. However, these results pinpoint to a connection between CLN5 and lipid metabolism in serum lipid components and peritoneal macrophage lipid transport. Interestingly, it has been shown that patients with MS display early cortical demyelination (Lucchinetti *et al.*, 2011). This observation was confirmed in this thesis work in *Cln5* ko mice as well. Lucchinetti *et al.*, (2011) suggest that cortical neuron loss may be directly linked to inflammatory demyelination, and hence recommend attempts to

inhibit inflammation to protect neurons. This is an interesting aspect which might be helpful for CLN5 patients or even for NCL diseases in general.

Herein, it was presented that CLN1/PPT1 can rescue the lysosomal trafficking of all analysed mutated CLN5 constructs *in vitro*. It was shown earlier that CLN1/PPT1 and CLN5 can interact *in vitro* and gene expression studies of *Cln1* ko and *Cln5* ko mouse brains pinpointed to common affected pathways (Lyly *et al.*, 2009; von Schantz *et al.*, 2008). Now, the basic characterisation of the newly generated *Cln1/5* dko mice further underlined the possible interactions of *Cln1* and *Cln5* gene products, as loss of both genes caused a more severe clinical NCL phenotype in these mice than in the single-knockouts. Enhanced accumulation of autofluorescence material, enhanced astrocytosis and microglial activation, defects in cortical myelination and the GROD ultrastructure in *Cln1/5* dko mice closer resemble the more severe pathological features of *Cln1* ko mice than *Cln5* ko mice, while the onset of neuronal loss closer resembles *Cln5* ko mice.

Finally, it was demonstrated in this thesis work that reactive astrocytosis and microglial activation precede neuronal death in *Cln5* ko and in *Cln1/5* dko mice. Glial cell pathology has been recognised before in several CNS degenerative disorders. Therefore, it may be that the basic causes in CLN5 disease are dysfunctions in glial cells leading to a disturbed cross-talk between neurons and glia, which in turn leads to neurodegeneration. Neuron-glia interaction studies and functional analyses of these diverse cells of the CNS are required to gain more insights into NCLs in general. As microglia and astrocytes seem to play an important role in the pathology of CLN5 it would be interesting to investigate the integrity of the blood-brain-barrier (BBB) in *Cln5* ko mice. For instance, the cortex is highly vascularised and the BBB is affected in many neurodegenerative diseases (Baeten and Akassoglou, 2011), and has been very recently shown to be affected in a *Cln1* ko mouse model (Saha *et al.*, 2012). Further, it would be important to check, whether some sort of peripheral cell recruitment to the affected BBB then takes place (e.g. leucocytes) due to a potential defective BBB in *Cln5* deficient models. A very recent publication has proposed a mechanism behind neurodegeneration (Sundaram *et al.*, 2012). They report that cyclin-dependent kinase 5 (Cdk5) is deregulated by p25 in several neurodegenerative diseases such as PD and AD (Sundaram *et al.*, 2012). Further, Sundaram *et al.* propose that hyperactivation of p25/Cdk5 leads to upregulation of phospholipase A2 (PLA2). PLA2 hydrolyses phosphatidylcholine to a soluble lipid factor lysophosphatidylcholine (LPC), which in turn activates glia to produce cytokines/chemokines and causes leucocytes to infiltrate the brain and subsequently trigger neurodegenerative disease progression. Whether this p25/Cdk5/LPC signalling plays a role also in NCL disease progression would be essential to be assessed.

It is known that astrocytes and microglia screen along the BBB. Astrocyte scars can be an attempt of neuroprotection to form barriers for microglia (Baeten and Akassoglou, 2011). Additionally, recent results indicate that astrocyte attenuation of *Cln1* ko mice by generating a *GFAP/Vimentin/Cln1* triple knockout mice exabertates neuroinflammation in the CNS (Macauley *et al.*, 2011). Therefore, they suggest a protective role for the upregulation of the intermediate filaments (vimentin and GFAP) in *Cln1*-deficiency, which might be a general phenomenon in NCLs and common in neurodegenerative diseases. Further, our studies present that two NCL mouse models share several features, like microglial activation, lipid disturbances and reactive astrocytosis, which are universal features for most neurodegenerative diseases and even are exabertated when both genes are dysfunctional. As defective cortical myelination is also found in MS patients, this may implicate that this pathology might be a common feature in NCLs or even in neurodegenerative diseases.

No therapeutic attempts have been made for CLN5 disease so far, but as CLN5 protein is a soluble lysosomal enzyme, combination of different therapy forms might be a fruitful approach. Combination therapy has been very recently reported to be extremely beneficial and superior to single therapy approaches in *Cln1* ko mice (Macauley *et al.*, 2012; Roberts *et al.*, 2012). *Cln1* ko mice were treated with adeno-associated virus (AAV) 2/5-PPT1 mediated gene therapy in combination with the systemic delivery of the lysosomotropic PPT1 mimetic phosphocysteamine (Roberts *et al.*, 2012). Also, a second approach using AAV2/5-PPT1 mediated gene therapy in combination with bone marrow transplantation in newborn *Cln1* ko mice was a fruitful approach (Macauley *et al.*, 2012). The treated *Cln1* ko mice presented biochemical and histological improvements, their lifespan was dramatically increased, and motor function was sustained. These findings are substantial for the development of therapeutic strategies to find a cure for NCLs patients in the future. Moreover, iPS cell research might be beneficial for the development of therapies as these cells have characteristics of self-renewal and pluripotency, which makes disease modelling, drug screening, and cell replacement therapy possible (Jung *et al.*, 2012). Neurons have been differentiated from iPS cells and represented the *in vivo* phenotype in Parkinson's disease (Jung *et al.*, 2012). In this case, iPS cell derived dopaminergic neurons gave a positive therapeutic effect in a rodent Parkinson's disease model (Jung *et al.*, 2012). Disease specific iPS cells could be derived from CLN5 patients and be utilised for drug screenings, disease modelling and may be even used for cell replacements therapy in the future.

7 Acknowledgements

Docents Eija Jokitalo and Mikko Hiltunen are thanked for reviewing my thesis and for providing helpful and encouraging comments. Elina Ikonen and Outi Kopra are warmly thanked for being part of my thesis committee, for providing valuable input for my thesis throughout the years and for the fruitful collaboration. Your encouragements in the thesis committee meetings meant a lot to me! I am grateful to Professor Anu Wartivaara for accepting the role of opponent in my thesis dissertation.

I am grateful to my supervisors, adjunct professor Anu Jalanko and adjunct professor Aija Kyttälä, for guiding me through the thesis jungle. Anu, you gave me the freedom to grow from a little biochemist to an independent scientist. You were always supportive. Aija, you guided me through the first part of the thesis and helped me with the paper jungle in the end. Thank you both for the motivation and encouragement. I learned how to write an article, submit and work through reviewers' comments. I wish you all the best for your future!

I also wish to warmly thank my collaborators Jonathan D. Cooper, Gil Ribeiro, Carlos Bessa, Tomas Blom, Matti Jauhiainen, Andrew Wong and Jarkko Soronen. Their contribution has been very valuable; especially the lab visits to Jon's lab will be always remembered with happy thoughts. Thank you for everything!

I wish to thank all the current and former members of the NCL group and neighbour labs for your company during my PhD life in and outside the lab: Tea, Kristiina, Tintti, Mari T., Annina, Mervi, Inken, Vilma, Saara, Olivier, Terhi, Riikka H., Will, Jenni L., Arjan, Manu, Mamun, Heidi, Alexandra R., Marius, Alex G., Anna L., Iulia, Roxana, Jonas D., Päivi, Regis, Jarkko, P-P, Mikko M., Markus, Marine, Mari R., Susanne and many others, which I may have forgotten to mention, it has been a pleasure to know you! Carlos, you were my best lab buddy and friend during the first 6 months of my PhD thesis. Tea, I will always remember our London stays with happiness and joy (apart from the fleas). Thank you for being a good companion! Cutbot and Mountbot, the perfect team! Terhi, I want to thank you for your friend-
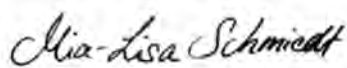
Helsinki, May 2012

Mia-Lisa Schmiedt

References

Abeliovich A, Schmitz Y, Farinas I, Choi-Lundberg D, Ho WH, Castillo PE, Shinsky N, Verdugo JM, Armanini M, Ryan A and others. 2000. Mice lacking alpha-synuclein display functional deficits in the nigrostriatal dopamine system. Neuron 25(1):239-52.

Aggarwal S, Yurlova L, Simons M. 2011. Central nervous system myelin: structure, synthesis and assembly. Trends Cell Biol 21(10):585-93.

Ahtiainen L, Kolikova J, Mutka AL, Luiro K, Gentile M, Ikonen E, Khiroug L, Jalanko A, Kopra O. 2007. Palmitoyl protein thioesterase 1 (Ppt1)-deficient mouse neurons show alterations in cholesterol metabolism and calcium homeostasis prior to synaptic dysfunction. Neurobiol Dis 28(1):52-64.

Aqul A, Liu B, Ramirez CM, Pieper AA, Estill SJ, Burns DK, Liu B, Repa JJ, Turley SD, Dietschy JM. 2011. Unesterified cholesterol accumulation in late endosomes/lysosomes causes neurodegeneration and is prevented by driving cholesterol export from this compartment. J Neurosci 31(25):9404-13.

Autti T, Raininko R, Launes J, Nuutila A, Santavuori P. 1992. Jansky-Bielschowsky variant disease: CT, MRI, and SPECT findings. Pediatr Neurol 8(2):121-6.

Autti T, Raininko R, Santavuori P, Vanhanen SL, Poutanen VP, Haltia M. 1997. MRI of neuronal ceroid lipofuscinosis. II. Postmortem MRI and histopathological study of the brain in 16 cases of neuronal ceroid lipofuscinosis of juvenile or late infantile type. Neuroradiology 39(5):371-7.

Baeten KM, Akassoglou K. 2011. Extracellular matrix and matrix receptors in blood-brain barrier formation and stroke. Dev Neurobiol 71(11):1018-39.

Bartke N, Hannun YA. 2009. Bioactive sphingolipids: metabolism and function. J Lipid Res 50 Suppl:S91-6.

Baumann N, Pham-Dinh D. 2001. Biology of oligodendrocyte and myelin in the mammalian central nervous system. Physiol Rev 81(2):871-927.

Bazan NG. 2003. Synaptic lipid signaling: significance of polyunsaturated fatty acids and platelet-activating factor. J Lipid Res 44(12):2221-33.

Bear MF, Connors BW, Paradiso MA. 2007. Neuroscience - Exploring the Brain, 3rd edition. Lippincott Williams & Wilkins.

Bellizzi JJ, 3rd, Widom J, Kemp C, Lu JY, Das AK, Hofmann SL, Clardy J. 2000. The crystal structure of palmitoyl protein thioesterase 1 and the molecular basis of infantile neuronal ceroid lipofuscinosis. Proc Natl Acad Sci U S A 97(9):4573-8.

Ben-David O, Futerman AH. 2010. The role of the ceramide acyl chain length in neurodegeneration: involvement of ceramide synthases. Neuromolecular Med 12(4):341-50.

Bessa C, Teixeira CA, Mangas M, Dias A, Sa Miranda MC, Guimaraes A, Ferreira JC, Canas N, Cabral P, Ribeiro MG. 2006. Two novel CLN5 mutations in a Portuguese patient with vLINCL: insights into molecular mechanisms of CLN5 deficiency. Mol Genet Metab 89(3):245-53.

Bible E, Gupta P, Hofmann SL, Cooper JD. 2004. Regional and cellular neuropathology in the palmitoyl protein thioesterase-1 null mutant mouse model of infantile neuronal ceroid lipofuscinosis. Neurobiol Dis 16(2):346-59.

Block ML, Zecca L, Hong JS. 2007. Microglia-mediated neurotoxicity: uncovering the molecular mechanisms. Nat Rev Neurosci 8(1):57-69.

Bonfanti L, Peretto P. 2011. Adult neurogenesis in mammals--a theme with many variations. Eur J Neurosci 34(6):930-50.

Bonifacino JS, Rojas R. 2006. Retrograde transport from endosomes to the trans-Golgi network. Nat Rev Mol Cell Biol 7(8):568-79.

Bossy-Wetzel E, Schwarzenbacher R, Lipton SA. 2004. Molecular pathways to neurodegeneration. Nat Med 10 Suppl:S2-9.

Braulke T, Bonifacino JS. 2009. Sorting of lysosomal proteins. Biochim Biophys Acta 1793(4):605-14.

Brecht WJ, Harris FM, Chang S, Tesseur I, Yu GQ, Xu Q, Dee Fish J, Wyss-Coray T, Buttini M, Mucke L and others. 2004. Neuron-specific apolipoprotein e4 proteolysis is associated with increased tau phosphorylation in brains of transgenic mice. J Neurosci 24(10):2527-34.

Bulankina AV, Deggerich A, Wenzel D, Mutenda K, Wittmann JG, Rudolph MG, Burger KN, Honing S. 2009. TIP47 functions in the biogenesis of lipid droplets. J Cell Biol 185(4):641-55.

Bullock TH, Bennett MV, Johnston D, Josephson R, Marder E, Fields RD. 2005. Neuroscience. The neuron doctrine, redux. Science 310(5749):791-3.

Bushong EA, Martone ME, Jones YZ, Ellisman MH. 2002. Protoplasmic astrocytes in CA1 stratum radiatum occupy separate anatomical domains. J Neurosci 22(1):183-92.

Camp LA, Hofmann SL. 1993. Purification and properties of a palmitoyl-protein thioesterase that cleaves palmitate from H-Ras. J Biol Chem 268(30):22566-74.

Cannelli N, Nardocci N, Cassandrini D, Morbin M, Aiello C, Bugiani M, Criscuolo L, Zara F, Striano P, Granata T and others. 2007. Revelation of a novel CLN5 mutation in early juvenile neuronal ceroid lipofuscinosis. Neuropediatrics 38(1):46-9.

Canuel M, Korkidakis A, Konnyu K, Morales CR. 2008. Sortilin mediates the lysosomal targeting of cathepsins D and H. Biochem Biophys Res Commun 373(2):292-7.

Chan WY, Kohsaka S, Rezaie P. 2007. The origin and cell lineage of microglia: new concepts. Brain Res Rev 53(2):344-54.

Chatterjee S. 1998. Sphingolipids in atherosclerosis and vascular biology. Arterioscler Thromb Vasc Biol 18(10):1523-33.

Chen ZY, Ieraci A, Teng H, Dall H, Meng CX, Herrera DG, Nykjaer A, Hempstead BL, Lee FS. 2005. Sortilin controls intracellular sorting of brain-derived neurotrophic factor to the regulated secretory pathway. J Neurosci 25(26):6156-66.

Choudhury A, Dominguez M, Puri V, Sharma DK, Narita K, Wheatley CL, Marks DL, Pagano RE. 2002. Rab proteins mediate Golgi transport of caveola-internalized glycosphingolipids and correct lipid trafficking in Niemann-Pick C cells. J Clin Invest 109(12):1541-50.

Choudhury A, Sharma DK, Marks DL, Pagano RE. 2004. Elevated endosomal cholesterol levels in Niemann-Pick cells inhibit rab4 and perturb membrane recycling. Mol Biol Cell 15(10):4500-11.

Chua CE, Tang BL. 2011. Rabs, SNAREs and alpha-synuclein--membrane trafficking defects in synucleinopathies. Brain Res Rev 67(1-2):268-81.

Cismondi IA, Cannelli N, Aiello C, Santorelli FM, Kohan R, Oller Ramirez AM, Halac IN. 2008. Gene symbol: CLN5. Disease: Neuronal Ceroid Lipofuscinosis, Finnish Variant. Hum Genet 123(5):554.

Compston A, Coles A. 2008. Multiple sclerosis. Lancet 372(9648):1502-17.

Cooper JD. 2010. The neuronal ceroid lipofuscinoses: the same, but different? Biochem Soc Trans 38(6):1448-52.

Coutinho MF, Prata MJ, Alves S. 2011. Mannose-6-phosphate pathway: A review on its role in lysosomal function and dysfunction. Mol Genet Metab 105(4):542-50.

Cramer PE, Cirrito JR, Wesson DW, Lee CY, Karlo JC, Zinn AE, Casali BT, Restivo JL, Goebel WD, James MJ and others. 2012. ApoE-directed therapeutics rapidly clear beta-amyloid and reverse deficits in AD mouse models. Science 335(6075):1503-6.

Daboussi L, Costaguta G, Payne GS. 2012. Phosphoinositide-mediated clathrin adaptor progression at the trans-Golgi network. Nat Cell Biol 14(3):239-48.

Das AM, Jolly RD, Kohlschutter A. 1999. Anomalies of mitochondrial ATP synthase regulation in four different types of neuronal ceroid lipofuscinosis. Mol Genet Metab 66(4):349-55.

De Duve C, Pressman BC, Gianetto R, Wattiaux R, Appelmans F. 1955. Tissue fractionation studies. 6. Intracellular distribution patterns of enzymes in rat-liver tissue. Biochem J 60(4):604-17.

DeMattos RB, Brendza RP, Heuser JE, Kierson M, Cirrito JR, Fryer J, Sullivan PM, Fagan AM, Han X, Holtzman DM. 2001. Purification and characterization of astrocyte-secreted apolipoprotein E and J-containing lipoproteins from wild-type and human apoE transgenic mice. Neurochem Int 39(5-6):415-25.

Dietschy JM. 2009. Central nervous system: cholesterol turnover, brain development and neurodegeneration. Biol Chem 390(4):287-93.

Dietschy JM, Turley SD. 2004. Thematic review series: brain Lipids. Cholesterol metabolism in the central nervous system during early development and in the mature animal. J Lipid Res 45(8):1375-97.

Dolman CL. 1991. in Textbook of Neuropathology, R. L. Davis, D. M. Robertson, Eds. (Williams & Wilkins, Baltimore, MD) 141-163.

Doray B, Ghosh P, Griffith J, Geuze HJ, Kornfeld S. 2002. Cooperation of GGAs and AP-1 in packaging MPRs at the trans-Golgi network. Science 297(5587):1700-3.

Durand G, Seta N. 2000. Protein glycosylation and diseases: blood and urinary oligosaccharides as markers for diagnosis and therapeutic monitoring. Clin Chem 46(6 Pt 1):795-805.

Elbein AD. 1987. Inhibitors of the biosynthesis and processing of N-linked oligosaccharide chains. Annu Rev Biochem 56:497-534.

Elleder M, Lake BD, Goebel HH, Rapola J, Haltia M, Carpenter S. 1999. Definitions of the Ultrastructural Patterns found in NCL. In: Goebel H.H., Mole S.E., Lake B.D. (eds) The Neuronal Ceroid Lipofuscinosis (Batten Disease). IOS Press, Amsterdam:5-15.

Fossale E, Wolf P, Espinola JA, Lubicz-Nawrocka T, Teed AM, Gao H, Rigamonti D, Cattaneo E, MacDonald ME, Cotman SL. 2004. Membrane trafficking and mitochondrial abnormalities precede subunit c deposition in a cerebellar cell model of juvenile neuronal ceroid lipofuscinosis. BMC Neurosci 5:57.

Freeman MR. 2010. Specification and morphogenesis of astrocytes. Science 330(6005):774-8.

Frugier T, Mitchell NL, Tammen I, Houweling PJ, Arthur DG, Kay GW, van Diggelen OP, Jolly RD, Palmer DN. 2008. A new large animal model of CLN5 neuronal ceroid lipofuscinosis in Borderdale sheep is caused by a nucleotide substitution at a consensus splice site (c.571+1G>A) leading to excision of exon 3. Neurobiol Dis 29(2):306-15.

Futerman AH, van Meer G. 2004. The cell biology of lysosomal storage disorders. Nat Rev Mol Cell Biol 5(7):554-65.

Galiano MR, Andrieux A, Deloulme JC, Bosc C, Schweitzer A, Job D, Hallak ME. 2006. Myelin basic protein functions as a microtubule stabilizing protein in differentiated oligodendrocytes. J Neurosci Res 84(3):534-41.

Galizzi G, Russo D, Deidda I, Cascio C, Passantino R, Guarneri R, Bigini P, Mennini T, Drago G, Guarneri P. 2011. Different early ER-stress responses in the CLN8(mnd) mouse model of neuronal ceroid lipofuscinosis. Neurosci Lett 488(3):258-62.

Gan KN, Smolen A, Eckerson HW, La Du BN. 1991. Purification of human serum paraoxonase/arylesterase. Evidence for one esterase catalyzing both activities. Drug Metab Dispos 19(1):100-6.

Ghosh P, Dahms NM, Kornfeld S. 2003. Mannose 6-phosphate receptors: new twists in the tale. Nat Rev Mol Cell Biol 4(3):202-12.

Giaume C, Koulakoff A, Roux L, Holcman D, Rouach N. 2010. Astroglial networks: a step further in neuroglial and gliovascular interactions. Nat Rev Neurosci 11(2):87-99.

Glass CK, Saijo K, Winner B, Marchetto MC, Gage FH. 2010. Mechanisms underlying inflammation in neurodegeneration. Cell 140(6):918-34.

Goebel HH. 1997. Morphologic diagnosis in neuronal ceroid lipofuscinosis. Neuropediatrics 28(1):67-9.

Gotz M, Huttner WB. 2005. The cell biology of neurogenesis. Nat Rev Mol Cell Biol 6(10):777-88.

Graeber MB. 2010. Changing face of microglia. Science 330(6005):783-8.

Graeber MB, Streit WJ. 1990. Microglia: immune network in the CNS. Brain Pathol 1(1):2-5.

Graeber MB, Streit WJ. 2010. Microglia: biology and pathology. Acta Neuropathol 119(1):89-105.

Guillery RW. 2007. Relating the neuron doctrine to the cell theory. Should contemporary knowledge change our view of the neuron doctrine? Brain Res Rev 55(2):411-21.

Gundersen HJ, Jensen EB. 1987. The efficiency of systematic sampling in stereology and its prediction. J Microsc 147(Pt 3):229-63.

Gupta P, Soyombo AA, Atashband A, Wisniewski KE, Shelton JM, Richardson JA, Hammer RE, Hofmann SL. 2001. Disruption of PPT1 or PPT2 causes neuronal ceroid lipofuscinosis in knockout mice. Proc Natl Acad Sci U S A 98(24):13566-71.

Haidar B, Kiss RS, Sarov-Blat L, Brunet R, Harder C, McPherson R, Marcel YL. 2006. Cathepsin D, a lysosomal protease, regulates ABCA1-mediated lipid efflux. J Biol Chem 281(52):39971-81.

Haltia M. 2003. The neuronal ceroid-lipofuscinoses. J Neuropathol Exp Neurol 62(1):1-13.

Haltia M. 2006. The neuronal ceroid-lipofuscinoses: from past to present. Biochim Biophys Acta 1762(10):850-6.

Haltia M, Rapola J, Santavuori P. 1973a. Infantile type of so-called neuronal ceroid-lipofuscinosis. Histological and electron microscopic studies. Acta Neuropathol 26(2):157-70.

Haltia M, Rapola J, Santavuori P, Keränen A. 1973b. Infantile type of so-called neuronal ceroid-lipofuscinosis. 2. Morphological and biochemical studies. J Neurol Sci 18(3):269-85.

Handunnetthi L, Handel AE, Ramagopalan SV. 2010. Contribution of genetic, epigenetic and transcriptomic differences to twin discordance in multiple sclerosis. Expert Rev Neurother 10(9):1379-81.

Hasilik A, Wrocklage C, Schröder B. 2009. Intracellular trafficking of lysosomal proteins and lysosomes. Int J Clin Pharmacol Ther 47 Suppl 1:S18-33.

Haucke V, Di Paolo G. 2007. Lipids and lipid modifications in the regulation of membrane traffic. Curr Opin Cell Biol 19(4):426-35.

Hayashi H. 2011. Lipid metabolism and glial lipoproteins in the central nervous system. Biol Pharm Bull 34(4):453-61.

Helenius A, Aebi M. 2001. Intracellular functions of N-linked glycans. Science 291(5512):2364-9.

Hellsten E, Vesa J, Olkkonen VM, Jalanko A, Peltonen L. 1996. Human palmitoyl protein thioesterase: evidence for lysosomal targeting of the enzyme and disturbed cellular routing in infantile neuronal ceroid lipofuscinosis. Embo J 15(19):5240-5.

Hirsch-Reinshagen V, Donkin J, Stukas S, Chan J, Wilkinson A, Fan J, Parks JS, Kuivenhoven JA, Lutjohann D, Pritchard H and others. 2009. LCAT synthesized by primary astrocytes esterifies cholesterol on glia-derived lipoproteins. J Lipid Res 50(5):885-93.

Holmberg V, Jalanko A, Isosomppi J, Fabritius AL, Peltonen L, Kopra O. 2004. The mouse ortholog of the neuronal ceroid lipofuscinosis CLN5 gene encodes a soluble lysosomal glycoprotein expressed in the developing brain. Neurobiol Dis 16(1):29-40.

Holmberg V, Lauronen L, Autti T, Santavuori P, Savukoski M, Uvebrant P, Hofman I, Peltonen L, Järvelä I. 2000. Phenotype-genotype correlation in eight patients with Finnish variant late infantile NCL (CLN5). Neurology 55(4):579-81.

Houweling PJ, Cavanagh JA, Palmer DN, Frugier T, Mitchell NL, Windsor PA, Raadsma HW, Tammen I. 2006. Neuronal ceroid lipofuscinosis in Devon cattle is caused by a single base duplication (c.662dupG) in the bovine CLN5 gene. Biochim Biophys Acta 1762(10):890-7.

Hu VW, Heikka DS. 2000. Radiolabeling revisited: metabolic labeling with (35)S-methionine inhibits cell cycle progression, proliferation, and survival. Faseb J 14(3):448-54.

Hua JY, Smith SJ. 2004. Neural activity and the dynamics of central nervous system development. Nat Neurosci 7(4):327-32.

Ikonen E. 2008. Cellular cholesterol trafficking and compartmentalization. Nat Rev Mol Cell Biol 9(2):125-38.

Isosomppi J, Vesa J, Jalanko A, Peltonen L. 2002. Lysosomal localization of the neuronal ceroid lipofuscinosis CLN5 protein. Hum Mol Genet 11(8):885-91.

Jabs S, Quitsch A, Käkelä R, Koch B, Tyynelä J, Brade H, Glatzel M, Walkley S, Saftig P, Vanier MT and others. 2008. Accumulation of bis(monoacylglycero)phosphate and gangliosides in mouse models of neuronal ceroid lipofuscinosis. J Neurochem 106(3):1415-25.

Jalanko A, Braulke T. 2009. Neuronal ceroid lipofuscinoses. Biochim Biophys Acta 4:697-709.

Jalanko A, Tyynelä J, Peltonen L. 2006. From genes to systems: new global strategies for the characterization of NCL biology. Biochim Biophys Acta 1762(10):934-44.

Jalanko A, Vesa J, Manninen T, von Schantz C, Minye H, Fabritius AL, Salonen T, Rapola J, Gentile M, Kopra O and others. 2005. Mice with Ppt1Deltaex4 mutation replicate the INCL phenotype and show an inflammation-associated loss of interneurons. Neurobiol Dis 18(1):226-41.

Jauhiainen M, Ehnholm C. 2005. Determination of human plasma phospholipid transfer protein mass and activity. Methods 36(2):97-101.

Jung YW, Hysolli E, Kim KY, Tanaka Y, Park IH. 2012. Human induced pluripotent stem cells and neurodegenerative disease: prospects for novel therapies. Curr Opin Neurol 25(2):125-30.

Järvelä I, Sainio M, Rantamäki T, Olkkonen VM, Carpen O, Peltonen L, Jalanko A. 1998. Biosynthesis and intracellular targeting of the CLN3 protein defective in Batten disease. Hum Mol Genet 7(1):85-90.

Kettenmann H, Hanisch UK, Noda M, Verkhratsky A. 2011. Physiology of microglia. Physiol Rev 91(2):461-553.

Kielar C, Maddox L, Bible E, Pontikis CC, Macauley SL, Griffey MA, Wong M, Sands MS, Cooper JD. 2007. Successive neuron loss in the thalamus and cortex in a mouse model of infantile neuronal ceroid lipofuscinosis. Neurobiol Dis 25(1):150-62.

Kim E, Lee Y, Lee HJ, Kim JS, Song BS, Huh JW, Lee SR, Kim SU, Kim SH, Hong Y and others. 2010. Implication of mouse Vps26b-Vps29-Vps35 retromer complex in sortilin trafficking. Biochem Biophys Res Commun 403(2):167-71.

Kim WS, Weickert CS, Garner B. 2008. Role of ATP-binding cassette transporters in brain lipid transport and neurological disease. J Neurochem 104(5):1145-66.

Kimelberg HK. 2010. Functions of mature mammalian astrocytes: a current view. Neuroscientist 16(1):79-106.

Koch S, Donarski N, Goetze K, Kreckel M, Stuerenburg HJ, Buhmann C, Beisiegel U. 2001. Characterization of four lipoprotein classes in human cerebrospinal fluid. J Lipid Res 42(7):1143-51.

Koehler RC, Roman RJ, Harder DR. 2009. Astrocytes and the regulation of cerebral blood flow. Trends Neurosci 32(3):160-9.

Kollmann K, Mutenda KE, Balleininger M, Eckermann E, von Figura K, Schmidt B, Lubke T. 2005. Identification of novel lysosomal matrix proteins by proteome analysis. Proteomics 5(15):3966-78.

Kolter T, Sandhoff K. 1999. Sphingolipids—Their Metabolic Pathways and the Pathobiochemistry of Neurodegenerative Diseases. Angewandte Chemie International Edition 38(11):1532-1568.

Kolter T, Sandhoff K. 2006. Sphingolipid metabolism diseases. Biochim Biophys Acta 1758(12):2057-79.

Kopra O, Vesa J, von Schantz C, Manninen T, Minye H, Fabritius AL, Rapola J, van Diggelen OP, Saarela J, Jalanko A and others. 2004. A mouse model for Finnish variant late infantile neuronal ceroid lipofuscinosis, CLN5, reveals neuropathology associated with early aging. Hum Mol Genet 13(23):2893-906.

Kousi M, Lehesjoki AE, Mole SE. 2012. Update of the mutation spectrum and clinical correlations of over 360 mutations in eight genes that underlie the neuronal ceroid lipofuscinoses. Hum Mutat 33(1):42-63.

Kousi M, Siintola E, Dvorakova L, Vlaskova H, Turnbull J, Topcu M, Yuksel D, Gokben S, Minassian BA, Elleder M and others. 2009. Mutations in CLN7/MFSD8 are a common cause of variant late-infantile neuronal ceroid lipofuscinosis. Brain 132(Pt 3):810-9.

Kratzer I, Wernig K, Panzenboeck U, Bernhart E, Reicher H, Wronski R, Windisch M, Hammer A, Malle E, Zimmer A and others. 2007. Apolipoprotein A-I coating of protamine-oligonucleotide nanoparticles increases particle uptake and transcytosis in an in vitro model of the blood-brain barrier. J Control Release 117(3):301-11.

Kwon HJ, Abi-Mosleh L, Wang ML, Deisenhofer J, Goldstein JL, Brown MS, Infante RE. 2009. Structure of N-terminal domain of NPC1 reveals distinct subdomains for binding and transfer of cholesterol. Cell 137(7):1213-24.

Käkelä R, Somerharju P, Tyynelä J. 2003. Analysis of phospholipid molecular species in brains from patients with infantile and juvenile neuronal-ceroid lipofuscinosis using liquid chromatography-electrospray ionization mass spectrometry. J Neurochem 84(5):1051-65.

Lawson LJ, Perry VH, Dri P, Gordon S. 1990. Heterogeneity in the distribution and morphology of microglia in the normal adult mouse brain. Neuroscience 39(1):151-70.

Lebrun AH, Storch S, Ruschendorf F, Schmiedt ML, Kyttälä A, Mole SE, Kitzmuller C, Saar K, Mewasingh LD, Boda V and others. 2009. Retention of lysosomal protein CLN5 in the endoplasmic reticulum causes neuronal ceroid lipofuscinosis in Asian Sibship. Hum Mutat 30(5):651-61.

Lee CW, Bang H, Oh YG, Yun HS, Kim JD, Coe CJ. 2003. A case of late infantile neuronal ceroid lipofuscinosis. Yonsei Med J 44(2):331-5.

Lee J, Gravel M, Zhang R, Thibault P, Braun PE. 2005. Process outgrowth in oligodendrocytes is mediated by CNP, a novel microtubule assembly myelin protein. J Cell Biol 170(4):661-73.

Lefrancois S, Zeng J, Hassan AJ, Canuel M, Morales CR. 2003. The lysosomal trafficking of sphingolipid activator proteins (SAPs) is mediated by sortilin. EMBO J 22(24):6430-7.

Legleiter J, DeMattos RB, Holtzman DM, Kowalewski T. 2004. In situ AFM studies of astrocyte-secreted apolipoprotein E- and J-containing lipoproteins. J Colloid Interface Sci 278(1):96-106.

Lehtovirta M, Kyttälä A, Eskelinen EL, Hess M, Heinonen O, Jalanko A. 2001. Palmitoyl protein thioesterase (PPT) localizes into synaptosomes and synaptic vesicles in neurons: implications for infantile neuronal ceroid lipofuscinosis (INCL). Hum Mol Genet 10(1):69-75.

Liu B, Xie C, Richardson JA, Turley SD, Dietschy JM. 2007. Receptor-mediated and bulk-phase endocytosis cause macrophage and cholesterol accumulation in Niemann-Pick C disease. J Lipid Res 48(8):1710-23.

Livak KJ, Schmittgen TD. 2001. Analysis of relative gene expression data using real-time quantitative PCR and the 2(-Delta Delta C(T)) Method. Methods 25(4):402-8.

Lloyd-Evans E, Morgan AJ, He X, Smith DA, Elliot-Smith E, Sillence DJ, Churchill GC, Schuchman EH, Galione A, Platt FM. 2008. Niemann-Pick disease type C1 is a sphingosine storage disease that causes deregulation of lysosomal calcium. Nat Med 14(11):1247-55.

Lonka L, Kyttälä A, Ranta S, Jalanko A, Lehesjoki AE. 2000. The neuronal ceroid lipofuscinosis CLN8 membrane protein is a resident of the endoplasmic reticulum. Hum Mol Genet 9(11):1691-7.

Lubke T, Lobel P, Sleat DE. 2009. Proteomics of the lysosome. Biochim Biophys Acta 1793(4):625-35.

Lucchinetti CF, Popescu BF, Bunyan RF, Moll NM, Roemer SF, Lassmann H, Bruck W, Parisi JE, Scheithauer BW, Giannini C and others. 2011. Inflammatory cortical demyelination in early multiple sclerosis. N Engl J Med 365(23):2188-97.

Lucin KM, Wyss-Coray T. 2009. Immune activation in brain aging and neurodegeneration: too much or too little? Neuron 64(1):110-22.

Luiro K, Kopra O, Lehtovirta M, Jalanko A. 2001. CLN3 protein is targeted to neuronal synapses but excluded from synaptic vesicles: new clues to Batten disease. Hum Mol Genet 10(19):2123-31.

Lutjohann D, Breuer O, Ahlborg G, Nennesmo I, Siden A, Diczfalusy U, Bjorkhem I. 1996. Cholesterol homeostasis in human brain: evidence for an age-dependent flux of 24S-hydroxycholesterol from the brain into the circulation. Proc Natl Acad Sci U S A 93(18):9799-804.

Luzio JP, Pryor PR, Bright NA. 2007. Lysosomes: fusion and function. Nat Rev Mol Cell Biol 8(8):622-32.

Lyly A, Marjavaara SK, Kyttälä A, Uusi-Rauva K, Luiro K, Kopra O, Martinez LO, Tanhuanpää K, Kalkkinen N, Suomalainen A and others. 2008. Deficiency of the INCL protein Ppt1 results in changes in ectopic F1-ATP synthase and altered cholesterol metabolism. Hum Mol Genet 17(10):1406-17.

Lyly A, von Schantz C, Heine C, Schmiedt ML, Sipila T, Jalanko A, Kyttälä A. 2009. Novel interactions of CLN5 support molecular networking between Neuronal Ceroid Lipofuscinosis proteins. BMC Cell Biol 10:83.

Lyly A, von Schantz C, Salonen T, Kopra O, Saarela J, Jauhiainen M, Kyttälä A, Jalanko A. 2007. Glycosylation, transport, and complex formation of palmitoyl protein thioesterase 1 (PPT1)--distinct characteristics in neurons. BMC Cell Biol 8:22.

Macauley SL, Pekny M, Sands MS. 2011. The role of attenuated astrocyte activation in infantile neuronal ceroid lipofuscinosis. J Neurosci 31(43):15575-85.

Macauley SL, Roberts MS, Wong AM, McSloy F, Reddy AS, Cooper JD, Sands MS. 2012. Synergistic effects of central nervous system-directed gene therapy and bone marrow transplantation in the murine model of infantile neuronal ceroid lipofuscinosis. Ann Neurol Epub ahead of print.

Macauley SL, Wozniak DF, Kielar C, Tan Y, Cooper JD, Sands MS. 2009. Cerebellar pathology and motor deficits in the palmitoyl protein thioesterase 1-deficient mouse. Exp Neurol 217(1):124-35.

Mahley RW, Innerarity TL, Rall SC, Jr., Weisgraber KH. 1984. Plasma lipoproteins: apolipoprotein structure and function. J Lipid Res 25(12):1277-94.

Maragakis NJ, Rothstein JD. 2006. Mechanisms of Disease: astrocytes in neurodegenerative disease. Nat Clin Pract Neurol 2(12):679-89.

Marshansky V, Futai M. 2008. The V-type H+-ATPase in vesicular trafficking: targeting, regulation and function. Curr Opin Cell Biol 20(4):415-26.

Martinez LO, Jacquet S, Esteve JP, Rolland C, Cabezon E, Champagne E, Pineau T, Georgeaud V, Walker JE, Terce F and others. 2003. Ectopic beta-chain of ATP synthase is an apolipoprotein A-I receptor in hepatic HDL endocytosis. Nature 421(6918):75-9.

Melville SA, Wilson CL, Chiang CS, Studdert VP, Lingaas F, Wilton AN. 2005. A mutation in canine CLN5 causes neuronal ceroid lipofuscinosis in Border collie dogs. Genomics 86(3):287-94.

Meng XL, Shen JS, Kawagoe S, Ohashi T, Brady RO, Eto Y. 2010. Induced pluripotent stem cells derived from mouse models of lysosomal storage disorders. Proc Natl Acad Sci U S A 107(17):7886-91.

Mole SE, Williams RE, Goebel HH. 2011. The Neuronal Ceroid Lipofuscinoses (Batten Disease). Oxford University Press.

Moore CS, Abdullah SL, Brown A, Arulpragasam A, Crocker SJ. 2010. How factors secreted from astrocytes impact myelin repair. J Neurosci Res 89(1):13-21.

Mukherjee A, Morales-Scheihing D, Gonzalez-Romero D, Green K, Taglialatela G, Soto C. 2011. Calcineurin inhibition at the clinical phase of prion disease reduces neurodegeneration, improves behavioral alterations and increases animal survival. PLoS Pathog 6(10):e1001138.

Mukherjee S, Maxfield FR. 2004. Lipid and cholesterol trafficking in NPC. Biochim Biophys Acta 1685(1-3):28-37.

Mullins C, Bonifacino JS. 2001. The molecular machinery for lysosome biogenesis. Bioessays 23(4):333-43.

Nakai M, Kawamata T, Taniguchi T, Maeda K, Tanaka C. 1996. Expression of apolipoprotein E mRNA in rat microglia. Neurosci Lett 211(1):41-4.

Nakamura T, Lipton SA. 2009. Cell death: protein misfolding and neurodegenerative diseases. Apoptosis 14(4):455-68.

Namba Y, Tomonaga M, Kawasaki H, Otomo E, Ikeda K. 1991. Apolipoprotein E immunoreactivity in cerebral amyloid deposits and neurofibrillary tangles in Alzheimer's disease and kuru plaque amyloid in Creutzfeldt-Jakob disease. Brain Res 541(1):163-6.

Narayan SB, Rakheja D, Tan L, Pastor JV, Bennett MJ. 2006. CLN3P, the Batten's disease protein, is a novel palmitoyl-protein Delta-9 desaturase. Ann Neurol 60(5):570-7.

Nave KA. 2008. Myelination and support of axonal integrity by glia. Nature 468(7321):244-52.

Nebenfuhr A, Ritzenthaler C, Robinson DG. 2002. Brefeldin A: deciphering an enigmatic inhibitor of secretion. Plant Physiol 130(3):1102-8.

Ni X, Morales CR. 2006. The lysosomal trafficking of acid sphingomyelinase is mediated by sortilin and mannose 6-phosphate receptor. Traffic 7(7):889-902.

Nieweg K, Schaller H, Pfrieger FW. 2009. Marked differences in cholesterol synthesis between neurons and glial cells from postnatal rats. J Neurochem 109(1):125-34.

Nimmerjahn A, Kirchhoff F, Helmchen F. 2005. Resting microglial cells are highly dynamic surveillants of brain parenchyma in vivo. Science 308(5726):1314-8.

Norio R. 2003. Finnish Disease Heritage I: characteristics, causes, background. Hum Genet 112(5-6):441-56.

Norton WT. 1981. Biochemistry of myelin. Adv Neurol 31:93-121.

Noskova L, Stranecky V, Hartmannova H, Pristoupilova A, Baresova V, Ivanek R, Hulkova H, Jahnova H, van der Zee J, Staropoli JF and others. 2011. Mutations in DNAJC5, encoding cysteine-string protein alpha, cause autosomal-dominant adult-onset neuronal ceroid lipofuscinosis. Am J Hum Genet 89(2):241-52.

Novikoff AB, Beaufay H, De Duve C. 1956. Electron microscopy of lysosomerich fractions from rat liver. J Biophys Biochem Cytol 2(4 Suppl):179-84.

Oram JF, Wolfbauer G, Vaughan AM, Tang C, Albers JJ. 2003. Phospholipid transfer protein interacts with and stabilizes ATP-binding cassette transporter A1 and enhances cholesterol efflux from cells. J Biol Chem 278(52):52379-85.

Oresic K, Mueller B, Tortorella D. 2009. Cln6 mutants associated with neuronal ceroid lipofuscinosis are degraded in a proteasome-dependent manner. Biosci Rep 29(3):173-81.

Oswald MJ, Palmer DN, Kay GW, Shemilt SJ, Rezaie P, Cooper JD. 2005. Glial activation spreads from specific cerebral foci and precedes neurodegeneration in presymptomatic ovine neuronal ceroid lipofuscinosis (CLN6). Neurobiol Dis 20(1):49-63.

Pagano RE, Chen CS. 1998. Use of BODIPY-labeled sphingolipids to study membrane traffic along the endocytic pathway. Ann N Y Acad Sci 845:152-60.

Pagano RE, Martin OC, Kang HC, Haugland RP. 1991. A novel fluorescent ceramide analogue for studying membrane traffic in animal cells: accumulation at the Golgi apparatus results in altered spectral properties of the sphingolipid precursor. J Cell Biol 113(6):1267-79.

Palop JJ, Chin J, Mucke L. 2006. A network dysfunction perspective on neurodegenerative diseases. Nature 443(7113):768-73.

Panzenboeck U, Balazs Z, Sovic A, Hrzenjak A, Levak-Frank S, Wintersperger A, Malle E, Sattler W. 2002. ABCA1 and scavenger receptor class B, type I, are modulators of reverse sterol transport at an in vitro blood-brain barrier constituted of porcine brain capillary endothelial cells. J Biol Chem 277(45):42781-9.

Pascual O, Ben Achour S, Rostaing P, Triller A, Bessis A. 2012. Microglia activation triggers astrocyte-mediated modulation of excitatory neurotransmission. Proc Natl Acad Sci U S A 109(4):E197-205.

Paxinos G, Franklin KBJ. 2001. The Mouse Brain in Stereotaxic Coordinates. Academic Press.

Perea G, Araque A. 2005. Glial calcium signaling and neuron-glia communication. Cell Calcium 38(3-4):375-82.

Perea G, Navarrete M, Araque A. 2009. Tripartite synapses: astrocytes process and control synaptic information. Trends Neurosci 32(8):421-31.

Perry VH, Nicoll JA, Holmes C. 2010. Microglia in neurodegenerative disease. Nat Rev Neurol 6(4):193-201.

Persaud-Sawin DA, Mousallem T, Wang C, Zucker A, Kominami E, Boustany RM. 2007. Neuronal ceroid lipofuscinosis: a common pathway? Pediatr Res 61(2):146-52.

Piccinini M, Scandroglio F, Prioni S, Buccinna B, Loberto N, Aureli M, Chigorno V, Lupino E, DeMarco G, Lomartire A and others. 2010. Deregulated sphingolipid metabolism and membrane organization in neurodegenerative disorders. Mol Neurobiol 41(2-3):314-40.

Pineda-Trujillo N, Cornejo W, Carrizosa J, Wheeler RB, Munera S, Valencia A, Agudelo-Arango J, Cogollo A, Anderson G, Bedoya G and others. 2005. A CLN5 mutation causing an atypical neuronal ceroid lipofuscinosis of juvenile onset. Neurology 64(4):740-2.

Pitas RE, Boyles JK, Lee SH, Foss D, Mahley RW. 1987. Astrocytes synthesize apolipoprotein E and metabolize apolipoprotein E-containing lipoproteins. Biochim Biophys Acta 917(1):148-61.

Pohlmann R, Boeker MW, von Figura K. 1995. The two mannose 6-phosphate receptors transport distinct complements of lysosomal proteins. J Biol Chem 270(45):27311-8.

Pont-Lezica L, Bechade C, Belarif-Cantaut Y, Pascual O, Bessis A. 2011. Physiological roles of microglia during development. J Neurochem 119(5):901-8.

Pontikis CC, Cella CV, Parihar N, Lim MJ, Chakrabarti S, Mitchison HM, Mobley WC, Rezaie P, Pearce DA, Cooper JD. 2004. Late onset neurodegeneration in the Cln3-/- mouse model of juvenile neuronal ceroid lipofuscinosis is preceded by low level glial activation. Brain Res 1023(2):231-42.

Pontikis CC, Cotman SL, MacDonald ME, Cooper JD. 2005. Thalamocortical neuron loss and localized astrocytosis in the Cln3Deltaex7/8 knock-in mouse model of Batten disease. Neurobiol Dis 20(3):823-36.

Pryor PR, Luzio JP. 2009. Delivery of endocytosed membrane proteins to the lysosome. Biochim Biophys Acta 1793(4):615-24.

Puertollano R, van der Wel NN, Greene LE, Eisenberg E, Peters PJ, Bonifacino JS. 2003. Morphology and dynamics of clathrin/GGA1-coated carriers budding from the trans-Golgi network. Mol Biol Cell 14(4):1545-57.

Puri V, Jefferson JR, Singh RD, Wheatley CL, Marks DL, Pagano RE. 2003. Sphingolipid storage induces accumulation of intracellular cholesterol by stimulating SREBP-1 cleavage. J Biol Chem 278(23):20961-70.

Puri V, Watanabe R, Dominguez M, Sun X, Wheatley CL, Marks DL, Pagano RE. 1999. Cholesterol modulates membrane traffic along the endocytic pathway in sphingolipid-storage diseases. Nat Cell Biol 1(6):386-8.

Qian M, Sleat DE, Zheng H, Moore D, Lobel P. 2008. Proteomics analysis of serum from mutant mice reveals lysosomal proteins selectively transported by each of the two mannose 6-phosphate receptors. Mol Cell Proteomics 7(1):58-70.

Rapola J, Lahdetie J, Isosomppi J, Helminen P, Penttinen M, Jarvelä I. 1999. Prenatal diagnosis of variant late infantile neuronal ceroid lipofuscinosis (vLINCL[Finnish]; CLN5). Prenat Diagn 19(7):685-8.

The CLN5 disease - protein maturation, trafficking and pathology

Rapp M, Yarom Y, Segev I. 1996. Modeling back propagating action potential in weakly excitable dendrites of neocortical pyramidal cells. Proc Natl Acad Sci U S A 93(21):11985-90.

Reczek D, Schwake M, Schröder J, Hughes H, Blanz J, Jin X, Brondyk W, Van Patten S, Edmunds T, Saftig P. 2007. LIMP-2 is a receptor for lysosomal mannose-6-phosphate-independent targeting of beta-glucocerebrosidase. Cell 131(4):770-83.

Reichenbach A, Derouiche A, Kirchhoff F. 2010. Morphology and dynamics of perisynaptic glia. Brain Res Rev 63(1-2):11-25.

Roberts MS, Macauley SL, Wong AM, Yilmas D, Hohm S, Cooper JD, Sands MS. 2012. Combination small molecule PPT1 mimetic and CNS-directed gene therapy as a treatment for infantile neuronal ceroid lipofuscinosis. J Inherit Metab Dis Epub ahead of print.

Rosenbaum AI, Maxfield FR. 2011. Niemann-Pick type C disease: molecular mechanisms and potential therapeutic approaches. J Neurochem 116(5):789-95.

Ruddock LW, Molinari M. 2006. N-glycan processing in ER quality control. J Cell Sci 119(Pt 21):4373-80.

Ruiperez V, Darios F, Davletov B. 2010. Alpha-synuclein, lipids and Parkinson's disease. Prog Lipid Res 49(4):420-8.

Saftig P, Klumperman J. 2009. Lysosome biogenesis and lysosomal membrane proteins: trafficking meets function. Nat Rev Mol Cell Biol 10(9):623-35.

Saftig P, Schröder B, Blanz J. 2010. Lysosomal membrane proteins: life between acid and neutral conditions. Biochem Soc Trans 38(6):1420-3.

Saha A, Sarkar C, Singh SP, Zhang Z, Munasinghe J, Peng S, Chandra G, Kong E, Mukherjee AB. 2012. The blood-brain barrier is disrupted in a mouse model of infantile neuronal ceroid lipofuscinosis: amelioration by resveratrol. Hum Mol Genet 21(10):2233-44.

Saijo K, Glass CK. 2011. Microglial cell origin and phenotypes in health and disease. Nat Rev Immunol 11(11):775-87.

Salonen T, Heinonen-Kopra O, Vesa J, Jalanko A. 2001. Neuronal trafficking of palmitoyl protein thioesterase provides an excellent model to study the effects of different mutations which cause infantile neuronal ceroid lipofuscinocis. Mol Cell Neurosci 18(2):131-40.

Salonen T, Järvelä I, Peltonen L, Jalanko A. 2000. Detection of eight novel palmitoyl protein thioesterase (PPT) mutations underlying infantile neuronal ceroid lipofuscinosis (INCL;CLN1). Hum Mutat 15(3):273-9.

Santavuori P. 1988. Neuronal ceroid-lipofuscinoses in childhood. Brain Dev 10(2):80-3.

Santavuori P, Haltia M, Rapola J, Raitta C. 1973. Infantile type of so-called neuronal ceroid-lipofuscinosis. 1. A clinical study of 15 patients. J Neurol Sci 18(3):257-67.

Santavuori P, Rapola J, Nuutila A, Raininko R, Lappi M, Launes J, Herva R, Sainio K. 1991. The spectrum of Jansky-Bielschowsky disease. Neuropediatrics 22(2):92-6.

Santavuori P, Rapola J, Sainio K, Raitta C. 1982. A variant of Jansky-Bielschowsky disease. Neuropediatrics 13(3):135-41.

Savukoski M, Klockars T, Holmberg V, Santavuori P, Lander ES, Peltonen L. 1998. CLN5, a novel gene encoding a putative transmembrane protein mutated in

Finnish variant late infantile neuronal ceroid lipofuscinosis. Nat Genet 19(3):286-8.

Schmiedt ML, Bessa C, Heine C, Ribeiro MG, Jalanko A, Kyttälä A. 2010. The neuronal ceroid lipofuscinosis protein CLN5: new insights into cellular maturation, transport, and consequences of mutations. Hum Mutat 31(3):356-65.

Schneider-Poetsch T, Ju J, Eyler DE, Dang Y, Bhat S, Merrick WC, Green R, Shen B, Liu JO. 2010. Inhibition of eukaryotic translation elongation by cycloheximide and lactimidomycin. Nat Chem Biol 6(3):209-217.

Schröder BA, Wrocklage C, Hasilik A, Saftig P. 2010. The proteome of lysosomes. Proteomics 10(22):4053-76.

Schultz ML, Tecedor L, Chang M, Davidson BL. 2011. Clarifying lysosomal storage diseases. Trends Neurosci 34(8):401-10.

Seifert G, Carmignoto G, Steinhauser C. 2010. Astrocyte dysfunction in epilepsy. Brain Res Rev 63(1-2):212-21.

Seifert G, Steinhauser C. 2011. Neuron-astrocyte signaling and epilepsy. Exp Neurol Epub ahead of print.

Shankar GM, Walsh DM. 2009. Alzheimer's disease: synaptic dysfunction and Abeta. Mol Neurodegener 4:48.

Sharifi A, Kousi M, Sagne C, Bellenchi GC, Morel L, Darmon M, Hulkova H, Ruivo R, Debacker C, El Mestikawy S and others. 2010. Expression and lysosomal targeting of CLN7, a major facilitator superfamily transporter associated with variant late-infantile neuronal ceroid lipofuscinosis. Hum Mol Genet 19(22):4497-514.

Sharma DK, Choudhury A, Singh RD, Wheatley CL, Marks DL, Pagano RE. 2003. Glycosphingolipids internalized *via* caveolar-related endocytosis rapidly merge with the clathrin pathway in early endosomes and form microdomains for recycling. J Biol Chem 278(9):7564-72.

Shields SA, Blakemore WF, Franklin RJ. 2000. Schwann cell remyelination is restricted to astrocyte-deficient areas after transplantation into demyelinated adult rat brain. J Neurosci Res 60(5):571-8.

Siakotos AN, Blair PS, Savill JD, Katz ML. 1998. Altered mitochondrial function in canine ceroid-lipofuscinosis. Neurochem Res 23(7):983-9.

Simons K, Vaz WL. 2004. Model systems, lipid rafts, and cell membranes. Annu Rev Biophys Biomol Struct 33:269-95.

Simons M, Trotter J. 2007. Wrapping it up: the cell biology of myelination. Curr Opin Neurobiol 17(5):533-40.

Sleat DE, Ding L, Wang S, Zhao C, Wang Y, Xin W, Zheng H, Moore DF, Sims KB, Lobel P. 2009. Mass spectrometry-based protein profiling to determine the cause of lysosomal storage diseases of unknown etiology. Mol Cell Proteomics 8(7):1708-18.

Sleat DE, Lackland H, Wang Y, Sohar I, Xiao G, Li H, Lobel P. 2005. The human brain mannose 6-phosphate glycoproteome: a complex mixture composed of multiple isoforms of many soluble lysosomal proteins. Proteomics 5(6):1520-32.

Sleat DE, Wang Y, Sohar I, Lackland H, Li Y, Li H, Zheng H, Lobel P. 2006. Identification and validation of mannose 6-phosphate glycoproteins in human plasma reveal a wide range of lysosomal and non-lysosomal proteins. Mol Cell Proteomics 5(10):1942-56.

Slezak M, Pfrieger FW. 2003. New roles for astrocytes: regulation of CNS synaptogenesis. Trends Neurosci 26(10):531-5.

Stahl SM. 2008. Stahl's Essential Psychopharmacology: Neuroscientific Basis and Practical Applications. Cambridge University Press.

Storch S, Pohl S, Quitsch A, Falley K, Braulke T. 2007. C-terminal prenylation of the CLN3 membrane glycoprotein is required for efficient endosomal sorting to lysosomes. Traffic 8(4):431-44.

Sundaram JR, Chan ES, Poore CP, Pareek TK, Cheong WF, Shui G, Tang N, Low CM, Wenk MR, Kesavapany S. 2012. Cdk5/p25-induced cytosolic PLA2-mediated lysophosphatidylcholine production regulates neuroinflammation and triggers neurodegeneration. J Neurosci 32(3):1020-34.

Suopanki J, Partanen S, Ezaki J, Baumann M, Kominami E, Tyynelä J. 2000. Developmental changes in the expression of neuronal ceroid lipofuscinoses-linked proteins. Mol Genet Metab 71(1-2):190-4.

Suzumura A, Takeuchi H, Zhang G, Kuno R, Mizuno T. 2006. Roles of glia-derived cytokines on neuronal degeneration and regeneration. Ann N Y Acad Sci 1088:219-29.

Takahashi K, Okita K, Nakagawa M, Yamanaka S. 2007. Induction of pluripotent stem cells from fibroblast cultures. Nat Protoc 2(12):3081-9.

Talbott JF, Loy DN, Liu Y, Qiu MS, Bunge MB, Rao MS, Whittemore SR. 2005. Endogenous Nkx2.2+/Olig2+ oligodendrocyte precursor cells fail to remyelinate the demyelinated adult rat spinal cord in the absence of astrocytes. Exp Neurol 192(1):11-24.

Tang Y, Li H, Liu JP. 2010. Niemann-Pick Disease Type C: from molecule to clinic. Clin Exp Pharmacol Physiol 37(1):132-40.

Trapp BD, Wujek JR, Criste GA, Jalabi W, Yin X, Kidd GJ, Stohlman S, Ransohoff R. 2007. Evidence for synaptic stripping by cortical microglia. Glia 55(4):360-8.

Tremblay ME, Lowery RL, Majewska AK. 2010. Microglial interactions with synapses are modulated by visual experience. PLoS Biol 8(11):e1000527.

Tremblay ME, Stevens B, Sierra A, Wake H, Bessis A, Nimmerjahn A. 2011. The role of microglia in the healthy brain. J Neurosci 31(45):16064-9.

Tyynelä J, Cooper JD, Khan MN, Shemilts SJ, Haltia M. 2004. Hippocampal pathology in the human neuronal ceroid-lipofuscinoses: distinct patterns of storage deposition, neurodegeneration and glial activation. Brain Pathol 14(4):349-57.

Tyynelä J, Palmer DN, Baumann M, Haltia M. 1993. Storage of saposins A and D in infantile neuronal ceroid-lipofuscinosis. FEBS Lett 330(1):8-12.

Tyynelä J, Suopanki J, Santavuori P, Baumann M, Haltia M. 1997. Variant late infantile neuronal ceroid-lipofuscinosis: pathology and biochemistry. J Neuropathol Exp Neurol 56(4):369-75.

Ulrich G, Ziessel R, Harriman A. 2008. The chemistry of fluorescent bodipy dyes: versatility unsurpassed. Angew Chem Int Ed Engl 47(7):1184-201.

Uvebrant P, Hagberg B. 1997. Neuronal ceroid lipofuscinoses in Scandinavia. Epidemiology and clinical pictures. Neuropediatrics 28(1):6-8.

Uversky VN. 2008. Alpha-synuclein misfolding and neurodegenerative diseases. Curr Protein Pept Sci 9(5):507-40.

Wake H, Moorhouse AJ, Jinno S, Kohsaka S, Nabekura J. 2009. Resting microglia directly monitor the functional state of synapses in vivo and determine the fate of ischemic terminals. J Neurosci 29(13):3974-80.

van der Velde AE. 2010. Reverse cholesterol transport: from classical view to new insights. World J Gastroenterol 16(47):5908-15.

van Vliet C, Thomas EC, Merino-Trigo A, Teasdale RD, Gleeson PA. 2003. Intracellular sorting and transport of proteins. Prog Biophys Mol Biol 83(1):1-45.

Vana AC, Flint NC, Harwood NE, Le TQ, Fruttiger M, Armstrong RC. 2007. Platelet-derived growth factor promotes repair of chronically demyelinated white matter. J Neuropathol Exp Neurol 66(11):975-88.

Vance JE, Hayashi H. 2010. Formation and function of apolipoprotein E-containing lipoproteins in the nervous system. Biochim Biophys Acta 1801(8):806-18.

Vance JE, Hayashi H, Karten B. 2005. Cholesterol homeostasis in neurons and glial cells. Semin Cell Dev Biol 16(2):193-212.

Watson P, Jones AT, Stephens DJ. 2005. Intracellular trafficking pathways and drug delivery: fluorescence imaging of living and fixed cells. Adv Drug Deliv Rev 57(1):43-61.

Wei H, Kim SJ, Zhang Z, Tsai PC, Wisniewski KE, Mukherjee AB. 2008. ER and oxidative stresses are common mediators of apoptosis in both neurodegenerative and non-neurodegenerative lysosomal storage disorders and are alleviated by chemical chaperones. Hum Mol Genet 17(4):469-77.

Vekrellis K, Xilouri M, Emmanouilidou E, Rideout HJ, Stefanis L. 2011. Pathological roles of alpha-synuclein in neurological disorders. Lancet Neurol 10(11):1015-25.

Verkhratsky A, Butt A. 2007. Glial Neurobiology : A Textbook. John Wiley & Sons Ltd.:21-24.

Verkruyse LA, Hofmann SL. 1996. Lysosomal targeting of palmitoyl-protein thioesterase. J Biol Chem 271(26):15831-6.

Vesa J, Chin MH, Oelgeschlager K, Isosomppi J, DellAngelica EC, Jalanko A, Peltonen L. 2002. Neuronal ceroid lipofuscinoses are connected at molecular level: interaction of CLN5 protein with CLN2 and CLN3. Mol Biol Cell 13(7):2410-20.

Vesa J, Hellsten E, Verkruyse LA, Camp LA, Rapola J, Santavuori P, Hofmann SL, Peltonen L. 1995. Mutations in the palmitoyl protein thioesterase gene causing infantile neuronal ceroid lipofuscinosis. Nature 376(6541):584-7.

Vikstedt R, Metso J, Hakala J, Olkkonen VM, Ehnholm C, Jauhiainen M. 2007. Cholesterol efflux from macrophage foam cells is enhanced by active phospholipid transfer protein through generation of two types of acceptor particles. Biochemistry 46(42):11979-86.

Vincze A, Mazlo M, Seress L, Komoly S, Abraham H. 2008. A correlative light and electron microscopic study of postnatal myelination in the murine corpus callosum. Int J Dev Neurosci 26(6):575-84.

Winter E, Ponting CP. 2002. TRAM, LAG1 and CLN8: members of a novel family of lipid-sensing domains? Trends Biochem Sci 27(8):381-3.

von Schantz C, Kielar C, Hansen SN, Pontikis CC, Alexander NA, Kopra O, Jalanko A, Cooper JD. 2009. Progressive thalamocortical neuron loss in Cln5 deficient mice: Distinct effects in Finnish variant late infantile NCL. Neurobiol Dis 34(2):308-19.

von Schantz C, Saharinen J, Kopra O, Cooper JD, Gentile M, Hovatta I, Peltonen L, Jalanko A. 2008. Brain gene expression profiles of Cln1 and Cln5 deficient mice unravels common molecular pathways underlying neuronal degeneration in NCL diseases. BMC Genomics 9:146.

Woodruff RH, Fruttiger M, Richardson WD, Franklin RJ. 2004. Platelet-derived growth factor regulates oligodendrocyte progenitor numbers in adult CNS and their response following CNS demyelination. Mol Cell Neurosci 25(2):252-62.

Xie C, Turley SD, Dietschy JM. 2000. Centripetal cholesterol flow from the extrahepatic organs through the liver is normal in mice with mutated Niemann-Pick type C protein (NPC1). J Lipid Res 41(8):1278-89.

Xin W, Mullen TE, Kiely R, Min J, Feng X, Cao Y, O'Malley L, Shen Y, Chu-Shore C, Mole SE and others. 2010. CLN5 mutations are frequent in juvenile and late-onset non-Finnish patients with NCL. Neurology 74(7):565-71.

Young SA, Mina JG, Denny PW, Smith TK. 2012. Sphingolipid and ceramide homeostasis: potential therapeutic targets. Biochem Res Int 2012:248135.

Zannis VI, Koukos G, Drosatos K, Vezeridis A, Zanni EE, Kypreos KE, Chroni A. 2008. Discrete roles of apoA-I and apoE in the biogenesis of HDL species: lessons learned from gene transfer studies in different mouse models. Ann Med 40 Suppl 1:14-28.

Zhang D, Hu X, Qian L, O'Callaghan JP, Hong JS. 2010. Astrogliosis in CNS pathologies: is there a role for microglia? Mol Neurobiol 41(2-3):232-41.

Zhang SC. 2001. Defining glial cells during CNS development. Nat Rev Neurosci 2(11):840-3.

Zhong NA, Moroziewicz DN, Ju W, Wisniewski KE, Jurkiewicz A, Brown WT. 2000. CLN-encoded proteins do not interact with each other. Neurogenetics 3(1):41-4.

Zipp F, Waiczies S, Aktas O, Neuhaus O, Hemmer B, Schraven B, Nitsch R, Hartung HP. 2007. Impact of HMG-CoA reductase inhibition on brain pathology. Trends Pharmacol Sci 28(7):342-9.

Zschoche A, Furst W, Schwarzmann G, Sanhoff K. 1994. Hydrolysis of lactosylceramide by human galactosylceramidase and GM1-beta-galactosidase in a detergent-free system and its stimulation by sphingolipid activator proteins, sap-B and sap-C. Activator proteins stimulate lactosylceramide hydrolysis. Eur J Biochem 222(1):83-90.